



An Environmental Survey of Serpentine Hot Springs

Geology, Hydrology, Geochemistry, and Microbiology

Natural Resource Report NPS/BELA/NRR—2015/1019



ON THE COVER

Bathhouse at Serpentine Hot Springs along Hot Springs Creek with granite tors in background
Photograph by: D. Kirk Nordstrom

An Environmental Survey of Serpentine Hot Springs

Geology, Hydrology, Geochemistry, and Microbiology

Natural Resource Report NPS/BELA/NRR—2015/1019

D. Kirk Nordstrom¹, Linda Hasselbach², Steven E. Ingebritsen³, Dana Skorupa⁴, R. Blaine McCleskey¹, Timothy R. McDermott⁴

¹U.S. Geological Survey
3215 Marine St.
Boulder, CO 80303

²National Park Service
Western Arctic National Parklands
PO Box 1029
Kotzebue, AK 99752

³U.S. Geological Survey, Mail Stop 439
345 Middlefield Rd.
Menlo Park, CA 94025

⁴Department of Land Resources and Environmental Sciences
Montana State University
Bozeman, MT 59717

September 2015

U.S. Department of the Interior
National Park Service
Natural Resource Stewardship and Science
Fort Collins, Colorado

The National Park Service, Natural Resource Stewardship and Science office in Fort Collins, Colorado, publishes a range of reports that address natural resource topics. These reports are of interest and applicability to a broad audience in the National Park Service and others in natural resource management, including scientists, conservation and environmental constituencies, and the public.

The Natural Resource Report Series is used to disseminate comprehensive information and analysis about natural resources and related topics concerning lands managed by the National Park Service. The series supports the advancement of science, informed decision-making, and the achievement of the National Park Service mission. The series also provides a forum for presenting more lengthy results that may not be accepted by publications with page limitations.

All manuscripts in the series receive the appropriate level of peer review to ensure that the information is scientifically credible, technically accurate, appropriately written for the intended audience, and designed and published in a professional manner.

Data in this report were collected and analyzed using methods based on established, peer-reviewed protocols and were analyzed and interpreted within the guidelines of the protocols. This report received formal peer review by subject-matter experts who were not directly involved in the collection, analysis, or reporting of the data, and whose background and expertise put them on par technically and scientifically with the authors of the information.

Views, statements, findings, conclusions, recommendations, and data in this report do not necessarily reflect views and policies of the National Park Service, U.S. Department of the Interior. Mention of trade names or commercial products does not constitute endorsement or recommendation for use by the U.S. Government.

This report is available in digital format from the Natural Resource Publications Management website (<http://www.nature.nps.gov/publications/nrpm/>). To receive this report in a format optimized for screen readers, please email irma@nps.gov.

Please cite this publication as:

Nordstrom, D. K., L. Hasselbach, S. E. Ingebritsen, D. Skorupa, R. B. McCleskey, and T. McDermott. 2015. An environmental survey of Serpentine Hot Springs: Geology, hydrology, geochemistry, and microbiology. Natural Resource Report NPS/BELA/NRR—2015/1019. National Park Service, Fort Collins, Colorado.

Contents

	Page
Figures	v
Tables	vii
Executive Summary	ix
Acknowledgments.....	xi
Introduction.....	1
Physiography and Climate	7
Permafrost	8
Climate	8
Regional Geology	9
Prior Geologic Investigations	9
Tectonics and Volcanism	10
Bedrock Geology.....	11
Methods.....	13
Field Measurements and Sampling	13
Water Sampling and Preservation for Chemical Analysis	13
Stable Isotope Sampling	13
Discharge Measurements.....	17
Microbiological Sampling	17
Methods for Chemical Analysis	18
Laboratory Methods	18
Quality Assurance Quality Control	18
Methods for Microbiological Analysis.....	18
DNA extraction and PCR	18
Pyrosequencing.....	19
Data Analysis.....	19
Results and Discussion	20
Water Chemistry.....	20
Chemical Character of Waters.....	20

Contents (continued)

	Page
Temperature and Conductance Profile of Diversion Ditch Water	22
Stable Isotope Hydrology	24
Overview: Stable Isotope Hydrology as applied to Geothermal Waters	24
Serpentine-area Stable Isotope Data Interpretation	26
Hydrologic Discharge and Chloride Load.....	30
Hot Springs Creek	30
Serpentine and Arctic Hot Springs	33
Thermal Discharge	37
Overview: Thermal Inventories.....	37
Serpentine-area Thermal Discharge	37
Microbiology and its Relation to Human Activity	38
Introduction	38
Total and Fecal Coliform Bacteria	40
Phylogenetic Diversity	41
Synthesis.....	47
Microbial Diversity in Thermal Waters	47
Serpentine Hot Springs.....	49
Arctic Hot Springs.....	53
Synthesis.....	58
Literature Cited	59
Appendix A : Details of analytical methods for water chemistry	68
Appendix B: Quality Assurance Quality Control	76
Appendix C: Water Chemistry Analyses	81

Figures

	Page
Figure 1. Location of Serpentine Hot Springs on Seward Peninsula within the Bering Land Bridge National Preserve, Alaska.....	1
Figure 2. Landscape of Serpentine Hot Springs environs, bathhouse (building on left) and bunkhouse (building on right) at right center of photo.	2
Figure 3. William Allokeok at Serpentine Hot Springs, 1923 (from Alaska State Library Edward Keithahn Collection, P360.823).	3
Figure 4. Study site photos: a) Arctic Hot Springs (HS) main hot vent, b) 1920's era hot tub remains, c) an algae sampling site, d) Hot Springs Creek, e) Serpentine HS hot pool, f) Hot Springs Creek, g) one of four beaver dams located on Hot Springs Creek immediately above cabins, h) airstrip, i) granite tors. Photos b, c, e, f and h courtesy of Greg Gusse, 2010.....	4
Figure 5. Serpentine Hot Springs with bunkhouse (left) and bathhouse (right) and Hot Springs Creek in foreground.	5
Figure 6. Seward Peninsula hot springs, granitic plutons (Miller et al., 1973), Late Cenozoic volcanic rocks (Moll-Stolcup et al., 1994), selected fault lines (Plafket et al., 1994), maars and other key features.	7
Figure 7. Serpentine Hot Springs drainage basin showing basic geology (modified from Hudson, 1979, plate 1), relief, streams, continental divide, and 37 sampling locations with range of specific conductance.....	12
Figure 8. Serpentine Hot Springs total and fecal coliform bacteria sampling site numbers, 2010.....	18
Figure 9. Plot of Na and Br concentrations relative to Cl concentrations with seawater dilution lines for each.....	22
Figure 10. Enlargement of sketch map from Gary Rosenlieb (NPS, written commun., 1998) shows field measurement locations (open circles) for temperature and specific conductance.....	23
Figure 11. Stable isotope sample locations and deuterium (δD) content of samples acquired in the Serpentine Hot Springs area, midsummer 2010.....	25
Figure 12. Relation between deuterium (δD) and oxygen-18 ($\delta^{18}O$) contents, showing the meteoric water line (Craig, 1961a) with a slope of 8, Vienna Standard Mean Ocean Water (VSMOW) and typical fractionation for geothermal waters that have undergone evaporation with a slope of approximately 3 (Craig, 1963; Panichi and Gonfiantini, 1977).	26
Figure 13. Relation between deuterium (δD) and oxygen-18 ($\delta^{18}O$) contents for samples acquired in the Serpentine Hot Springs area, midsummer 2010, relative to the global meteoric water line (Craig, 1961).	27

Figures (continued)

	Page
Figure 14. Relation between deuterium (δD) content and elevation for samples acquired in the Serpentine Hot Springs area, 2010.....	29
Figure 15. Midsummer 2010 conductance-temperature-depth records from Hot Springs Creek below Serpentine Hot Springs (A) and below Arctic Hot Springs (B).	31
Figure 16. Plot of conductivity against stream height in Hot Springs Creek below Serpentine and Arctic Hot Springs discharges, 2010.....	32
Figure 17. Discharge plotted against downstream distance.....	32
Figure 18. Block diagram illustrating chloride-flux method of measuring thermal-spring discharge.	34
Figure 19. Plot of Cl concentrations against conductivity for Hot Springs Creek samples.....	35
Figure 20. Plot of conductivity against the fraction of river water.	36
Figure 21. Chloride load plotted against distance with red bars showing the loading from the two hot spring areas.	36
Figure 22. The Three Domains of Life classification system.	39
Figure 23. Photographs of microbial growth in and adjacent to the hot pool at Serpentine Hot Springs.	48
Figure 24. Photographs of microbial growth in Arctic Hot Springs, 2010.....	48
Figure 25. Arctic Hot Springs microbiology collection sites, 2010.....	53

Tables

	Page
Table 1. Sample site locations with identification number (Site ID), collection date, longitude, latitude, and type of sample collected. Sample site locations are shown in Figures 7, 8, and 25.....	14
Table 2. Container preparation and stabilization methods for water samples.	16
Table 3. Field measurement and main chemical constituents of waters sampled.....	20
Table 4. Saturation indices calculated with the WATEQ4F code (Ball and Nordstrom, 1991).	22
Table 5. Field measurements of temperature and specific conductance along cold water diversion ditch from Hot Springs Creek to the bathhouse.	23
Table 6. Chemical geothermometer results for the four hottest waters sampled using equations listed in Fournier (1991).	27
Table 7. Discharge values for key locations along Hot Spring Creek	30
Table 8. Estimates of hot spring discharge by two methods.....	34
Table 9. Total and fecal coliform bacteria in Hot Springs Creek upstream, downstream, and surrounding the bunkhouse and bathhouse structures.....	40
Table 10. Archaeal, bacterial, and eukaryotic phylotype richness (97% ID) in water quality analysis of Hot Springs Creek.....	42
Table 11. Dominant Archaea phyla observed in the various sampling sites surrounding the bathhouse and bunkhouse	42
Table 12. Dominant Bacteria phyla observed in the various sampling sites surrounding the bathhouse and bunkhouse.	44
Table 13. Dominant Eukarya phyla observed in the various sampling sites surrounding the bathhouse and bunkhouse.	46
Table 14. Archaeal, bacterial, and eukaryotic phylotype richness (97% ID) in the Serpentine Hot Spring study location.	49
Table 15. Dominant Archaea phyla in Serpentine Hot Spring sampling site 44.	50
Table 16. Dominant Bacteria phyla observed in the Serpentine Hot Spring sampling sites. Genus level taxonomy is highlighted in orange.....	51
Table 17. Dominant Eukarya phyla observed in Serpentine and Arctic Hot Springs. Family or Genus level taxonomy is highlighted in orange.	52
Table 18. Archaeal, bacterial, and eukaryotic phylotype richness (97% ID) in the Arctic hot springs sampling sites.	54
Table 19. Dominant Archaea phyla observed in the Arctic Hot Springs sampling sites. Dominant genera are highlighted in orange.....	55

Tables (continued)

	Page
Table 20. Dominant Bacteria phyla observed in the Arctic Hot Springs sampling sites. Dominant genera are highlighted in orange.	56
Table A-1. Analytical techniques, detection limits, typical precision, equipment used, and analytical method references.	69
Table B-1. Results for standard reference water samples.	76
Table C-1. Results of water analyses, field parameters, and sampling coordinates.	82
Table C-2. Water analyses for trace elements (<0.002 mg/L).	85
Table C-3. Water isotope data.	88

Executive Summary

Serpentine Hot Springs is the most visited site in the Bering Land Bridge National Preserve. The hot springs have traditionally been used by the Native people of the Seward Peninsula for religious, medicinal and spiritual purposes and continue to be used in many of the same ways by Native people today. The hot springs are also popular with non-Native users from Nome and other communities, recreational users and pilots from out of the area, and hunters and hikers. The constituency is diverse and vocal. Many users have divergent views with regard to management priorities at the site.

Serpentine Hot Springs are located on Hot Springs Creek near the headwaters of the Serpentine River, named for its meandering course. The site consists of two distinct thermal areas; Serpentine Hot Springs proper and Arctic Hot Springs, located approximately 600 m downstream. Little is known about the hydrology and water chemistry of the system. The current study was undertaken to address identified data gaps by describing the hydrology, geochemistry, water quality, and microbiology of Serpentine Hot Springs in an integrated fashion.

Late Cenozoic volcanic fields, mainly north and east of Serpentine Hot Springs, cover about 10,000 km² of the Seward Peninsula. The four Espenberg Maars occur just 40 km north of Serpentine Hot Springs. These maars are shallow, broad craters attributed to Late Pleistocene (17,500-200,000 years B.P.) volcanic eruptions through thick permafrost. All four maars are larger than Kilauea caldera, Hawaii, and about an order of magnitude larger than any other known maars on Earth. The associated eruptive products are farther north than any other Late Pleistocene-to-present volcanoes in North America.

In the Serpentine Hot Springs area, a Late Cretaceous (67-69 Ma) biotite granite stock named the Oonatut Granite Complex intruded a diverse suite of older metamorphic rocks, pelitic and mixed schists, and is exposed over an area of about 70 km². Most known hot springs in central and northern Alaska are, like Serpentine Hot Springs, spatially associated with granitic plutons; in fact, Miller et al. (1975) showed that all 23 northern Alaska hot springs for which bedrock geology is known occur within 5 km of a granitic pluton. The Cretaceous-aged granites are unlikely heat sources, as even the largest plutons cool to ambient temperature in about 1 Ma. The association is most likely hydraulic, in that hot springs require deep circulation of meteoric water in order to reach high temperature. The two most likely candidates for sustaining vertical permeability to requisite depths are normal faults and the contact zones between granitic plutons and intruded country rocks.

Two main water types were sampled in the catchment area, variably dilute surface water of Ca-HCO₃ type and hot-spring water of Na-Cl type. Serpentine and Arctic Hot Springs have virtually identical chemical composition and similar inferred maximum subsurface temperatures of 127±3°C and, hence, must be coming from the same source. Water-isotope data (hydrogen and oxygen isotopes) suggest that the thermal waters are of meteoric and possibly local origin. Both the Na/Cl and Br/Cl ratios of the thermal waters and their water-isotope composition are compatible with the suggestion that they contain a seawater component. A ~7% seawater component would fit the chloride data and would also account for the 10-12 ‰ deuterium shift between the thermal waters and the mean of the non-thermal waters.

During fieldwork in June 2010 the discharge of Hot Springs Creek was approximately 450 L/s. Approximately 25% of this flow was diverted around the Serpentine Hot Springs structures by an extensive series of beaver dams, as determined by the difference between the sum of the north and south forks and a measurement in the main stem just upstream from the structures. The diverted flow returns to the main stem below Serpentine Hot Springs.

The chloride load in Hot Springs Creek downstream of Arctic Hot Springs (~2000 kg/d, 90% of which is from the hot-spring groups) was used to estimate a thermal-water discharge rate of ~14 kg/s, 2/3 of which is from Serpentine Hot Springs. Both the thermal-water discharge value and the inferred subsurface temperatures are the highest observed in central or western Alaska, and combine to indicate a hydrothermal heat discharge of ~8 MW_t (MW of thermal output). Hydrothermal heat output in excess of the likely conductive heat input to the local catchment (~3 MW_t assuming 0.1 W/m² over a 30-km² area) suggests the possibility of a subsurface flow system that extends well beyond the surface catchment, or a cryptic magmatic heat source that augments the expected conductive heat flux. However a helium-isotope ratio (³He/⁴He) of R/R_a = 0.343 at Arctic Hot Springs does not support the existence of a cryptic magmatic heat source.

The sites assessed near the Serpentine Hot Springs structures contain few potentially pathogenic prokaryotic microorganisms, and water resources were not impaired at the time of sampling in June 2010. Total coliform bacteria (TC) counts were elevated in the four sampling sites closest to the structures. However fecal coliform (FC) levels were within range of Alaska's bacteriological standards for drinking water supply (20 FC/100mL) and water recreation (100 FC/100mL). As the time of sampling did not correspond to peak seasonal human visitation, the peak seasonal TC and FC counts may be higher. The upstream beaver dam complex was not a contributing factor to the elevated TC counts measured near the bunkhouse.

The identification and distribution of eukaryotic 18S rDNA sequences from the genera *Naegleria* at Serpentine Hot Spring intake ditch sites includes the possibility of the deadly free-living amoeba *N. fowleri*, which proliferates at elevated water temperatures. However, taxonomic resolution achieved by the molecular-based data could not determine whether the *Naegleria* detected was the pathogenic species *fowleri*. Additional molecular work employing other techniques is warranted in order to clarify this particular issue.

Assessment of the microbial diversity at Serpentine and Arctic Hot Springs considerably expands the current understanding of thermophilic microbial communities in Bering Land Bridge National Preserve. The *Eimeriidae* family of *Apicomplexa* eukaryotes are not known to tolerate elevated temperature and thus sequences detected at Serpentine could potentially represent a new genus of thermophilic protozoa. Dominant *Philodinida* phylotypes detected at both Serpentine and Arctic Hot Springs provide evidence for the prevalence of these poorly understood organisms in hot spring ecosystems. Finally, the sequence signature of numerous fly, water mite, protozoa, and rotifer species at Arctic Hot Springs represents a novel contribution to our understanding of the diversity and prevalence of eukaryotes in geothermal hot spring systems, suggesting that the prevalence and contribution of eukaryotic life to hot spring ecosystems is perhaps more important than previously thought.

Acknowledgments

The USGS researchers would like to thank Randall Chiu for assistance with the chemical analyses and the Geothermal / National Research / Volcano Hazards Programs of the USGS and the National Park Service for funding this project. USGS reviews by W.C. Evans and J.C. Underwood and NPS reviews by Paul Burger and Jon O'Donnell are gratefully acknowledged.

Introduction

Serpentine Hot Springs are located in Bering Land Bridge National Preserve, a remote National Park Service (NPS) unit on the Seward Peninsula in northwestern Alaska (Figure 1). The 2.7 million acre Preserve was established in 1980 under the Alaska National Interest Lands Conservation Act. One of its primary purposes is to protect, study and interpret a portion of the land bridge that allowed humans, other animals and plants to migrate from Asia to North America during the last glacial maximum (ending ca. 12,000 years ago, NPS, 2009; NPS, 2011). Additional directives include (but are not limited to) protection of the “integrity of Serpentine Hot Springs, its natural setting, and its cultural and spiritual significance” and protection and study of high latitude volcanic features unique to North America (NPS, 2009).

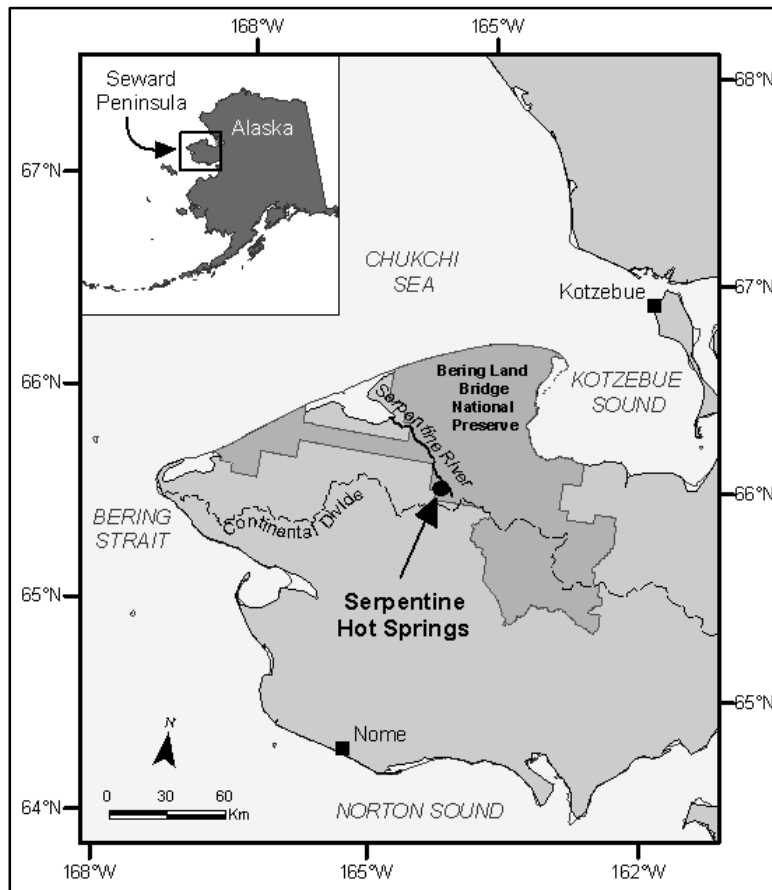


Figure 1. Location of Serpentine Hot Springs on Seward Peninsula within the Bering Land Bridge National Preserve, Alaska.

The northern Seward Peninsula is broadly characterized by gently rolling tundra uplands and flat coastal plains. Serpentine Hot Springs lie in a ‘bowl-shaped valley’ surrounded by granite tors (i.e., pinnacles or spires) (NPS, 2003). Together, the hot springs and the surrounding tors form a unique and visually striking setting in contrast to the undulating tundra backdrop of the surrounding area (Figure 2).



Figure 2. Landscape of Serpentine Hot Springs environs, bathhouse (building on left) and bunkhouse (building on right) at right center of photo.

Serpentine Hot Springs is the most visited site in the Preserve. The hot springs have traditionally been used by the Native people of the Seward Peninsula for religious, medicinal, and spiritual purposes (Figure 3), as well as for subsistence and recreational activities, for hundreds of years or more (Book et al., 1983; NPS, 2003). The site continues to be used in many of the same ways by Native people today. The hot springs are also popular with non-Native users from Nome and other communities, recreational users and pilots from out of the area, and hunters and hikers. The constituency is diverse and vocal. Many users have divergent views with regard to management priorities at the site.

Serpentine Hot Springs are located on Hot Springs Creek near the headwaters of the Serpentine River, named for its meandering course (Hudson, 1979, Figure 1). The site consists of two distinct thermal areas; Serpentine Hot Springs proper and Arctic Hot Springs, located approximately 600 m downstream (Figure 4). Little is known about the hydrology and water chemistry of the system. Previous studies are limited to a 1975 USGS paper on hot springs in central Alaska (Miller et al., 1975), a draft report describing basic water quality and chemistry conditions at Serpentine Hot Springs proper (G. Rosenlieb, NPS, written comm., 1998), and a 2009 water-resource draft assessment for the entire Preserve which included five data points from the Serpentine area (L.A. Munk et al., University of Alaska-Anchorage, written comm., 2009).



Figure 3. William Allokeok at Serpentine Hot Springs, 1923 (from Alaska State Library Edward Keithahn Collection, P360.823).

Aquatic thermophilic communities are well developed and are likely adapted to specific water quality, chemistry, and hydrothermal conditions at Serpentine. Given the latitude and isolation of the site, there is a high likelihood of rare and/or endemic aquatic flora and/or fauna, however, no previous studies have examined these communities. Because the hydrologic, chemical, and microbiological environments at Serpentine Hot Springs are largely undescribed, the range of natural variability and ecosystem diversity is unknown. Insufficient data exist with which to adequately assess threats and concerns related to the hot spring ecosystem.

Thermal and non-thermal water resources at Serpentine are threatened by anthropogenic and natural phenomena. Infrastructure includes a privy and a 400 m gravel airstrip on a dry terrace above the river. A World War II-era bunkhouse and small bathhouse (for soaking) are located on the river gravels below the terrace (Figure 5). Surrounded by water, these buildings are currently accessed via boardwalk. All facilities are in poor condition. The proximity of human structures to the aquatic environment has water-quality implications that may influence human health and safety, as well as the health of the aquatic ecosystem and long-term viability of the facilities.

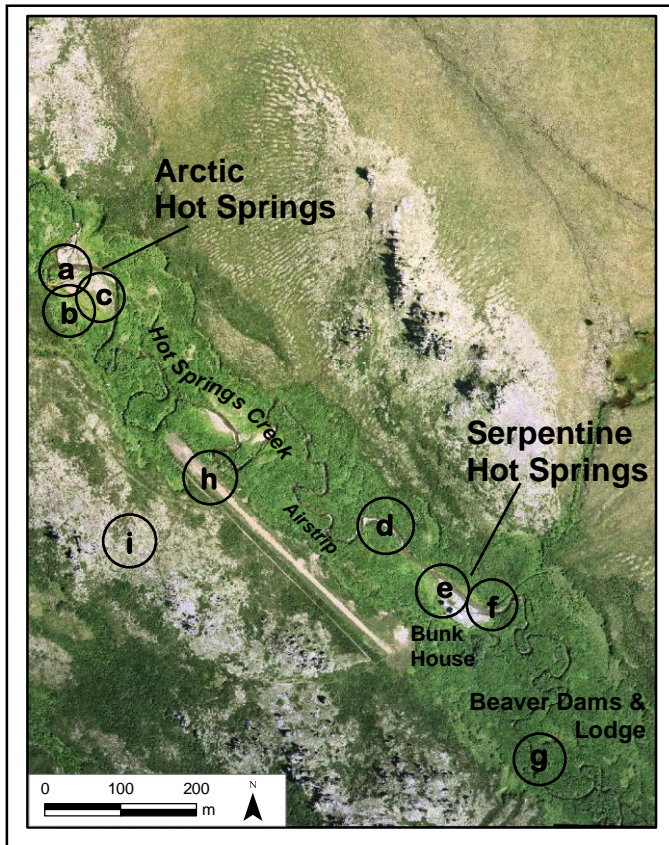


Figure 4. Study site photos: a) Arctic Hot Springs (HS) main hot vent, b) 1920's era hot tub remains, c) an algae sampling site, d) Hot Springs Creek, e) Serpentine HS hot pool, f) Hot Springs Creek, g) one of four beaver dams located on Hot Springs Creek immediately above cabins, h) airstrip, i) granite tors. Photos b, c, e, f and h courtesy of Greg Gusse, 2010.



Figure 5. Serpentine Hot Springs with bunkhouse (left) and bathhouse (right) and Hot Springs Creek in foreground.

Specific anthropogenic threats to water resources include:

- Inadequate human-waste disposal
- Bathhouse grey-water effluent (e.g., shampoos, soap)
- Improper fuels management (e.g., heating fuel, snow-machine fuel)
- Trampling in sensitive areas
- Facility development, replacement, maintenance
- Possible increase in visitor use

Natural threats include recently documented beaver activity (including an active lodge and dams) immediately upstream of the bunkhouse. Beavers are relatively new additions to the Serpentine basin ecosystem and little is known about their current population numbers and/or viability. However, in a warming climate, beaver habitat is likely to expand and it is reasonable to expect the species to gain a foothold. Additional natural threats include natural flooding, geothermal variability and climate change.

In December 2009, NPS managers and park planners began developing a site management plan for Serpentine (in the form of a General Management Plan Amendment / Environmental Assessment). Key issues included facility repair and/or replacement, disposal of human waste, questions involving site access (airstrip improvements, etc.) and future visitation levels. Initial planning efforts were hampered by an almost complete lack of baseline data. The current study was undertaken to address identified data gaps by describing the hydrology, geochemistry, water chemistry, and microbiology of Serpentine Hot Springs in an integrated fashion. In addition to being relevant to ongoing planning efforts, the information presented here will assist scientists in developing a long-term monitoring protocol to describe natural variation in water resources and detect long-term anthropogenic and natural change at Serpentine, thus assisting Preserve staff in making informed decisions regarding water-resource protection and management in future years.

Physiography and Climate

The northern Seward Peninsula is a treeless, subarctic landscape containing dynamic shoreline environments, broad coastal plains, wetlands, rolling uplands, low mountains, extensive lava fields, thaw and maar lakes, and an abundance of streams and rivers. The diverse physiography supports a wide variety of tundra plant communities. The area is remote, accessible only by aircraft, boat, or snow machine. The Continental Divide bisects the Peninsula from east to west, reaching a maximum elevation of 803 m at the headwaters of Hot Springs Creek. Serpentine Hot Springs (65.85N 164.71W) are located immediately north of the Divide and drain to the Chukchi Sea via the Serpentine River (Figure 6). They are approximately 70 km south of the Arctic Circle, 150 km north of Nome, and 160 km east of the Bering Strait.

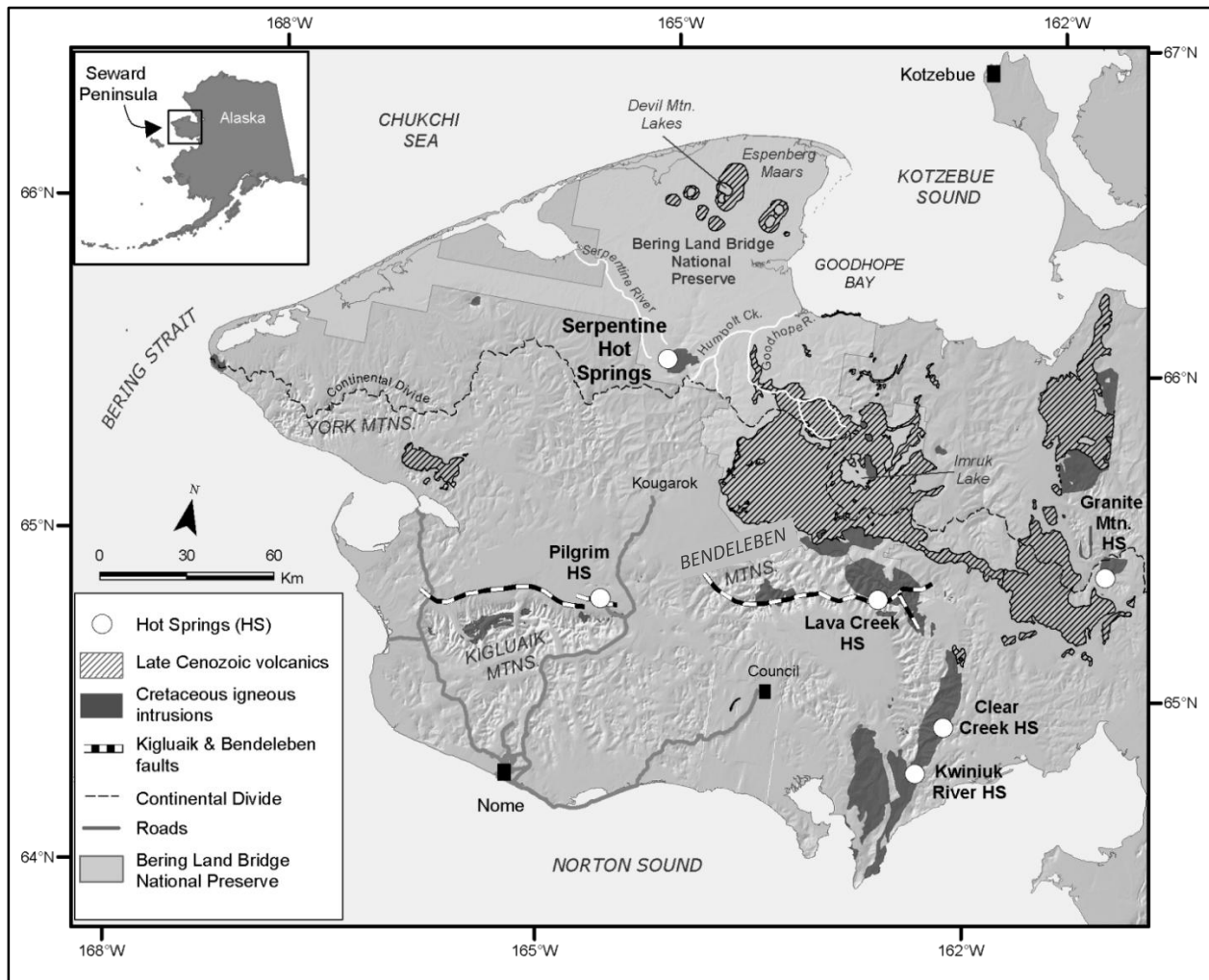


Figure 6. Seward Peninsula hot springs, granitic plutons (Miller et al., 1973), Late Cenozoic volcanic rocks (Moll-Stolcup et al., 1994), selected fault lines (Plafket et al., 1994), maars and other key features.

Permafrost

Permafrost is continuous in the northern Seward Peninsula with the exception of local anomalies in the vicinity of hot springs and along large rivers (Hudson, 1979; L.A. Munk et al., University of Alaska-Anchorage, written comm., 2009). Depth of the frozen layer is approximately 100 m (Pewe, 1975; Beget et al., 1996). The presence of permafrost strongly influences natural hydrologic conditions and is responsible for a variety of surface features including thaw lakes, ice wedge polygons, patterned ground, solifluction lobes, and cryoturbation (NPS, 1987; L.A. Munk et al., University of Alaska-Anchorage, written comm., 2009).

Climate

The Seward Peninsula experiences long, cold winters and cool, wet summers. A maritime climate prevails from mid-June to November when marine waters are ice-free. From November through May, the maritime influence is minimized by the presence of oceanic pack ice which produces a colder, drier continental climate (NPS, 1987).

The nearest National Weather Service station is in Kotzebue, Alaska (on the Baldwin Peninsula, 150 km northeast of the study area) and provides a rough approximation of conditions on the northern Seward Peninsula. Mean daily temperatures in Kotzebue (Climate Zone, 2011) range from 7 °C to 12 °C in summer (June – August) and from -20 °C to -17 °C in winter (January – March). Mean annual precipitation is approximately 23 cm, most of which occurs during summer months when warm, moist air moves in from the southwest (L.A. Munk et al., University of Alaska-Anchorage, written comm., 2009). August is the wettest month with a mean precipitation of 45 mm (Climate Zone, 2011). Average annual snowfall is 114 cm. Water content in the snowpack is low (NPS, 1987).

Winds are generally from the east in winter months and from the south – southwest in summer (NPS, 1987). Average monthly wind speeds are 7 – 9 knots throughout the year, reaching 40 – 60 knots during storm events (NPS, 1987).

Regional Geology

Prior Geologic Investigations

Gold is reported to have been discovered on the Seward Peninsula in 1865-66 by a survey party led by Baron von Bendeleben (Hopkins and Hopkins, 1958), whose name is now used for the topographic quadrangle that contains the Serpentine Hot Springs as well as the mountains located to the southeast of Serpentine (Figure 6). A gold rush did not begin until 1898 when rich placers were found near Nome and Council. Placer tin was found in 1900 in the York Mountains by Alfred H. Brooks (Brooks, 1901) of the U.S. Geological Survey (USGS), and his team produced the first geologic maps for the Seward Peninsula (Brooks et al., 1901).

Collier (1902), a colleague of Brooks, reports Charles McLennan to be the first non-Native to explore the Serpentine River and probably the first to reach the hot springs on Hot Springs Creek (named Spring Creek in Collier, 1902) in May, 1900. McLennan staked claims and prepared a map of the region. Collier found a small settlement at the hot springs in September, 1901, with a small garden. He also noted the needles and pinnacles of granite and reported that bedrock above the fluvial gravels was dark graphitic and feldspathic schists intruded by granite with limestones and mica schists nearby belonging to the Kugruk group. Placer gold had already been found in some tributaries of the Serpentine. Collier is credited with finding the first lode tin deposit in Alaska, a significant find because there were no known tin deposits in the rest of the United States, and this find was confirmed by Knopf (1908). Placer deposits of cassiterite (tin oxide, SnO_2) were found in Humboldt Creek (Sainsbury et al., 1968), which flows northeast into the Goodhope River and Goodhope Bay in Kotzebue Sound. The headwaters of Humboldt Creek are located just on the other side of the watershed divide from the headwaters of Hot Springs Creek, near the contact between the granitic intrusion of the Serpentine drainage and the metamorphic rocks to the east.

Wimmeler (1926) noted that several hundred lode deposits had been found in the Seward Peninsula but that most did not go beyond the prospecting stage because of low metal contents, discontinuous ore mineralization and poor economic conditions. During 1944-46 field work was undertaken by the USGS to find lode and placer deposits of radioactive minerals. Nothing of commercial value was found, but small quantities of radioactive minerals were documented in the granite near the headwaters of the Serpentine River (Moxham and West, 1953).

A heavy-metals program by the USGS led to further detailed mapping and mineral deposit evaluations in the area (Sainsbury et al., 1968; Hudson, 1979). Within the granitic complex of the Serpentine Hot Springs area, nothing commercial was found, but just outside of the drainage basin, on the east side of the continental divide, geochemical anomalies in stream sediments were reported for the Humboldt Creek area (Sainsbury et al., 1968; Sainsbury, 1975). The anomalies were elevated concentrations of gold, silver, mercury, arsenic, antimony, cobalt, copper, lead, molybdenum, tin, nickel, tungsten, and zinc. During the 1980s a mineral resource mapping study of Bendeleben and Soloman quadrangles marked the tin vein occurrences at the headwaters of Humboldt Creek which included a designation at the headwaters of the north fork of Hot Springs Creek (Gamble and Till, 1993). That survey also identified the area of the granite outcrop as having a high level of

favorability for tin vein and greisen deposits. Greisenization is the hydrothermal alteration of granite by a high-fluoride fluid at high temperatures ($> 350^{\circ}\text{C}$) to sericite or muscovite and quartz, often accompanied by topaz, tourmaline, and fluorite. Lode tin deposits are often greisens.

Robinson and Stevens (1984) published a complete geologic map of the Seward Peninsula from a compilation of other reports. The most recent bedrock geology map for the Seward Peninsula (scale 1:500,000) is the preliminary map of Till et al. (2010) that includes conodont data.

Tectonics and Volcanism

The hot springs are located 1100 km north of the Aleutian volcanic arc, which is the surface expression of the major, active tectonic-plate boundary where the Pacific plate plunges beneath North America. The surrounding Seward Peninsula is a region of active Late Cenozoic (0-6 Ma) volcanism (Moll-Stalcup, 1994) and ongoing north-south tectonic extension of enigmatic origin (Dumitru et al., 1995; Mackey et al., 1997).

The active volcanism on the Seward Peninsula consists mainly of large basalt fields overlain by steep cones and maars. Late Cenozoic volcanic fields, mainly north and east of Serpentine Hot Springs, cover about 10,000 km² (Till and Dumoulin, 1994). The four Espenberg Maars occur just 40 km north of Serpentine Hot Springs. Maars are shallow, broad craters formed by phreatomagmatic eruptions. These maars are attributed to Late Pleistocene (17,500-200,000 years B.P.) volcanic eruptions through thick permafrost (Beget et al., 1996). The largest, Devil Mountain Lakes Maar (Figure 6), is about the size of Oregon's Crater Lake. All four maars are larger than Kilauea caldera, Hawaii, and about an order of magnitude larger than any other known maars on Earth. The Espenberg Maars and associated eruptive products are farther north than any other Late Pleistocene-to-present volcanoes in North America (Wood and Kienle, 1990).

The entire Seward Peninsula is subject to ongoing north-south extension, which has continued, at least episodically, since the middle to late Cretaceous (Dumitru et al., 1995). The ongoing extension is expressed in the focal mechanisms of modern seismicity (Eastbrook et al., 1988; Page et al., 1991; Mackey et al., 1997), large active normal faults such as those that bound the Kigluaik Mountains and Bendeleben Mountains (Figure 6), and basin-range topography. Ongoing extension is also compatible with the active basaltic volcanism and existence of hot springs. Both the north-south extension and the active volcanism remain somewhat enigmatic, however, because of the great distance from any well-established tectonic-plate boundary and the generally compressive tectonics in northern Alaska east of about longitude 154°W. The "demise of the Brooks Range going west towards the Bering Strait" may be associated with a transition from north-south shortening to north-south extension at about 154° longitude (Dumitru et al., 1995). It has been further suggested that the Seward Peninsula represents the northern boundary of an independent Bering block that is rotating clockwise relative to the North American plate (Mackey et al., 1997). Thus a proposed east-west-trending rift through the central Seward Peninsula at the latitude of Pilgrim Hot Springs (Turner and Swanson, 1981) may be part of an extensional system similar to the Basin and Range of the western United States, although smaller in scale. The active basaltic volcanism on the Seward Peninsula is the local expression of a larger "Bering Sea basalt province" (Akinin et al., 2009) that spans the Bering Strait and also includes the Saint Michaels and Nunivak Island volcanic fields to the south (Moll-

Stalcup, 1994). Many authors refer to this volcanism as “back-arc volcanism” despite the very large distance (~1000 km) to the Aleutian volcanic arc. Some link to distant plate-boundary processes is suggested by the timing of the onset of voluminous “Bering Sea” basaltic eruptions at ~ 6 Ma, contemporaneous with small changes in Pacific plate motion (Cox and Engebretson, 1985) and a major pulse of activity in the Aleutian arc (Moll-Stalcup, 1994).

Bedrock Geology

Despite the conspicuous Late Cenozoic volcanism, the bedrock geology of the Seward Peninsula consists mainly of much older rocks. Regionally metamorphosed sedimentary rocks (metasediments) of Precambrian and Paleozoic age (more than 245 Ma) are widespread, and are locally intruded by mainly Cretaceous age (70-140 Ma) granitic plutons (see Figure 6 for generalized distribution of exposed granitic plutons on the Seward Peninsula and adjacent areas to the east).

Much of the Seward Peninsula is a tundra-mantled low-relief landscape, such that bedrock exposures are scarce. However, bedrock exposures in the immediate vicinity of Serpentine Hot Springs are unusually good, owing to 700+ m of topographic relief associated with resistant granite outcrops and to the continental divide, locally expressed as a ridgeline that partly bounds the Serpentine catchment and attains a maximum elevation of 803 m (Figure 7). In the Serpentine Hot Springs area, a Late Cretaceous (67-69 Ma) biotite granite stock named the Oonatut Granite Complex intruded a diverse suite of older metamorphic rocks, pelitic and mixed schists, and is exposed over an area of about 70 km² (Figure 7; Hudson, 1979). Oonatut is the local Yupic-language name for the area, and means “place where hot water exists”. The granite exerts the main influence on water chemistry in the Hot Springs Creek drainage, but the south fork of Hot Springs Creek begins in the mixed schists, and some water samples in this area were found to have higher solute concentrations than those in the north fork. This effect is reflected in the conductivities shown in Figure 7.

Most known hot springs in central and northern Alaska are, like Serpentine Hot Springs, spatially associated with granitic plutons. This association was first noted by Waring (1917), and Miller et al. (1975) later showed that all 23 northern Alaska hot springs for which bedrock geology is known occur within 5 km of a granitic pluton (a subset of these springs and associated plutons appear on Figure 6). This association is independent of the exposed size, age, or composition of the plutons, and in fact the Cretaceous-aged (70-140 Ma) granites are unlikely heat sources, as even the largest plutons cool to ambient temperature in about 1 Ma. The association is most likely hydraulic, in that hot springs require deep circulation of meteoric water in order to reach high temperature. In this terrane the two most likely candidates for sustaining vertical permeability to requisite depths are normal faults and the contact zones between granitic plutons and intruded country rocks. However, hot springs in northern and central Alaska are associated with faults or lineaments only where those faults and lineaments are themselves near plutons (Miller et al., 1975).

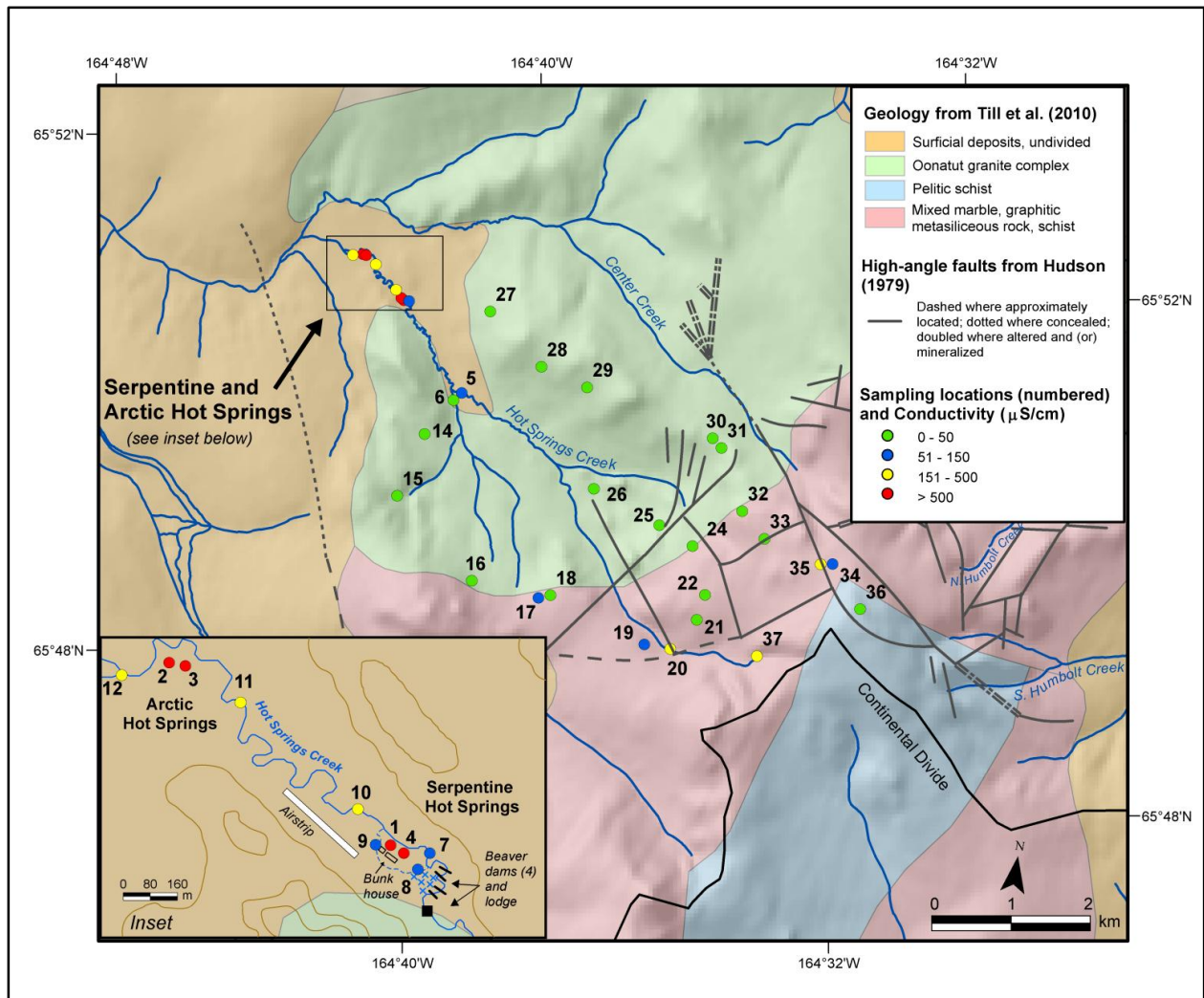


Figure 7. Serpentine Hot Springs drainage basin showing basic geology (modified from Hudson, 1979, plate 1), relief, streams, continental divide, and 37 sampling locations with range of specific conductance. Additional information on site locations is shown in Table 1.

Methods

Field Measurements and Sampling

Water Sampling and Preservation for Chemical Analysis

Sample site locations and types of samples collected are summarized in Table 1 and the sample sites are shown on Figure 7. Measurements for temperature, pH, Eh, electrical conductivity, dissolved oxygen (DO), and H₂S (hydrogen sulfide) were performed on site. Measurements for Eh and pH were made on unfiltered sample water pumped from the source through an acrylic plastic flow-through cell, which minimized sample contact with air. The flow-through cell contained a combination redox electrode, a combination pH electrode, a thermistor, and test tubes containing buffer solutions for calibration of the pH electrode. All components were thermally equilibrated with the sample water before obtaining measurements. Where possible, electrical conductivity and temperature were measured by immersing the combined conductivity/temperature probe directly into the main source of discharge as close to the sampling point as possible. Otherwise, the probe was immersed in the flow-through cell. Dissolved oxygen was determined using the azide modification of the Winkler titration (American Public Health Association (APHA), 1980).

Container preparation, sample stabilization, and sample storage methods for filtered samples are summarized in Table 2. Samples were filtered on site through a disposable capsule filter having a nominal pore size of 0.45 µm. Several sample splits were collected for determination of concentrations of inorganic constituents, redox species, and dissolved organic carbon (DOC). Samples for the determination of concentrations of cations and trace metals (As, Al, B, Ba, Be, Bi, Ca, Cd, Ce, Co, Cr, Cs, Cu, Dy, Er, Eu, Fe, Gd, Hf, Ho, K, La, Li, Lu, Mg, Mn, Mo, Na, Nd, Ni, Pb, Pr, Rb, Re, Sb, Se, SiO₂, Sm, Sr, Ta, Tb, Te, Th, Tl, Tm, U, V, W, Y, Yb, Zr, and Zn), major anions (Br, Cl, F, NO₃, and SO₄), alkalinity, and DOC were filtered, and then stabilizing reagents were added when necessary. Sample bottles were pre-rinsed with filtered water prior to sample collection. Samples for the determination of DOC concentrations were filtered through the same filter used to collect the inorganic constituents. At least 1 L of sample was passed through the filter assembly before a DOC sample was collected.

Stable Isotope Sampling

Raw, unfiltered water samples for stable isotope analysis were collected at 37 sites in the Serpentine Hot Springs catchment (Table 1). Sample sites included 4 hot spring orifices and 25 sites distributed throughout the Hot Springs Creek watershed between Arctic Hot Springs and the continental divide (Figure 7).

Table 1. Sample site locations with identification number (Site ID), collection date, longitude, latitude, and type of sample collected. Sample site locations are shown in Figures 7, 8, and 25.

Site ID	Location	Collection Date	Longitude	Latitude	Chemistry	Isotopes	Microbiology
1	Serpentine Hot Spring	6/23/2010	65°51'9.4"	164°41'43.7"	x	x	x
2	Arctic Hot Springs - above old bathhouse	6/24/2010	65°51'26.5"	164°42'32.7"	x	x	
3	Arctic Hot Springs - upper site	6/24/2010	65°51'22.7"	164°42'23.2"	x	x	x
4	Cold water intake for bathhouse	6/23/2010	65°51'0.90"	164°41'41.9"	x	x	x
5	Hot Springs Creek - North Fork	6/25/2010	65°50'30.8"	164°40'31.1"	x	x	
6	Hot Springs Creek - South Fork	6/25/2010	65°50'30.6"	164°40'31.7"	x	x	
7	Hot Springs Creek - upstream from bathhouse	6/23/2010	65°51'9.2"	164°41'38.8"	x	x	x
8	Pooled up water south east of bathhouse	6/23/2010	--	--	x	x	x
9	outflow from bathhouse / stream south of bathhouse	6/23/2010	65°51'10.2"	164°41'45.5"	x	x	x
10	Hot Springs Creek - 200 m downstream from bathhouse	6/23/2010	65°51'12.1"	164°41'55.8"	x	x	
11	Hot Springs Creek - above Arctic Hot Springs	6/24/2010	65°51'23.7"	164°42'21.7"	x	x	
12	Hot Springs Creek - downstream from Arctic Hot Springs	6/24/2010	65°51'27.3"	164°42'49.7"	x	x	
13	Spring/pool	6/23/2010	65°50'46.8"	165°41'15.6"	x	x	
14	Thermokarst outflow	6/23/2010	65°50'7.8"	164°40'57.4"		x	
15	Stream headwaters	6/23/2010	65°49'37"	164°41'17.3"		x	
16	Stream headwaters	6/23/2010	65°49'3.1"	164°39'37.4"		x	
17	Pool/seep	6/23/2010	65°49'0.2"	164°38'19.1"		x	
18	Snowbank	6/23/2010	65°49'2.3"	164°38'6.2"		x	
19	Headwaters spring	6/23/2010	65°48'46.4"	164°36'11.4"		x	
20	High-gradient stream	6/23/2010	65°48'46.3"	164°35'41.3"	x	x	
21	Headwaters spring	6/23/2010	65°49'1.8"	164°35'16.6"		x	
22	Snowbank	6/23/2010	65°49'14.0"	164°35'12.0"		x	
23	Snowbank	6/23/2010	64°49'24.2"	164°35'11.0"		x	
24	Seep	6/23/2010	65°49'35.7"	164°35'35.0"		x	
25	Steam below tors	6/23/2010	65°49'43.0"	164°36'16.2"		x	
26	Mid-valley stream	6/23/2010	65°49'55.0"	164°37'36.6"		x	
27	Hillside seep	6/24/2010	65°51'9.7"	164°40'6.0"	x	x	
28	Hillside spring	6/24/2010	65°50'47.8"	164°38'58.1"		x	
29	Ridgetop spring	6/24/2010	65°50'41.7"	164°38'2.8"		x	
30	Snowbank	6/24/2010	65°50'27.4"	164°35'31.6"		x	
31	Spring near divide	6/24/2010	65°50'23.6"	164°35'20.0"		x	
32	Headwaters spring	6/24/2010	65°49'55.7"	164°34'45.2"		x	
33	Headwaters spring	6/24/2010	65°49'44.5"	164°34'15.2"		x	
34	Spring (C. palustra)	6/24/2010	65°49'37.9"	164°32'53.5"	x	x	

Table 1 (cont'd). Sample site locations with identification number (Site ID), collection date, longitude, latitude, and type of sample collected. (continued)

Site ID	Location	Collection Date	Longitude	Latitude	Chemistry	Isotopes	Microbiology
35	Pool on divide	6/24/2010	65°49'36.8"	164°33'7.2"	x	x	
36	Ephemeral(?) spring	6/24/2010	65°49'18.9"	164°32'14.2"		x	
37	Headwaters N fork	6/24/2010	65°48'49.4"	164°34'2.4"	x	x	
38	Outflow from bathhouse	6/25/2010	--	--			x
39	Cold water intake for bathhouse	6/24/2010	--	--			x
40	SB bath	6/24/2010	--	--			x
41	Main Below	6/25/2010	--	--			x
42	Hot Springs Creek	6/24/2010	--	--			x
43	Cold water diversion	6/25/2010	--	--			x
44	Serpentine Hot Spring- Green Mat	6/25/2010	--	--			x
45	Serpentine Hot Spring- Pink Mat	6/23/2010	--	--			x
46	Arctic Hot Springs- Upstream 02	6/25/2010	--	--			x
47	Arctic Hot Springs- Upstream 04	6/25/2010	--	--			x
48	Arctic Hot Springs- Upstream 05	6/25/2010	--	--			x
49	Arctic Hot Springs- Main 02	6/25/2010	--	--			x
50	Arctic Hot Springs- Main 04	6/25/2010	--	--			x
51	Arctic Hot Springs- Main 05	6/25/2010	--	--			x
52	Arctic Hot Springs- Main 06	6/25/2010	--	--			x
53	Arctic Hot Springs- Main 07	6/25/2010	--	--			x
54	Arctic Hot Springs- Main 08	6/25/2010	--	--			x
55	Arctic Hot Springs- Main 09	6/25/2010	--	--			x
56	Arctic Hot Springs- Main 10	6/25/2010	--	--			x
57	Arctic Hot Springs- Main 11	6/25/2010	--	--			x

Table 2. Container preparation and stabilization methods for water samples.

Constituent(s) to be determined	Storage container and preparation	Stabilization treatment in addition to refrigeration
Major cations and trace metals	Polyethylene bottles, soaked in 5% HCl and rinsed 3 times with deionized water	1% (v/v) concentrated redistilled HNO ₃ added; samples were not chilled
Total mercury (Hg(T))	Borosilicate glass bottles, soaked with 5% HNO ₃ and rinsed 3 times with deionized water	1 % (v/v) concentrated redistilled HNO ₃ / 1 % (w/v) K ₂ Cr ₂ O ₇ added
Iron and As redox species (Fe(T), Fe(II), As(T), and As(III))	Opaque polyethylene bottles, soaked in 5% HCl and rinsed 3 times with deionized water	1% (v/v) redistilled 6 M HCl added
Major anions (Br, Cl, F, and SO ₄), alkalinity as HCO ₃ , acidity, density, and nitrate (NO ₃)	Polyethylene bottles filled with distilled water and allowed to stand for 24 hours, then rinsed 3 times with deionized water	None
Ammonium (NH ₄)	Same as major cations and trace metals	1% (v/v) 1:9 H ₂ SO ₄ added
Silica (SiO ₂)	Same as major anions, alkalinity, and density	1 mL diluted to 25 mL with distilled water on-site; samples were not chilled
Thiosulfate (S ₂ O ₃)	30-mL polyethylene bottle	1.7% (v/v) 0.6 M ZnCl ₂ plus 1% (v/v) 1 M NaOH added; 1.7% (v/v) 1 M KCN also added to S _n O ₆ bottle
Dissolved organic carbon (DOC)	Amber glass bottle baked at 600°C	None
Water Isotopes (δD and δ ¹⁸ O)	60-mL glass bottle	None (unfiltered sample collected when filtration was not possible); samples were not chilled
Sulfide	30-mL polyethylene bottle	15-mL sulfide anti-oxidant buffer followed by 15-mL sample

°C, degrees Celsius; HCO₃, bicarbonate; HCl, hydrochloric acid; HNO₃, nitric acid; 1:9 H₂SO₄, one part sulfuric acid plus 9 parts water; KCN, potassium cyanide; K₂Cr₂O₇, potassium dichromate; M, molar; mL, milliliter; N, normal; NaOH, sodium hydroxide; (S-II), sulfide; v/v, volume per volume; w/v, weight per volume; ZnCl₂, zinc chloride; %, percent

Discharge Measurements

Discharge data were obtained using standard U.S. Geological Survey velocity-area methods (Carter and Davidian, 1968; Buchanan and Somers, 1969; Rantz, 1982). All velocity measurements were wading measurements made with a Type SK magnetic head pygmy meter with a digital counter. The number of velocity-area sections was not always optimal, varying between 12 and 27, because of the narrow width or shallow depth of the stream in several locations. Also, as discussed later, there was some variation in stream discharge during the course of a day of measurements. To quantify this variability, Aqua TROLL 200 (In-Situ Corporation) instruments were deployed at Hot Springs Creek downstream of Serpentine Hot Springs (site 10) and at Hot Springs Creek downstream of Arctic Hot Springs (site 12). These instruments measured electrical conductivity, water temperature, and water level hourly.

Microbiological Sampling

Microbial biomass samples were taken from various locations within the Serpentine and Arctic Hot Springs area. Sampling locations were selected so as to target either thermophilic microbial communities or microbial communities potentially affecting water quality. A schematic diagram of sampling sites in the Serpentine Hot Springs area is shown in Figure 8. Water was evaluated from 10 locations and included influent bathhouse waters, effluent bathhouse waters, and the surrounding waters of Hot Springs Creek. Surface water (1 L) was collected in Whirl-Pak bags (Nasco, Fort Atkinson, Wisconsin) and maintained on ice until processed within 1 hour. Total coliform and *E. coli* plate counts were conducted in triplicate by the membrane filtration technique; volumes of 1, 10, and 100 mL were filter-treated and incubated on a selective medium (m-Coliblu24, HACH, USA) at 37°C for 24 hours. The dilutions were used to estimate the concentration of total and *E. coli* colony-forming units (CFU), with CFU enumeration calculated from sample volumes that yielded between 20 and 80 colonies per membrane. The remaining water from each location was filtered (0.2 µm polyethersulfone (PES) membrane), and the filters stored at -20 °C until used for DNA extraction and subsequent microbial community analysis. In a separate thrust, biomass from thermophilic microbial mats was sampled for microbial diversity at Arctic and Serpentine Hot springs. This sampling scheme targeted visual gradients occurring in the microbial community as a result of temperature shifts. Microbial mat material was collected in 15-mL Falcon™ tubes using sterilized spatulas, frozen at -20°C during field sampling, and then frozen at -80°C until DNA extraction.

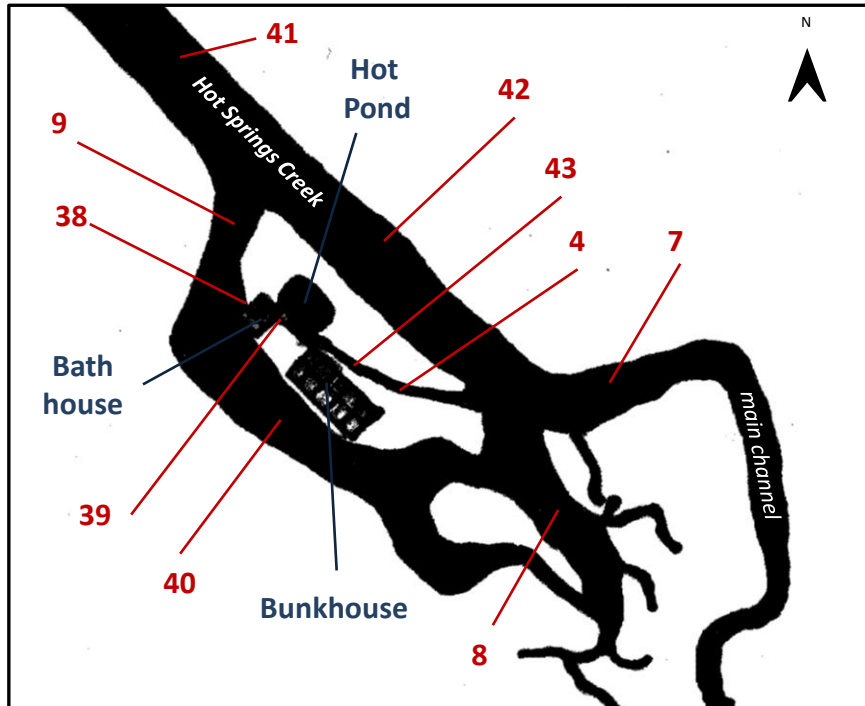


Figure 8. Serpentine Hot Springs total and fecal coliform bacteria sampling site numbers, 2010.

Methods for Chemical Analysis

Laboratory Methods

Analytical techniques, detection limits, equipment used, pertinent references, and comments are described briefly in Appendix A. Oxygen and hydrogen isotopic determinations of water samples were performed at the USGS Stable Isotope Laboratory in Reston, Virginia. Analyses of all other water samples were performed by the USGS Branch of Regional Research Laboratory in Boulder, Colorado.

Quality Assurance Quality Control

Several techniques were used to assure the quality of the analytical data (McCleskey et al., 2004). These techniques included use of field blanks, standard reference water samples, charge imbalance, and determination by alternative methods. Quality-assurance and quality-control checks for DOC included analyses of laboratory reagent blanks and synthetic samples made from potassium biphthalate, sodium bicarbonate, and sodium benzoate.

Methods for Microbiological Analysis

DNA extraction and PCR

DNA was extracted using a modified version of the FastDNA Spin Kit for Soil (MP Biomedicals, Solon, Ohio). For microbial biomass derived from thermal hot springs, 500 mg of frozen sample was first thawed to the point of convenient removal from the Falcon™ tube, and transferred to a Lysing Matrix E tube. Filters containing microbial biomass from water quality samples were cut into

quarters using a sterilized Exacto™ knife, with one quarter transferred directly to a Lysing Matrix E tube using sterilized forceps. Following sample addition, DNA extraction for both sample types continued according to the manufacturer's instructions. The DNA was cleaned and concentrated using a Qiaquick PCR Purification Kit (Qiagen, Valencia, California), and stored at -20°C until further use.

Pyrosequencing

The V1 and V2 regions of the bacterial and archaeal 16S rRNA encoding genes was amplified for 454 pyrosequencing using bacterial primers 27F (5'-AGAGTTTGATCCTGGCTCAG-3') and 533R (5'-TNACCGCGGCTGCTGGCAC-3') and archaeal primers A2Fa (5'-TTCCGGTTGATCCYGCCGGA-3') and A571R (5'-GCTACGGNYSCTTTARGC-3'). The V7 region of the eukaryotic 18S rRNA encoding gene was amplified using primers 907F (5'-GAGGTGAAATTCTTRGA-3') and 1428R (5'-CTAAGGGCATCACAGACC-3'). For all primer sets, the PCR volume was 50µl and contained: 1.5mM MgCl₂, 20µg BSA, 0.2mM each dNTP, 1µM each primer, and 1.25U Taq polymerase. The PCR program was 94°C for 5 min., 25 cycles of 94°C for 1 min., 48°C for 1 min, and 72°C for 1 min., 72°C for 7 min., and 4°C hold. After the primary amplification, five additional cycles were carried out to add the sample specific barcodes and the A and B adaptor sequences required for 454 pyrosequencing. The barcoded rRNA gene amplicons were pooled in equal concentrations and pyrosequenced on a 454 GS-FLX sequencer (EnGenCore, Columbia, South Carolina).

Data Analysis

Sequences were trimmed and quality-controlled according to Kunin et al. (2010), followed by abundance-sorted pre-clustering as per Huse et al. (2010) and a final complete linkage clustering using the mothur software package (Schloss et al., 2009). The RDP pyrosequencing pipeline was used to classify 16S rRNA sequences, while taxonomic assignment for eukaryotic-derived 18S rRNA sequences was performed in the CANGS pipeline (Pandey et al., 2010). Statistical analysis of operational taxonomic unit (OTU) richness via rarefaction, Chao1, and ACE estimates were performed in mothur, with the pyrosequencing data sets all normalized to the same number of reads. DNA pyrosequences are available in GenBank SRA accession SRA046059.

Results and Discussion

Water Chemistry

Chemical Character of Waters

Two main water types were sampled in the catchment area, variably dilute surface water of Ca-HCO₃ type and hot-spring water of Na-Cl type. The main field measurements and chemical constituents are compiled in Table 3. Complete chemical analyses and isotope determinations are provided in Appendix C for all samples.

Comparison of these values indicates that Serpentine and Arctic Hot Springs have virtually identical chemical composition and similar maximum temperatures and, hence, must be coming from the same source.

Table 3. Field measurement and main chemical constituents of waters sampled.

Site ID	Location	Collection Date	pH	Conductivity	Temperature	Ca	Na	Cl	Alkalinity
				$\mu\text{S}\cdot\text{cm}^{-1}$ at 25 °C	°C	----- mg·L ⁻¹ -----			as HCO ₃ ⁻
1	Serpentine Hot Spring	6/23/2010	7.52	4535	74.8	84.5	789	1456	56.8
2	Arctic Hot Springs - above old bath house	6/24/2010	7.47	4570	72.8	84.6	789	1434	56.1
3	Arctic Hot Springs - upper site	6/24/2010	7.23	4750	36.3	79.3	807	1455	59.5
4	Cold water intake for bath house	6/23/2010	7.64	4660	61	84.1	797	1477	58
5	Hot Springs Creek - North Fork	6/25/2010	7.47	126	6.5	15.6	2.20	6.28	24.9
6	Hot Springs Creek - South Fork	6/25/2010	6.32	28	5.2	1.3	2.24	2.53	10.5
7	Hot Springs Creek - upstream from bath house	6/23/2010	6.87	99	7.2	11.0	2.98	3.55	19.6
9	outflow from bath house / stream south of bath house	6/23/2010	6.96	121	6.8	11.1	6.78	10	19.8
10	Hot Springs Creek - about 200 m downstream from bath house	6/23/2010	7.15	198	6.6	12.1	18.7	31.4	20.3
11	Hot Springs Creek - above Arctic Hot Springs	6/24/2010	7.25	232	9.5	10.5	21.45	37.2	18.4
12	Hot Springs Creek - downstream from Arctic Hot Springs	6/24/2010	7.30	235	7.8	10.8	26.85	46.1	18.8

Two constituents that can suggest whether seawater is the source of the salinity for the hot springs are bromide and sodium. Bromide is generally quite conservative in groundwater systems and, because sodium is such a major constituent in seawater, it can also be indicative. When the Br/Cl ratio is distinctly different from seawater then other types of saline sources must be considered. If the ratio is similar to seawater then seawater must be considered as a possible source. In Figure 9 both Na and Br are plotted against Cl concentration and compared to the seawater dilution line for each. The values for Na and Cl plot directly on the seawater dilution line whereas Br and Cl are close but slightly enriched for Br. The data from Miller et al. (1973, 1975) are included for comparison, showing slight depletion. Considering the uncertainties in measuring Br concentrations these values are virtually the same as those for diluted seawater. These data tend to favor a seawater origin. This idea was mentioned by Miller et al. (1975), who discounted a seawater origin because this area has not been below sea level since the Cretaceous. However, it would not be necessary for the area to be below sea level if the presumed seawater is entrained by a large convective hydrothermal system in which permeable fault zones connect with sediments or metasediments containing modern or ancient seawater.

The hot spring waters also contain high concentrations of fluoride, 7-8 mg/L, which is typical of many thermal waters. The mineral fluorite, CaF_2 , is often thought to be a solubility control for fluoride concentrations in thermal waters and has been found in the Oonatut Granite (Hudson, 1979). The possibility of fluorite solubility equilibrium was checked by looking at saturation indices for the hot spring waters using the geochemical speciation code WATEQ4F (Ball and Nordstrom, 1991 with updates). These values are shown in Table 4 along with saturation indices for calcite, CaCO_3 . Saturation indices are calculated as $\log(\text{IAP}/\text{Ksp})$ where IAP = ion-activity product and Ksp = solubility-product constant, and values greater than 0 are supersaturated and values less than 0 are undersaturated. From the values in Table 4 it is clear that these thermal waters are saturated to supersaturated with respect to both calcite and fluorite. Most other minerals are well undersaturated.

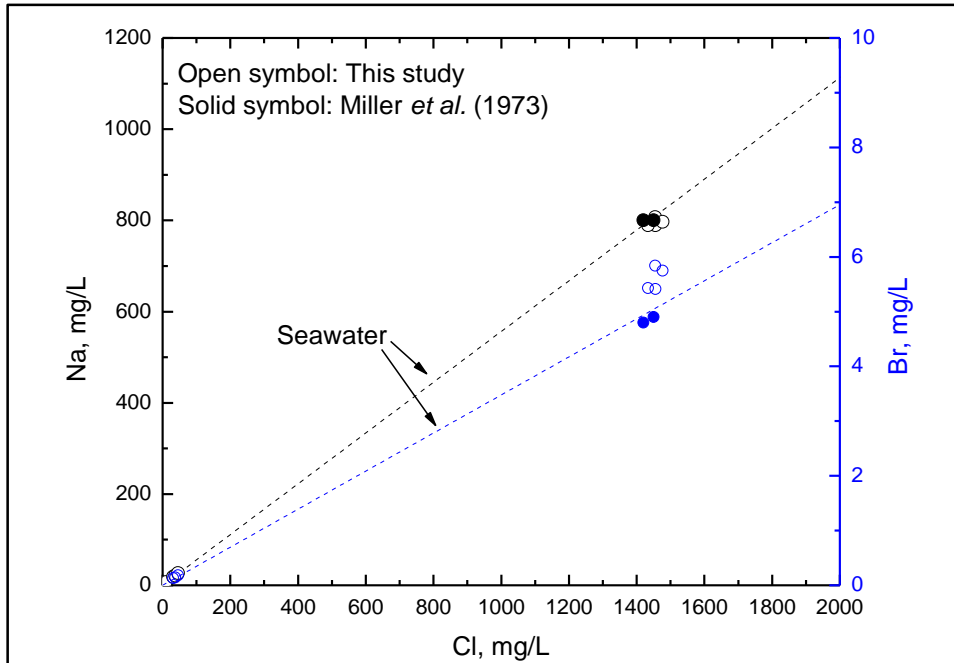


Figure 9. Plot of Na and Br concentrations relative to Cl concentrations with seawater dilution lines for each. Data from Miller *et al.* (1973, closed circles) is included for comparison. Hot spring compositions are those with about 1450 mg/L of Cl. Seawater composition is about 19,800 mg/L Cl, 422 mg/L Na, and 4.55 mg/L Br.

Table 4. Saturation indices calculated with the WATEQ4F code (Ball and Nordstrom, 1991).

Site ID	Sample Location	Saturation Index	
		Calcite	Fluorite
1	Serpentine Hot Spring	0.1	0.2
2	Arctic Hot Springs - above old bath house	0.0	0.2
3	Arctic Hot Springs - upper site	-0.6	0.5
4	Cold water intake for bath house	0.1	0.2

Temperature and Conductance Profile of Diversion Ditch Water

During a field survey of the diversion ditch that brings water from Hot Springs Creek to cool the hot spring water to a temperature suitable for bathing, a thermal anomaly was found. Consequently, a series of temperature and conductivity measurements were made along the diversion ditch and these results are shown in Table 5. Figure 10 shows the measurement locations along the diversion ditch with the corresponding temperature measurements in degrees Celsius. At about 8 meters from the separation of the diversion ditch water from Hot Springs Creek a temperature maximum of 58°C was measured. This observation indicates seepage of thermal water branches off to the east of Serpentine Hot Springs. The hot seepage in the gravel bar should be taken into consideration in planning any further construction in the area.

Table 5. Field measurements of temperature and specific conductance along cold water diversion ditch from Hot Springs Creek to the bathhouse.

Distance from Hot Springs Creek m	Temperature °C	Conductivity $\mu\text{S}\cdot\text{cm}^{-1}$ at 25 °C
0	48.9	4670
4	53.9	4680
8	58.3	4640
11	47.7	4660
15	44.2	4700
18	43.1	4740
21	42.8	4750
24	45.7	4730
28	43.7	4760
31	42.8	4710
34	40.8	4730
37	39.5	4810
40	37.5	4830

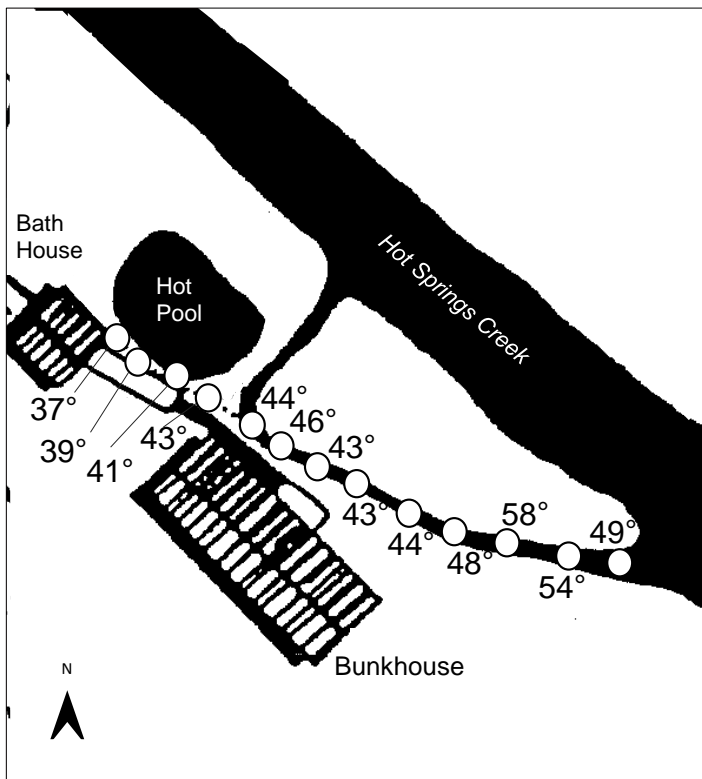


Figure 10. Enlargement of sketch map from Gary Rosenlieb (NPS, written commun., 1998) shows field measurement locations (open circles) for temperature and specific conductance. Number next to circle is the temperature in degrees Celsius. Distance between sample sites is 3-4 meters.

Stable Isotope Hydrology

In midsummer 2010 we collected water samples for stable isotope analysis at 37 sites in the Serpentine Hot Springs catchment (Table 1), including 4 hot-spring orifices and 25 other sites distributed in the Hot Springs Creek watershed between Arctic Hot Springs and the continental divide (Figure 11 and Table C-3). Here we briefly review some elements of stable-isotope hydrology before describing the 2010 stable-isotope sampling results and preliminary interpretations.

Overview: Stable Isotope Hydrology as applied to Geothermal Waters

Oxygen- and hydrogen-isotope data from water and rocks provide convincing evidence that most geothermal (hot spring) waters are mainly meteoric (atmospherically derived) fluids, and that meteoric fluids can circulate to midcrustal depths (as deep as ~10 km) in tectonically active continental crust. This conclusion is based on the isotopic composition of precipitation (Craig, 1961a), of geothermal waters (Craig, 1963), and of igneous rocks (Taylor, 1968).

There are two stable isotopes of hydrogen: ^1H and ^2H (deuterium or D) and three of oxygen: ^{16}O , ^{17}O , and ^{18}O , of which ^{16}O and ^{18}O are the more abundant. Because the vapor pressure of water molecules is inversely proportional to their masses, water vapor is depleted in the heavier isotopes, D and ^{18}O , relative to coexisting liquid water (e.g., Faure, 1986). The D and ^{18}O content of water is usually reported in “ δ -notation” relative to Craig’s (1961b) Standard Mean Ocean Water (SMOW):

$$\delta = [(R_{\text{sample}} / R_{\text{SMOW}}) - 1] \times 1000 \quad (1)$$

where R is the D/H or $^{18}\text{O}/^{16}\text{O}$ ratio and the units of δ are permil (‰). Craig (1961a) showed that meteoric waters worldwide define the relation $\delta\text{D} = 8\delta^{18}\text{O} + 10$ (Figure 12), with δD and $\delta^{18}\text{O}$ values becoming increasingly more negative at higher latitudes.

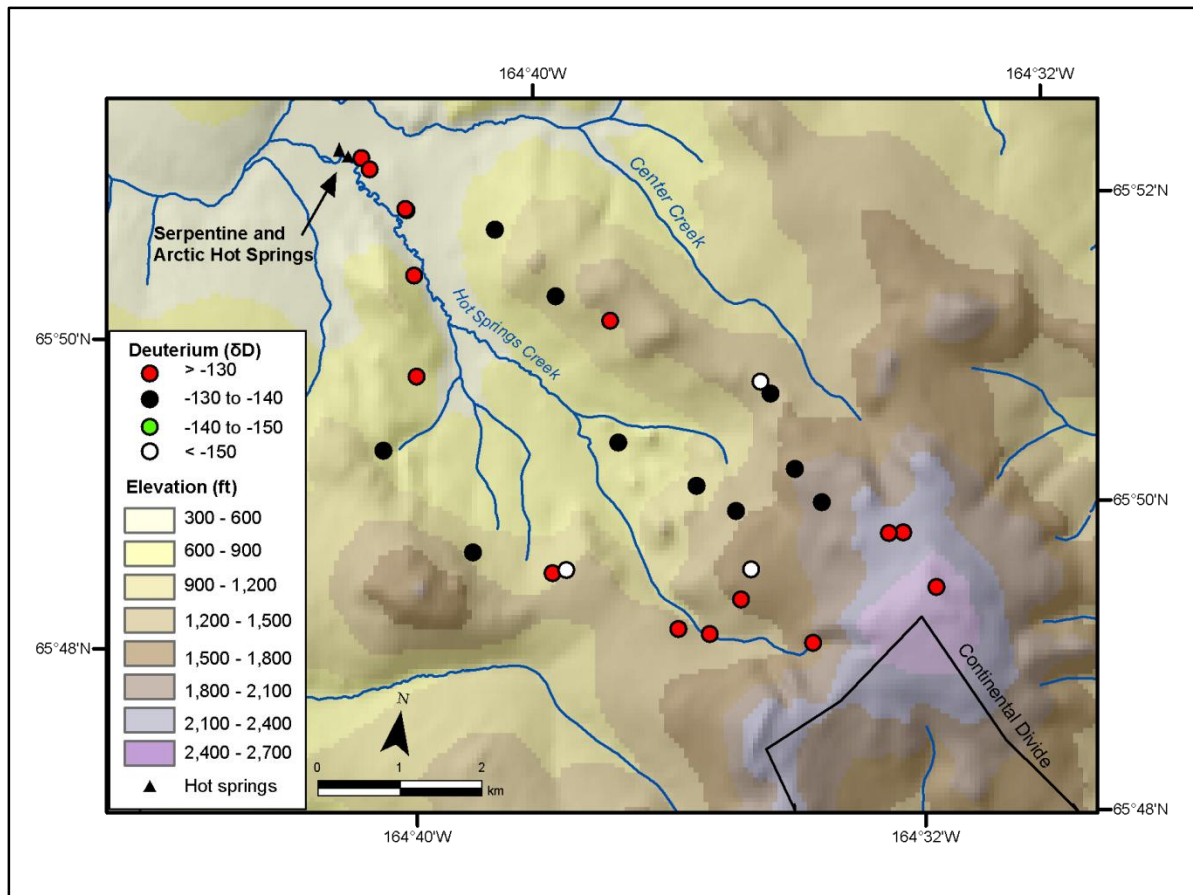


Figure 11. Stable isotope sample locations and deuterium (δD) content of samples acquired in the Serpentine Hot Springs area, midsummer 2010.

In general, the water vapor in an air mass becomes progressively more depleted in heavier isotopes as precipitation falls from it. The mean isotopic composition of precipitation at a particular location is approximately constant over time periods that are long enough to minimize the effect of seasonal variations and short enough to preclude significant climate change. Characteristic spatial variations in isotopic composition are often used to infer groundwater recharge areas, indicate mixing, or delineate different groundwater systems (e.g., Scholl et al., 1996; Kendall and McDonnell, 1998).

Most groundwater samples, like precipitation, lie near the “global meteoric water line” defined by $\delta D = 8\delta^{18}O + 10$, but high-temperature geothermal waters are sometimes an exception. Near-neutral-pH geothermal waters that have been heated to temperatures in excess of about 150°C frequently show an “oxygen shift” away from the meteoric water line toward an increasing abundance of the heavier isotope, ^{18}O . This phenomenon is due to oxygen-isotope exchange between water and rock at elevated temperatures (Craig, 1963). The hydrogen-isotope values of the water remain largely unaffected because of the low hydrogen content of most rocks (relative to H_2O). A hypothesized link between the oxygen-isotope composition of geothermal waters and hydrothermally altered rock was confirmed by Taylor (1968), who found that the original $\delta^{18}O$ composition of igneous rocks is typically 5.5 to 7 ‰ (versus -2 to -17 ‰ for groundwaters) but that many hydrothermally altered

igneous rocks are depleted in ^{18}O due to exchange with meteoric waters. Thermal waters also experience a shift in $\delta^{18}\text{O}$ and D because of boiling at depth and evaporation at the surface (Figure 12). Mixing with dilute surface waters or shallow groundwaters will bring the water isotopes back closer to meteoric values.

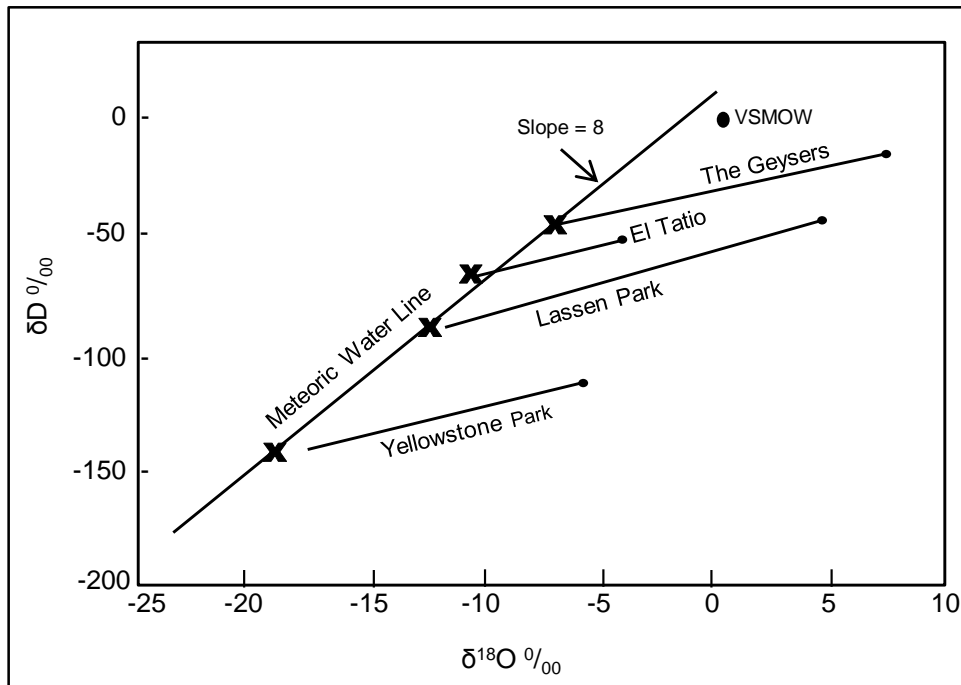


Figure 12. Relation between deuterium (δD) and oxygen-18 ($\delta^{18}\text{O}$) contents, showing the meteoric water line (Craig, 1961a) with a slope of 8, Vienna Standard Mean Ocean Water (VSMOW) and typical fractionation for geothermal waters that have undergone evaporation with a slope of approximately 3 (Craig, 1963; Panichi and Gonfiantini, 1977).

Serpentine-area Stable Isotope Data Interpretation

Deuterium (δD) values in the study area range from about -161 to -119 and $\delta^{18}\text{O}$ values from about -21 to -15. The samples generally fall near the global meteoric water line defined by $\delta\text{D} = 8\delta^{18}\text{O} + 10$ (Figure 13). The hot-spring waters have relatively small “oxygen shifts” of only about 1 ‰, perhaps because they do not attain very high temperatures at depth. Chemical geothermometers are estimates of the geothermal reservoir temperature based on the chemical composition of dissolved solutes in thermal waters and their assumed temperature-dependent equilibria with common minerals or gases found in most rock types such as feldspars, quartz, micas, and anhydrite (Fournier, 1977; Giggenbach, 1981; Reed and Spycher, 1984). Mean chemical-geothermometer temperature estimates for the hot-spring waters are only $\sim 127 \pm 3$ °C (Table 6).

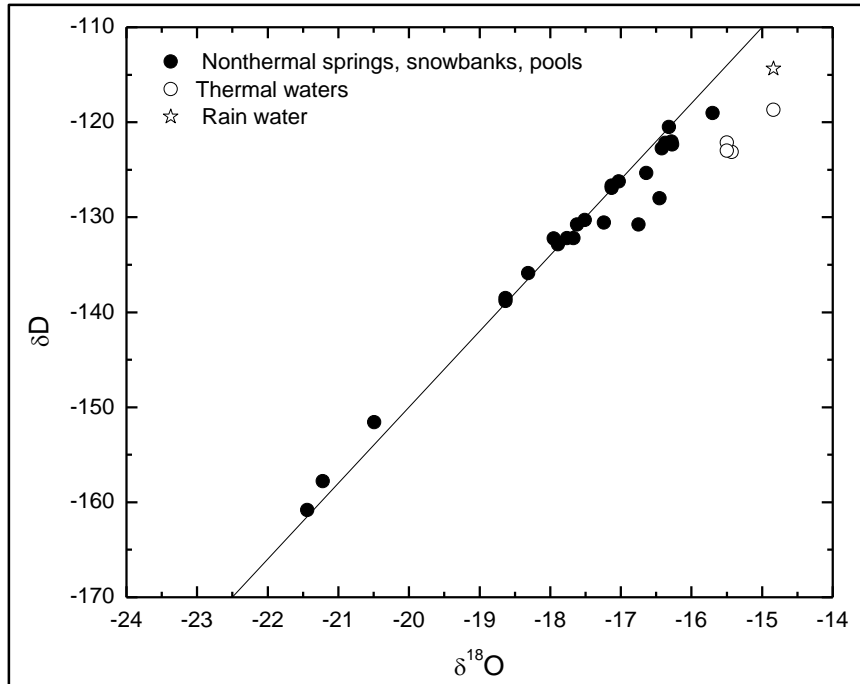


Figure 13. Relation between deuterium (δD) and oxygen-18 ($\delta^{18}O$) contents for samples acquired in the Serpentine Hot Springs area, midsummer 2010, relative to the global meteoric water line (Craig, 1961).

Table 6. Chemical geothermometer results for the four hottest waters sampled using equations listed in Fournier (1991).

Site ID	1	2	3	4
Description	Serpentine Hot Spring	Arctic Hot Springs - above old bath house	Arctic Hot Springs - upper site	Cold water intake for bath house
Geothermometer	t/°C	t/°C	t/°C	t/°C
Quartz-no steam loss	125	126	124	126
Quartz-maximum steam loss	123	123	121	123
Chalcedony	97	98	96	98
Na/K, Fournier (1983)	160	159	166	160
Na/K, Truesdell (1976)	119	118	126	118
Na/K, Tonani (1980)	123	121	130	122
Na/K 25-250 °C, Arnorsson (1983)	129	128	136	129
Na/K, Nieva and Nieva (1987)	148	147	154	148
Na/K, Giggenbach et al. (1983)	179	178	185	178
Median	125	126	130	126
Median Absoluted Deviation	9	12	13	11

Isotope compositions for some of the non-thermal waters lie to the right of the meteoric water line along a slope of ~ 5 (Figure 13), a signature that often indicates evaporation. Evaporated waters are fairly common in permafrost terrane (e.g. Yoshikawa and Hinzman, 2003, their Figure 6).

In nearly every region of the world, δD and $\delta^{18}O$ values decrease with elevation (Poage and Chamberlain, 2001). Well-constrained isotopic lapse rates in the western United States range from $-10 \text{ ‰ } \delta D/\text{km}$ in windward Hawaii (Scholl et al., 1996) to $-40 \text{ ‰ } \delta D/\text{km}$ on the west flank of the Sierra Nevada, California (Friedman and Smith, 1970). Such systematic variability is often used to estimate the recharge provenance of thermal waters (e.g. Ingebritsen et al., 1989). However, the δD data from the Serpentine area, which span an elevation range of $\sim 0.5 \text{ km}$, show no statistically significant correlation with elevation (Figure 14). The hot-spring waters are among the heaviest (least depleted) in deuterium (Figures 13 and 14), but similarly heavy waters can be found both in low-elevation seeps south of the hot springs and on the continental divide (Figures 11 and 14).

Any explanation of the stable isotope data from the Serpentine area must consider the unusual hydrogeology of permafrost terrane. This part of the Seward Peninsula is considered to have “continuous” permafrost (Woo, 1986). At Kougurok, about 50 km south of Serpentine Hot Springs, the continuous permafrost is known to be 15-50 m thick, overlain in summer by an active (unfrozen) layer about 0.5 m thick. Permafrost is generally considered to be an aquiclude, greatly inhibiting exchange between the active layer and subpermafrost groundwater. However, even on the North Slope of Alaska – another area of continuous permafrost – subpermafrost groundwater flow redistributes geothermal heat (Deming et al., 1992) and indicates some degree of exchange between shallow and deep groundwater. Such exchange may be focused in taliks (unfrozen zones) that connect subpermafrost groundwater with the active layer and can be maintained by perennial streams, ponds, or upflow of warm groundwater (Woo, 1986).

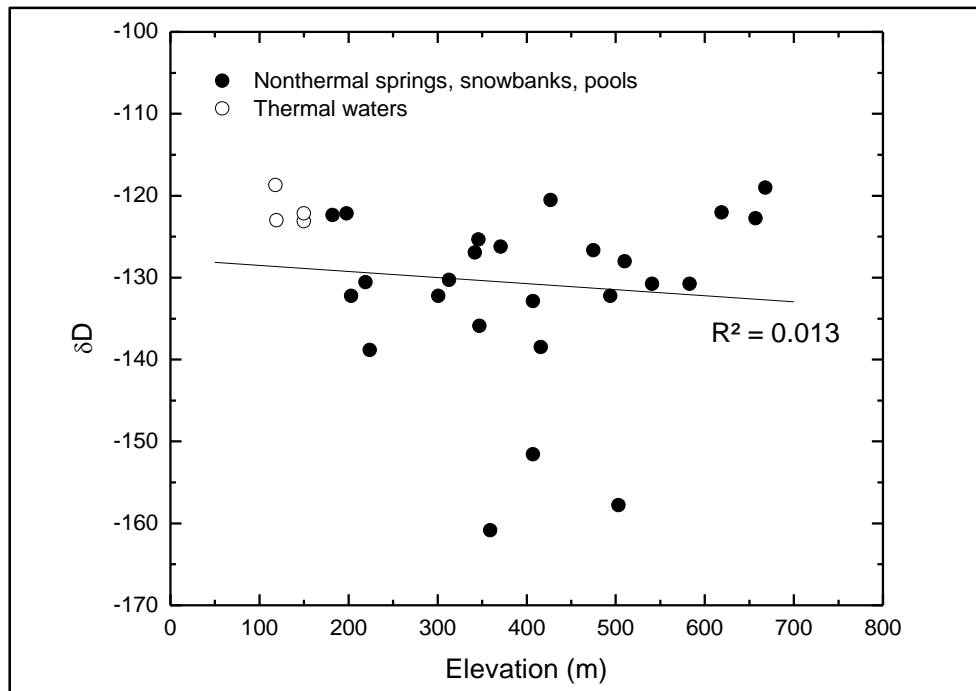


Figure 14. Relation between deuterium (δD) content and elevation for samples acquired in the Serpentine Hot Springs area, 2010.

What might account for the lack of an isotopic lapse rate in the Serpentine Hot Springs area?

Downslope flow of suprapermafrost groundwater in the active layer (Woo, 1986) would tend to obscure any systematic lapse rate that does exist, as would scouring of snow from exposed ridges towards shrubby slopes, a process that is known to be hydrologically significant on the Seward Peninsula (Hinzman et al., 2003). Further, the low precipitation near Serpentine Hot Springs would accentuate the isotopic influence of relatively chaotic extreme events (precipitation is only ~18 cm/year at Kougarak; Hinzman et al., 2003). The limited International Atomic Energy Agency (IAEA) isotopic data from western Alaska and easternmost Russia indeed suggests large variability in isotopic composition on a monthly to annual time scale (online data from IAEA stations Adak, Barrow, Bethel, Cherskiy, Mayo). Each of these factors would tend to obscure any systematic isotopic lapse rate.

The isotopic data suggest that the thermal waters are of meteoric and possibly local origin and, consistent with the geothermometer estimates, never attained temperatures much in excess of 150°C. Because of the semi-continuous permafrost, recharge to the subpermafrost groundwater system is likely localized, rather than widely distributed. However, in the absence of a local isotopic lapse rate (Figure 14), the thermal waters cannot be linked to any particular recharge elevation or locality.

Both the Na/Cl and Br/Cl ratios of the thermal waters (Figure 9) and their isotopic composition (Figure 13) are compatible with the suggestion that the hot springs contain a seawater component. A ~7% seawater component would fit the chloride data and would also account for the 10-12 ‰ deuterium shift between the thermal waters and the mean of the nonthermal waters (Figure 13).

Hydrologic Discharge and Chloride Load

Hot Springs Creek

Stream velocity-area measurements were made in the north and south forks of Hot Springs Creek above an area pooled by beaver dams, in Hot Springs Creek above and below the bathhouse and bunkhouse, in the flow that was diverted by the beaver dams just before it rejoined Hot Springs Creek, and in Hot Springs Creek just below Arctic Hot Springs (Figure 7, sites 5, 6, 7, 9, 10 and 12). The discharge value for each of these locations is shown in Table 7.

Table 7. Discharge values for key locations along Hot Spring Creek

Site ID	Location	Discharge, L s ⁻¹	
		Hot Springs Creek	Inflows/loss
5	Hot Springs Creek - North Fork		323
6	Hot Springs Creek - South Fork		118
	Downstream of the North and South Fork Confluence	441 ^A	
	Beaver Dam diversions		-121 ^A
7	Hot Springs Creek - upstream from bath house	320	
9	outflow from bath house / stream south of bath house		142
10	Hot Springs Creek - about 200 m downstream from bath house	486	
12	Hot Springs Creek - downstream from Arctic Hot Springs	461	

^Acalculated values

Hourly conductance-temperature-depth measurements were obtained from Hot Springs Creek below Serpentine and Arctic Hot Springs (Figure 15). During the duration of the study, the depth of Hot Springs Creek varied by 6-8 cm as a result of intermittent precipitation. Conductivities decreased with increasing stream height from 220 to 136 $\mu\text{s}\cdot\text{cm}^{-1}$ below Serpentine Hot Spring and from 313 to 191 $\mu\text{s}\cdot\text{cm}^{-1}$ below Arctic Hot Springs (Figure 16). The curves shown in Figure 16 are mixing lines that result from two-end-member mixing between a high conductivity water and a low conductivity water.

The temporal variation of discharge below Serpentine and Arctic Hot Springs was approximated by assuming the stream velocity remained constant and only the cross-sectional area varied during the duration of the study. This approach likely underestimates the maximum discharge and overestimates minimum discharge, but nonetheless allows the measured variation in stream height to be converted to a record of discharge during the study. The maximum, minimum, and mean discharges from the two stream sites are shown in Figure 17.

Figure 17 also shows the discharge of Hot Springs Creek along with the inflows from the north and south forks, the geothermal inputs from Serpentine and Arctic Hot Springs, and return flow from the bathhouse. Approximately 120 L·s⁻¹ (or 25%) of the flow in Hot Springs Creek was diverted around the bathhouse as a result of the extensive series of beaver dams, as determined by the difference between the sum of north and south forks and the measurement in the main stem just upstream from the bunkhouse. This value compares well with the measurement of 142 L·s⁻¹ for the return flow just

west of the bathhouse. About 95% of the combined discharge was accounted for downstream of Serpentine Hot Springs.

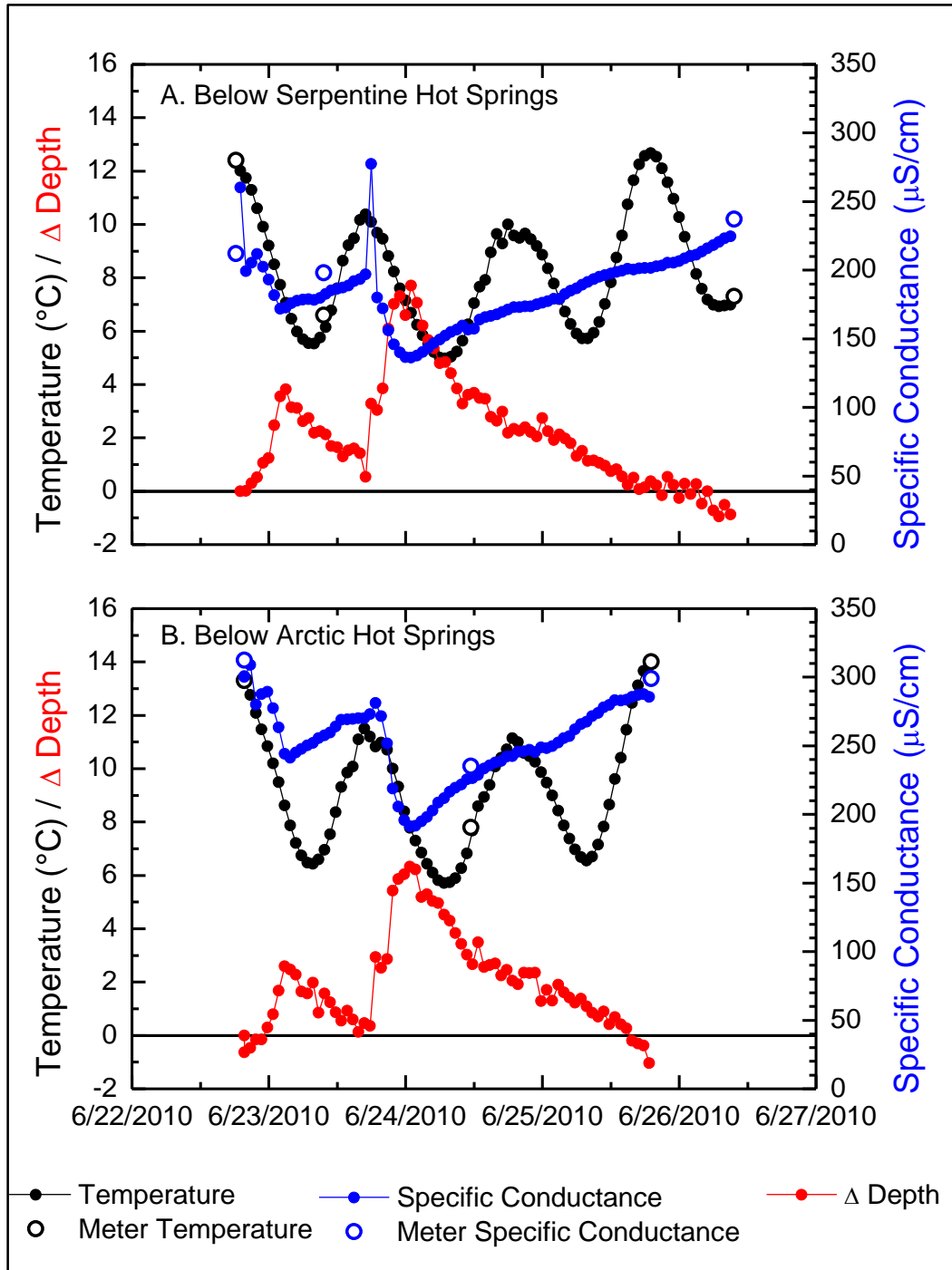


Figure 15. Midsummer 2010 conductance-temperature-depth records from Hot Springs Creek below Serpentine Hot Springs (A) and below Arctic Hot Springs (B).

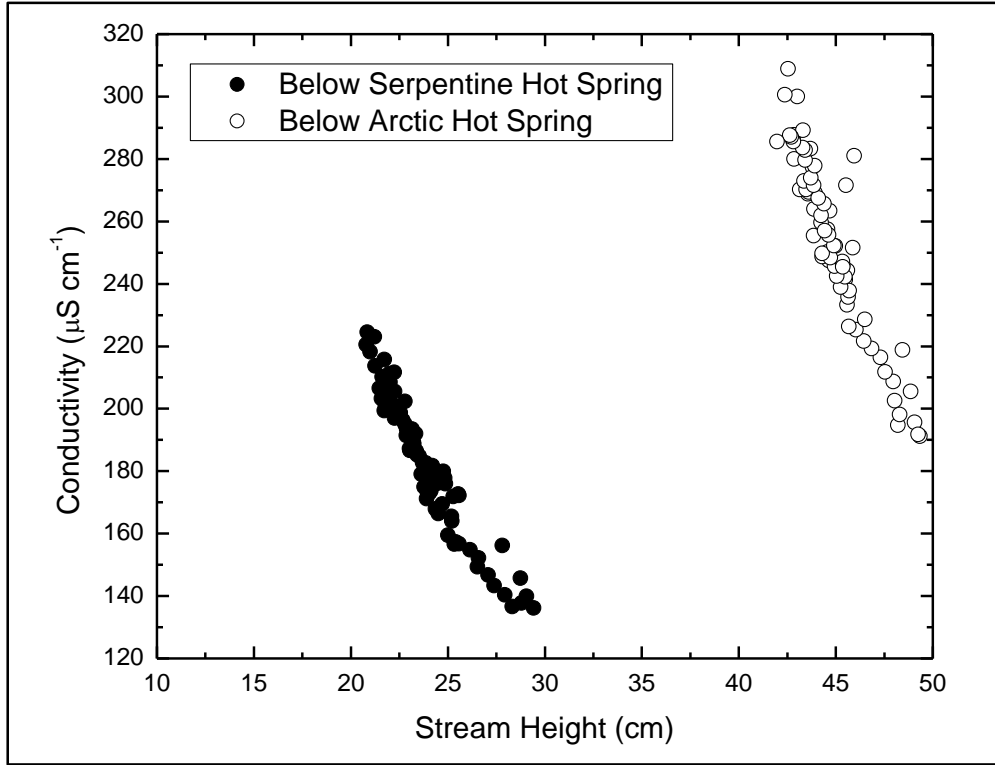


Figure 16. Plot of conductivity against stream height in Hot Springs Creek below Serpentine and Arctic Hot Springs discharges, 2010.

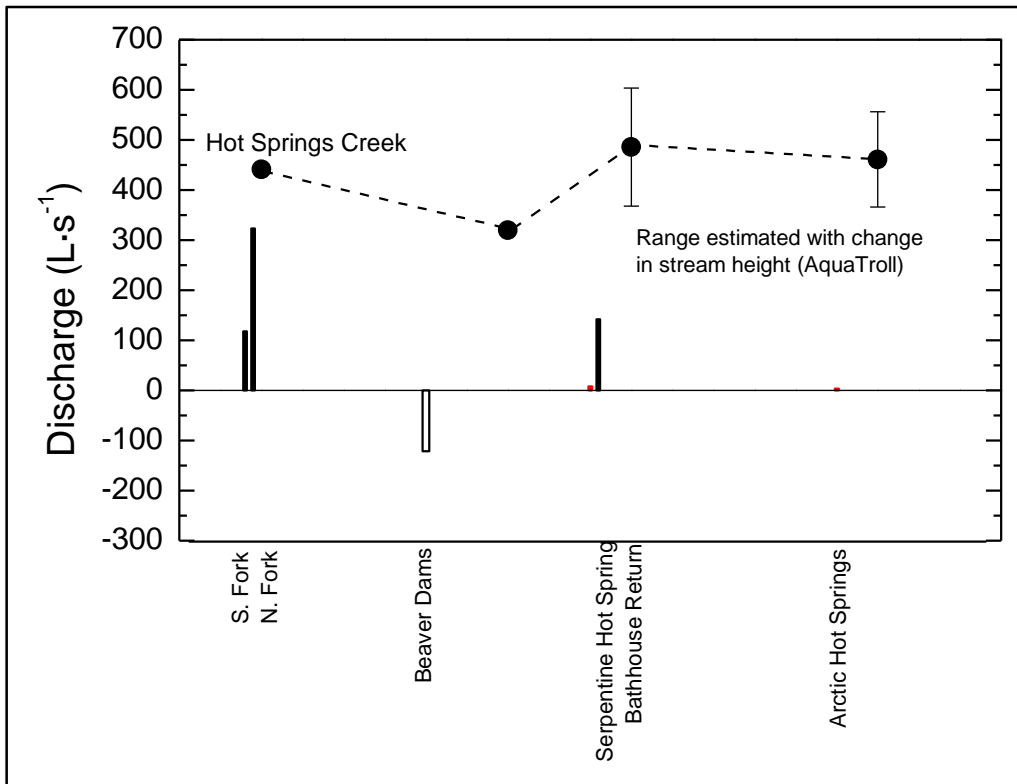


Figure 17. Discharge plotted against downstream distance.

Serpentine and Arctic Hot Springs

Most hot-spring discharge areas include numerous vents, some of which may be beneath streams or lakes or otherwise inaccessible, so that measurements of individual vents can rarely succeed in capturing the total hydrothermal discharge. However, most hot springs, like Serpentine Hot Springs, occur in valleys, near streams that eventually capture most of the thermal fluid. Thus their total discharge can often be gauged by measuring the flux of a geothermal solute in the streams (Ellis and Wilson, 1955). Chloride is the most commonly used indicator of thermal-spring discharge because it behaves conservatively in solution and because thermal waters are usually much higher in chloride than nearby surface water and/or shallow groundwater. In midsummer 2010, chloride concentrations in Serpentine Creek above the hot springs were 3-4 mg/L and chloride concentrations in the thermal waters were ~1450 mg/L, providing a strong contrast (Table 3). Although other ions present in elevated concentrations in thermal waters (e.g., As, B, Na, SO₄) can be used in solute inventories, they are much more likely to be affected by reactions in streams or the shallow subsurface.

The discharge from Serpentine Hot Springs and Arctic Hot Springs was calculated using two independent approaches (Table 8). Both approaches are based on mass balance. The first approach was the Cl-flux method (Figure 18) using the equation

$$Q_{HS} = (\Delta Cl_{stream} Q_{stream}) / Cl_{HS} \quad (1)$$

Because the difference in discharge between upstream and downstream sites is less than the error of the measurement, the median discharge and Cl concentration from Hot Springs Creek below Serpentine and Arctic Hot Springs were used to calculate the hydrothermal inputs.

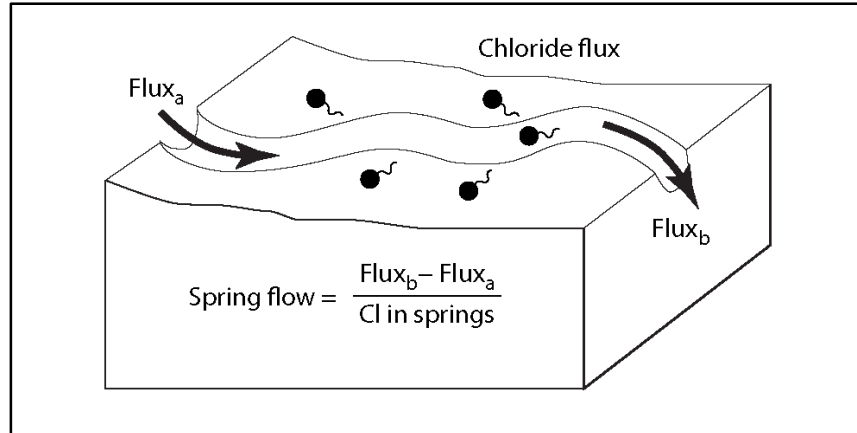


Figure 18. Block diagram illustrating chloride-flux method of measuring thermal-spring discharge. The difference between chloride flux upstream ($Flux_a$ or Q_a , g/s) and downstream ($Flux_b$ or Q_b) of a thermal-spring group is divided by the chloride concentration in the thermal-spring waters (Cl_{HS} , g/L) to determine thermal-spring discharge, Q_{HS} (L/s). That is, $Q_{HS} \sim (Q_s[Cl_b - Cl_a] / Cl_{HS})$, assuming that $Q_{HS} \ll Q_s$ and $Cl_{HS} \gg Cl_a$ or Cl_b , where Q_s is stream discharge, Cl_a and Cl_b are stream chloride concentrations above and below the thermal springs, respectively, and Cl_{HS} is the chloride concentration in the thermal springs themselves.

Table 8. Estimates of hot spring discharge by two methods.

	Discharge (L·s ⁻¹)	
	Cl flux	Conductivity
Serpentine Hot Springs	10	10
Arctic Hot Springs	4	5
Total Geothermal	14	15

The second approach was to use the conductivity to approximate the fraction of flow contributed by the hot springs and nonthermal river water. Chloride concentrations are positively correlated with conductivity in Hot Springs Creek (Figure 19). Using this correlation, instantaneous chloride concentrations can be calculated from the continuous conductivity measurements obtained downstream of Serpentine and Arctic Hot Springs. When the fraction of river water is 0, the conductivity is equal to the conductivity of Serpentine Hot Springs. And when the fraction of the river is 1, the conductivity is equal to the conductivity of the river upstream of any geothermal inputs (Figure 20). The two approaches produced similar results (Table 8) as expected because chloride is

the dominant contributor to the conductivity. About two-thirds of the thermal input in Hot Springs Creek comes from Serpentine Hot Springs.

The Cl load in Hot Springs Creek and the Cl load from the various inflows were determined (Figure 21). Downstream of the thermal areas, approximately 90% of the Cl load ($\sim 2000 \text{ kg d}^{-1}$) is hydrothermal even though only 3% of the water flow is hydrothermal.

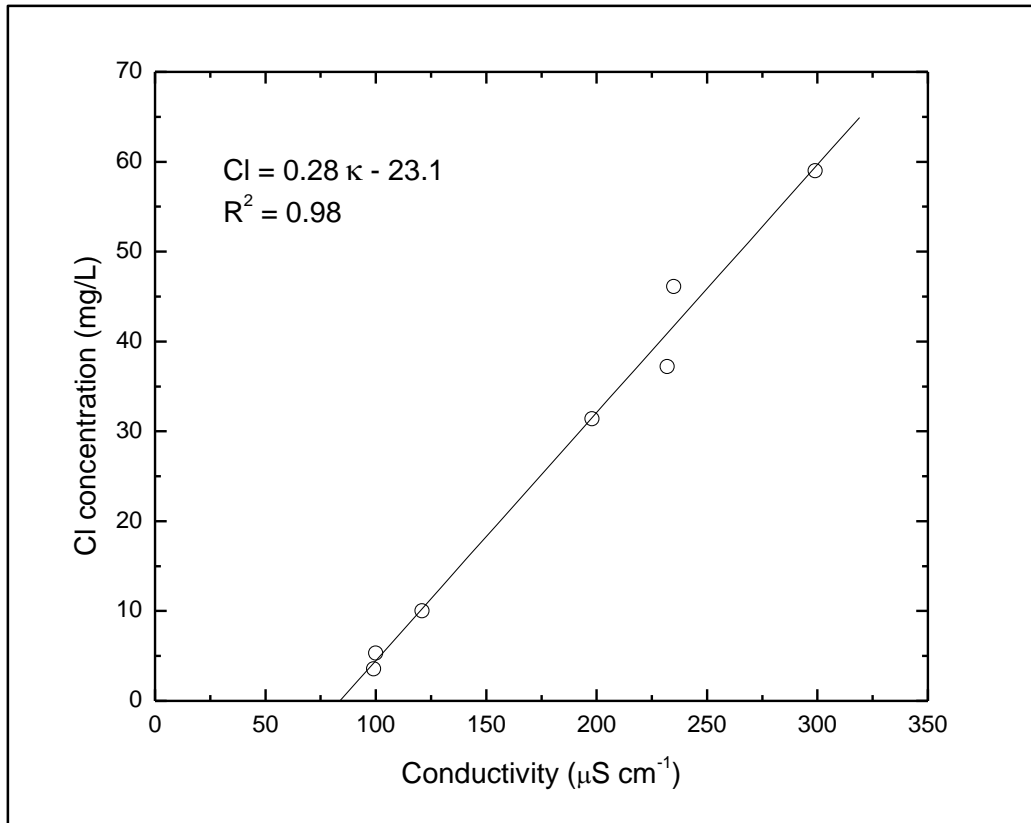


Figure 19. Plot of Cl concentrations against conductivity for Hot Springs Creek samples.

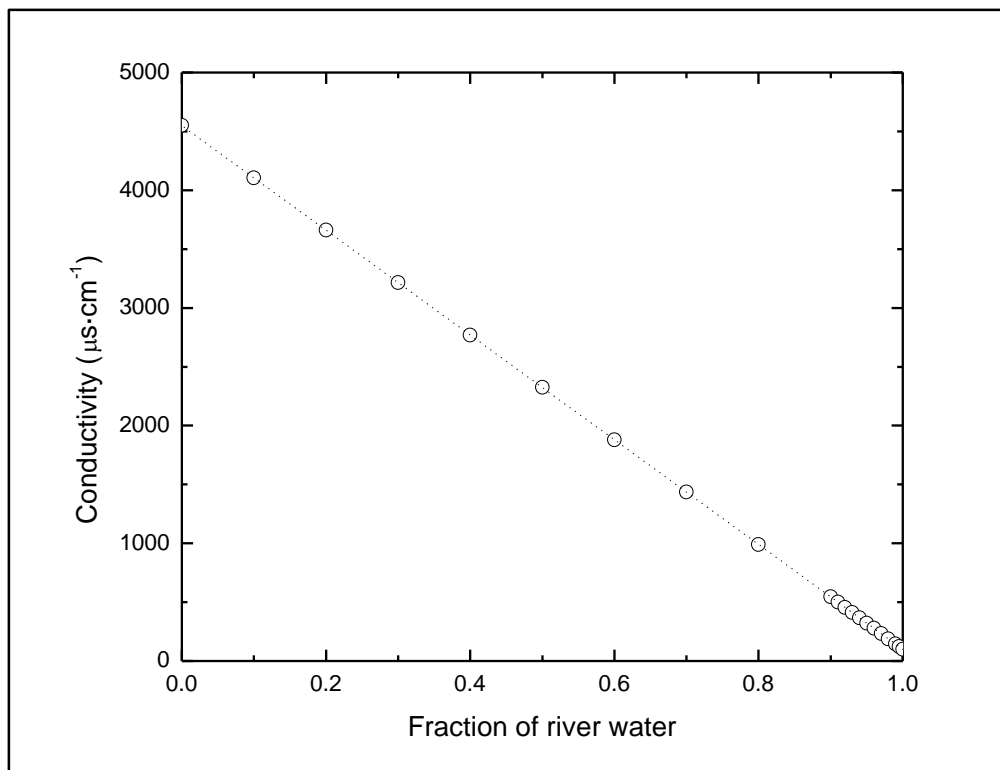


Figure 20. Plot of conductivity against the fraction of river water.

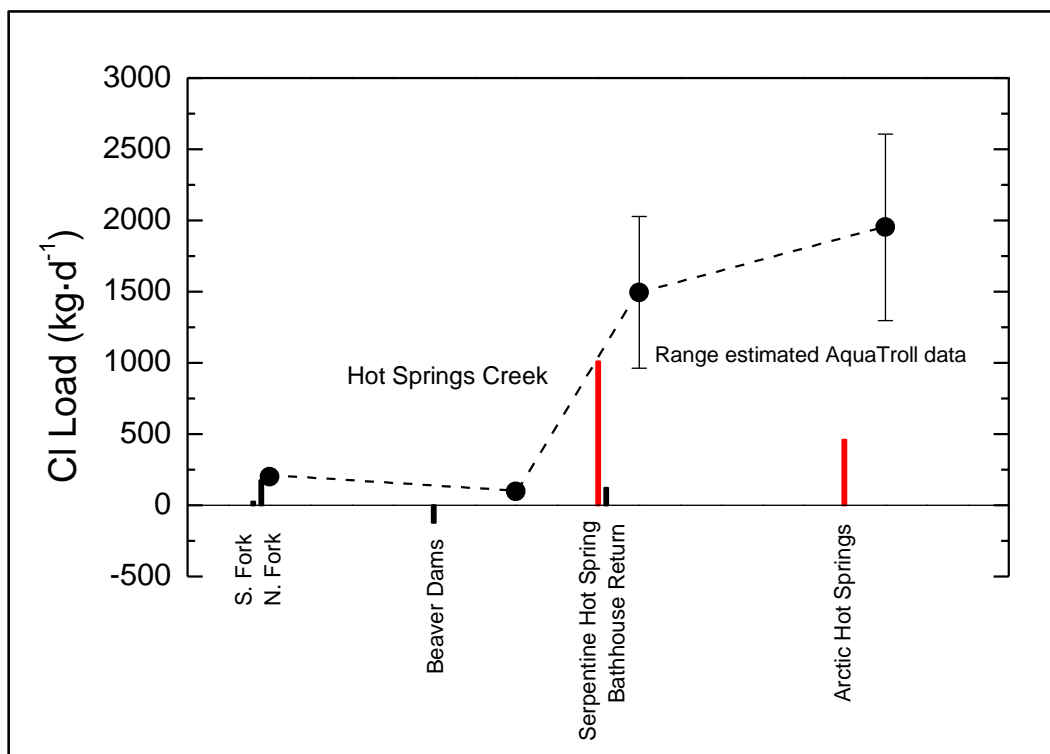


Figure 21. Chloride load plotted against distance with red bars showing the loading from the two hot spring areas.

Thermal Discharge

Overview: Thermal Inventories

A useful estimate of hot-spring heat discharge is given by

$$Q_{\text{thermal}} = Q_{\text{HS}} c(T_{\text{geo}} - T_{\text{rch}}), \quad (2)$$

where Q_{HS} is the hydrothermal discharge (Table 8), c is the specific heat of the fluid, T_{geo} is the maximum fluid temperature at depth, as determined by chemical geothermometry or other means, and T_{rch} is the recharge temperature (assumed to be 0°C on the Seward Peninsula). As thus defined, Q_{thermal} is a measure of the heat advected away from depth, rather than the heat discharged directly by the thermal springs; hot-spring discharge temperatures (up to $\sim 75^{\circ}\text{C}$ at Serpentine) are often much less than T_{geo} , due to conductive, advective, or radiative heat loss as the fluid rises from depth toward the thermal-spring orifices.

Chemical geothermometers estimate the temperature of water-rock equilibrium at depth, based on the temperature-dependent solubility of silica, various cation ratios that reflect temperature-dependent chemical equilibria, isotopic equilibria, and gas equilibria. Application of various standard silica and cation geothermometers to the Serpentine Hot Springs waters yields subsurface temperature estimates of $\sim 100\text{-}185^{\circ}\text{C}$ (Table 5). Both discharge and geothermometer temperatures for Serpentine Hot Springs are the highest observed in central or western Alaska (Miller et al., 1973, 1975).

USGS hydrothermal-monitoring data spanning several decades indicate fairly steady discharge from most high-chloride hot-spring systems in the western United States, although frequent measurements often reveal sensitivity to local hydrologic conditions, sometimes expressed as seasonal variability (Ingebritsen et al., 2001; Ingebritsen and Mariner, 2010). This general “steadiness” of continental hydrothermal systems is in marked contrast to mid-ocean ridge systems, which seem to exhibit much more short-term variability (cf. Von Damm et al., 1997). The absence of decadal-scale variability in continental systems seems sensible in light of the longevity of the probable heat sources and the likely spatial and temporal scales. Likely flow-path lengths range from a few kilometers to tens of km, likely fluid travel times are on the order of 10^2 to 10^4 years (Ingebritsen et al., 1994), and the heat sources for magmatically based systems are large enough to retain significant heat for 10^4 to 10^6 years (Smith and Shaw, 1975, 1979; Hayba and Ingebritsen, 1997). Continental hydrothermal systems differ in these respects from the dynamic subsea hydrothermal systems associated with shallow magmatism along the mid-ocean ridge

Serpentine-area Thermal Discharge

Several days of continuous (hourly) conductance-temperature-depth data from Hot Springs Creek in midsummer 2010 suggest that chloride-flux-based estimates of hydrothermal discharge will be sensitive to local hydrologic conditions, and therefore time-dependent. For instance, brief intermittent precipitation on 24-25 June raised stream levels by 6-8 cm and decreased specific conductance by $\sim 70 \mu\text{S}/\text{cm}$ ($>25\%$) (Figure 15). We have sufficient data for a single estimate of hot-spring mass and heat discharge, but insufficient data to estimate temporal variability. Whereas hydrothermal upflow from great depth can reasonably be supposed to be steady, its mixing with the unsteady shallow hydrologic system is a transient process. Confident estimates of the variability in

hydrothermal discharge will require extended conductance-temperature-depth records complemented by calibration samples and measurements.

Using an average total hot spring discharge value of 14 L/s from Table 8 and equation 2, the associated hydrothermal heat discharge is $\sim 5 \text{ MW}_t$ (MW of thermal output) based on the maximum observed discharge temperature of $\sim 75^\circ\text{C}$ (Appendix Table C-1) or $\sim 8 \text{ MW}_t$ based on a geothermometer temperature of $\sim 126^\circ\text{C}$ (Table 5). For comparison, thermal outputs from individual hot-spring systems of the Cascade Range volcanic arc range from <1 to $\sim 100 \text{ MW}_t$ and the thermal output of the entire Yellowstone hydrothermal system is about $6,000 \text{ MW}_t$ (Ingebritsen et al., 2001). Global experience with geothermal-electrical-power production indicates that electrical-power potential in MW electricity (MW_e) is typically in the range of 0.1 to 10 times the natural heat output in MW_t (Richards and Blackwell, 2002).

It is useful to compare the measured hydrothermal heat discharge from Serpentine Hot Springs to the likely conductive heat input to the contributing watershed. The area of the surface catchment upstream from Serpentine Hot Springs is $\sim 30 \text{ km}^2$. There are no actual conductive-heat-flow data on the Seward Peninsula and the nearest datum, more than 250 km north of Serpentine Hot Springs on Cape Thompson, indicates a heat flux of 0.06 W/m^2 (Deming et al., 1992). However, existing heat-flow maps (http://smu.edu/geothermal/heatflow/Alaska_hf.gif) suggest a much higher conductive heat flux of about 0.1 W/m^2 for the Seward Peninsula – a reasonable value for a region of Late Cenozoic volcanism and extensional tectonics (cf. Ingebritsen et al., 1989). Assuming a heat flux of 0.1 W/m^2 yields a conductive heat flow of 3 MW_t for the surface catchment. This value is less than the measured hydrothermal heat loss and represents the maximum capture of conductive heat flux that could be achieved via a subhorizontal aquifer system that sweeps heat from the entire catchment. Hydrothermal heat output in excess of the likely conductive heat input suggests the possibility of a subsurface flow system that extends well beyond the surface catchment, or a cryptic magmatic heat source that augments the expected conductive heat flux. The latter possibility can be explored via sampling of helium and carbon isotopes, which can indicate magmatic contributions. In particular, ^3He comes only from the mantle (magma) whereas ^4He is produced by radioactive decay in the crust. A single He-isotope sample collected on 12 July 2011 at Arctic Hot Springs (Table 1, Figure 7, site 3) yielded a $^3\text{He}/^4\text{He}$ ratio of $R/R_a = 0.343$ (Andy Hunt, U.S. Geological Survey, written comm., 2012). This is a relatively low ratio for a hot spring in western North America and does not support the existence of a cryptic magmatic heat source. Instead, it lends credence to the suggestion that the subsurface contributing area is more areally extensive than the surface catchment.

Microbiology and its Relation to Human Activity

Introduction

When assessing water quality in relation to human health, total and fecal coliform bacteria levels are often measured. Coliform bacteria are commonly found in the environment (e.g., soil or vegetation) and are generally not harmful. However, at very high levels, total coliform bacteria may include species capable of causing infection to humans. Fecal coliform bacteria are a sub-group of total coliform bacteria. Fecal coliform bacteria appear in great quantities in the intestines and feces of humans and animals. Confirmation of fecal coliform bacteria in water samples indicates recent

human and/or animal fecal contamination, which may pose an immediate health risk to anyone consuming the water. Disease symptoms may include diarrhea, cramps, and nausea. Both total and fecal coliform bacteria were enumerated in samples taken near and around the bathhouse and bunkhouse.

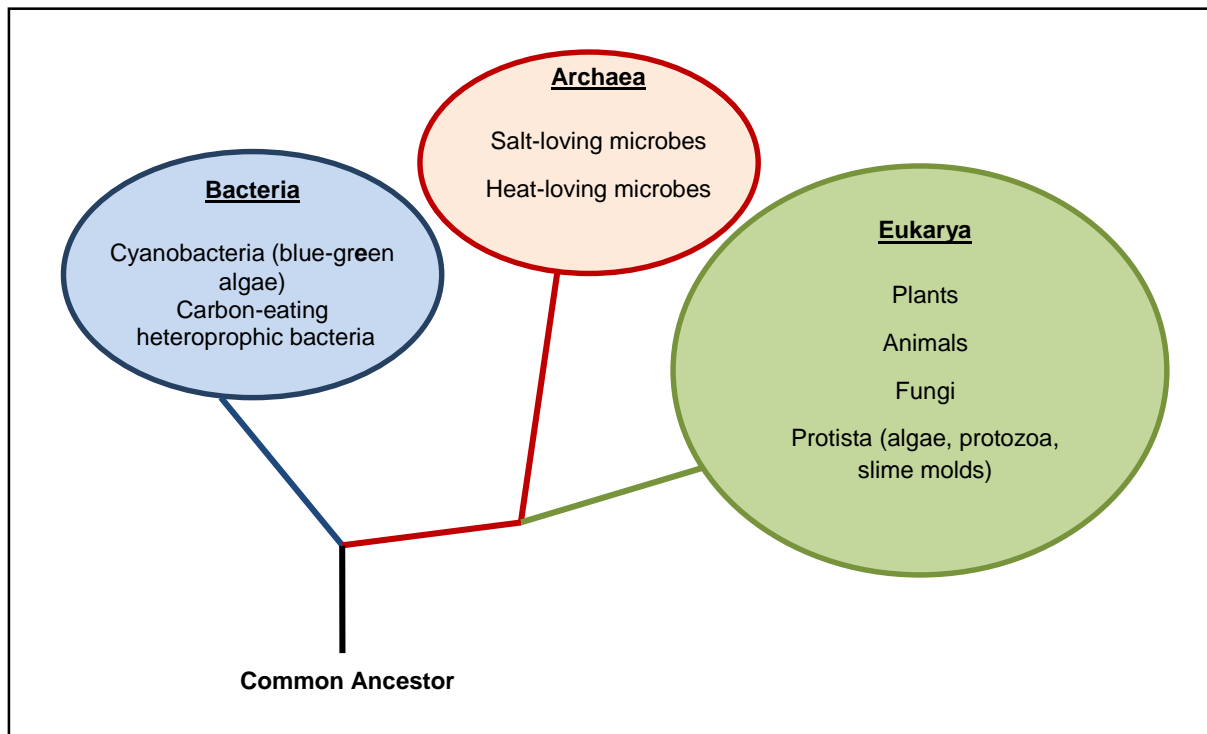


Figure 22. The Three Domains of Life classification system.

Molecular based techniques were also used as a more comprehensive tool to document total microbial diversity in addition to enumerating coliform bacteria. These data are presented using terminology that corresponds to microbial taxonomy currently in use. Life on Earth is commonly classified into 3 separate domains: *Bacteria*, *Archaea* and *Eukarya* (Figure 22) based on differences in 16S rRNA genes. The *Archaea* domain contains single celled organisms best known for their ability to survive in extreme environments, including hot springs and high salt environments. They also commonly occur in a wide variety of more hospitable habitats. While pathogenic species are fairly common in the *Bacteria* and *Eukarya* domains, pathogenic *Archaea* are not yet known to exist. Representatives from the *Bacteria* domain are present in most habitats and are considered to be much more common than *Archaea*. The *Eukarya* domain is distinguished from the *Bacteria* and *Archaea* domains in part by the presence of a cell nucleus. Although this domain includes plants, animals, fungi and protists, it represents a much smaller number of species than the other domains. With regard to the *Eukarya*, the current study focused on algae and protists, which are mostly unicellular eukaryotes such as protozoa (including amoebas) and slime molds.

Total and Fecal Coliform Bacteria

Total and fecal coliform bacteria counts and microbial phylogenetic diversity of waters upstream, downstream, and immediately adjacent to the structures were examined to assess the potential effects of human and animal activity in the vicinity of the bathhouse and bunkhouse (Figure 8). Though quite variable, total coliform bacteria (TC) counts were elevated in the four sampling sites closest to the structures (Figure 8: sites 38, 39, 40, 43), averaging $175 \pm 160/100$ mL (TC counts per 100 ml of sample) for all four sites (Table 9). Within Hot Springs Creek itself (Figure 8: sites 7 and 42), an area considered to experience less intensive human activity, TC counts averaged $30 \pm 10/100$ mL (Table 9). TC levels at site 8 (Figure 8) were of particular interest because the site was located upstream of the structures but downstream of an active beaver dam complex. This location was considered to be a potential TC source due to the beaver dam complex having a more focused and constant wildlife presence and activity. However, TC levels at site 8 were equivalent to levels measured at Hot Springs Creek sites 7 and 42 (Figure 8; Table 9). Results suggest that at the time of sampling the beaver dam complex was not a contributing factor to the elevated TC counts measured in the study area surrounding the bunkhouse.

Fecal coliform (FC) counts were relatively low at all sites and again variable. FCs at sites 38, 39, 40, 43 (locations surrounding the structures) averaged $3.8 \pm 4.3/100$ mL (Table 9) as compared to $2.0 \pm 1.4/100$ mL at sites 7 and 42 in Hot Springs Creek. Sites 8 and 38 displayed elevated FC levels ($6/100$ mL and $10/100$ mL, respectively; Table 9), suggesting that if FCs are being introduced in the area immediately surrounding the structures, their survival is short-lived. Based on these data, it appears that FC levels were within range of Alaska's bacteriological standards (<http://www.dec.state.ak.us/water/wqsar/index.htm>) for a drinking water supply (20 FC/100mL) and water recreation (100 FC/100mL). As the timing of this study did not correspond to peak seasonal human visitation, it is possible that the peak seasonal TC and FC counts may be higher.

Table 9. Total and fecal coliform bacteria in Hot Springs Creek upstream, downstream, and surrounding the bunkhouse and bathhouse structures. Counts are shown as colony forming units (CFU) with standard deviation (SD). See Figure 1 as a key for sampling locations referred to in the table.

Sample Site	(CFU/100 mL)	
	Total Coliform (mean \pm SD)	Fecal Coliform (mean \pm SD)
9	26 \pm 3	2 \pm 1
7	37 \pm 9	1 \pm 1
4	1 \pm 1	0
8	30 \pm 4	6 \pm 2
39	405 \pm 21	3 \pm 2
43	163 \pm 29	0
38	78 \pm 5	10 \pm 4
40	55 \pm 4	2 \pm 1
42	23 \pm 3	3 \pm 2
41	37 \pm 10	1 \pm 1

Phylogenetic Diversity

In addition to the use of TC and FC counts to assess water quality, we examined microbial phylogenetic diversity in waters in the vicinity of the bathhouse and bunkhouse to assess potential effects from human activity. *Archaea*-specific PCR amplicons were only detected from three sampling locations (sites 38, 39 and 43; Table 10; Figure 8), which were each elevated in water temperature and localized to the intake ditch flowing either into (sites 39 and 43) or out of (site 38) the bathhouse. Elevated water temperature readings were not unexpected for samples collected directly below the bathhouse (i.e., site 38), as this site represents a mixture of water from Serpentine Hot Spring and Hot Springs Creek. Several cryptic thermal vents were also observed in the portions of the intake ditch above the bathhouse, suggesting that the elevated water temperatures measured at sampling sites 39 and 43 are likely caused by these vents, and contribute to the maintenance of thermophilic microbial populations.

DNA extracted from sites 7, 8, 9, and 41 were amplifiable with bacterial-specific primers (see below), which implies that there were no inhibitors in the various PCRs, so that failure to amplify *Archaea* 16S rRNA genes with validated domain-specific primers (Baker et al., 2003) suggests that these organisms were either absent or present at extremely low densities. Samples from sites 4, 40, and 42 did not amplify with either the *Archaea*- or *Bacteria*-specific primers, indicating the possible presence of PCR inhibitors. Humic contaminants are specifically suspected because the samples were visually off-colored and brown in appearance. Following DNA extraction, the samples remained brown in appearance, again suggesting that a significant amount of humic contaminants was present in these DNA extracts.

Based on the studies conducted by Kunin et al. (2010) and Huse et al. (2010), OTU assignments based on 97% DNA sequence identity provide a reasonable assessment of the microbial taxonomic diversity in environmental samples. As such, the data indicate that there were between 203-230 definable archaeal OTUs identifiable among amplicons obtained from sites located within the intake ditch (i.e., sites 38, 39 and 43; Table 10). These data were then extrapolated using the richness estimators ACE and Chao1. Site 43, a sampling site located directly in front of the bunkhouse (Figure 8), appeared to contain the greatest potential archaeal diversity; 1226 and 684 OTUs were predicted using the ACE and Chao1 diversity extrapolations, respectively (Table 10).

Taxonomic resolution of archaeal 16s rDNA amplicons found that the vast majority (92.4-95%) of pyroreads were classified as *Archaea* (Table 11), with classification below the domain-level strikingly similar across locations. Microbial community composition across all three intake ditch sites showed that the *Euryarchaeota* were clearly a dominant phylum, comprising 77 to 89% of the total number of reads across all sites, with *Halobacteria*-like organisms appearing to be the most dominant class (20-41%) within the phyla (Table 11). *Crenarchaeota* were apparently absent at site 39 and were minor components of the microbial community at sites 38 and 43 (Table 11). Although widespread in nature, the *Crenarchaeota* are more frequently found in the highest temperature hot spring environments. Their absence here suggests that hot spring temperatures were not high enough to be considered optimum for thermophilic *Crenarchaeota*.

Table 10. Archaeal, bacterial, and eukaryotic phylotype richness (97% ID) in water quality analysis of Hot Springs Creek. Sites 38, 39, 43 are within the cold water ditch; the remaining sites are in the immediate vicinity of the bunkhouse and bathhouse (Table 1, Fig. 8). ACE and Chao are estimates of OTUs.

Sample	Temp (°C)	OTU	ACE (95% CI)	Chao (95% CI)
Archaea				
43	45	230	1226 (1040 - 1454)	684 (520 - 942)
38	44	203	1140 (971 - 1345)	533 (409 - 734)
39	37	216	1150 (982 - 1354)	567 (417 - 820)
Bacteria				
43	45.0	78	373 (203 - 772)	873 (700 - 1095)
38	44.0	148	345 (2223 - 589)	838 (657 - 1078)
39	37.0	114	295 (210 - 457)	676 (548 - 841)
41	8.0	290	994 (678 - 1524)	1021 (702 - 1545)
8	7.4	425	804 (557 - 1219)	815 (577 - 1199)
7	7.2	439	687 (478 - 1041)	1974 (1539 - 2547)
9	6.8	343	1054 (709 - 1634)	1217 (799 - 1930)
Eukarya				
43	45	30	38 (32 - 58)	37 (31 - 58)
38	44	84	507 (403 - 643)	197 (127 - 357)
39	37	126	394 (317 - 497)	296 (199 - 493)

Table 11. Dominant Archaea phyla observed in the various sampling sites surrounding the bathhouse and bunkhouse. Class level taxonomy is highlighted in yellow.

Phylum	Site #	43	38	39
	Temp (°C)	45	44	37
Unclassified_Root		5.6	4.9	3.6
Bacteria		1.7		1.0
Archaea		92.7	94.2	95.4
Unclassified_Archaea		12.9	9.0	5.4
Crenarchaeota		2.2	2.0	
Thermoprotei		2.2	2.0	
Euryarchaeota		77.6	83.3	89.6
Unclassified_Euryarchaeota		45.6	52.1	46.7
Halobacteria		20.4	26.9	40.7
Methanobacteria		5.9	1.1	1.2
Methanomicrobia		5.1	2.7	

Bacterial species richness at the sampling locations around the structures varied considerably, with water temperature apparently being an influencing factor (Table 10). Bacterial OTU counts were significantly lower at sites with water temperature readings $\geq 37^{\circ}\text{C}$, ranging from 78-148 OTUs (97% ID cut-off) (Table 10; sites 38, 39, and 43). As water temperature decreased, the total number of

OTU's increased significantly, ranging from 290 – 439 OTUs (Table 10; sites 7-9 and 41). OTU counts were consistent with the total richness estimates derived from ACE and Chao1 extrapolations (Table 10), being significantly higher for low water temperature sites relative to locations with higher water temperatures. Water temperature is known to be an important environmental selection pressure that can constrain microbial diversity, so these observations are not necessarily unexpected.

Temperature also appeared to influence the distribution of some *Bacteria* phyla and genera identified in the pyrosequencing libraries (Table 12). Among the total of 14 bacterial phyla detected, *Firmicutes* clearly dominated at higher temperatures, comprising ~10-26% of the total reads where water temperature was $\geq 37^{\circ}\text{C}$. Locations with lower water temperatures (i.e., sites 7, 8, 9, and 41) had a much higher prevalence of *Actinobacteria* phyla members, comprising ~11-17% of the pyroreads; (Table 12). Phylotype distribution was used to assess whether microbes found near the structures were being shed, and thus occurring downstream. Signs of microbial shedding could serve as an indicator of possible water contamination issues. The most prevalent bacterial phylum detected from samples collected near the bunkhouse and bathhouse (i.e., sites 38, 39 and 43; Table 12) were the α - and β -*Proteobacteria* (Table 12). These phyla were also noticeably elevated in abundance at sites 9 and 41, locations sampled downstream from the structures. However, α - and β -*Proteobacteria* were also equally prevalent at sites 7 and 8, both of which lie upstream of the bunkhouse and bathhouse (Figure 8), suggesting that water contamination is not a significant confounding problem at the Serpentine location. The pyrosequencing data for samples taken around the structures also suggest low representation of the γ -*Proteobacteria* taxonomic class, a phylogenic group containing the vast majority of pathogenic coliform species. Though γ -*Proteobacteria* sequences were detected at some locations (Table 12, sites 7, 8, and 41), the typical genera of pathogenic coliform bacteria, including *Citrobacter*, *Enterobacter*, *Escherichia*, *Hafnia*, *Klebsiella*, and *Serratia*, were noticeably absent from all the sampling sites. The lack of a coliform molecular signature in the pyrosequencing libraries is consistent with the low FC counts detected using the membrane filtration method discussed above.

Table 12. Dominant Bacteria phyla observed in the various sampling sites surrounding the bathhouse and bunkhouse. Family level taxonomy is highlighted in orange.

Phylum	Site # Temp (°C)	9 6.8	7 7.2	8 7.4	41 8.0	39 37.0	38 44.0	43 45.0
Acidobacteria		3.7	3.8	3.3	3.5			
Actinobacteria		16.4	11.1	13.6	17.2	3.9	1.8	
Actinobacteria								
Micrococcineae		5.1	4.0	6.7	5.6	1.6		
Micromonosporineae					1.1			
Solirubrobacteraceae		1.4	1.9		1.1			
Bacteroidetes		8.1	6.7	7.4	7.5	5.9	7.3	4.7
Bacteroidia		2.1	1.1	2.1	1.6			1.6
Flavobacteria		3.0	3.0	1.3	3.2	1.6		
Flavobacterium		1.2	2.1		1.3			
Sphingobacteria		1.9	2.1	1.6		3.5	3.3	1.6
Chloroflexi		3.0		1.0	1.1	2.0	2.5	2.6
Chloroflexi		1.6					1.8	
Chloroflexus		1.6					1.8	
Anaerolineae		1.2	1.4	1.0	1.1	1.6		
Caldilineae								1.1
Caldilinea								1.1
Cyanobacteria		3.7		1.0	1.3	3.1	3.3	1.1
Bacillariophyta		1.9				1.2		
Deinococcus-Thermus						1.6		
Firmicutes		5.1	5.5	5.2	5.6	25.5	9.0	10.5
Bacilli						4.3	1.8	4.2
Aneurinibacillus								2.1
Clostridia		3.5	3.8	4.2	3.8	17.3	6.8	5.3
Clostridiaceae						7.5		2.1
Gemmatimonadetes		1.4						
OD1		1.2			1.6			
Proteobacteria		19.2	33.9	27.1	26.3	38.0	65.6	69.5
Alphaproteobacteria		5.6	7.6	8.3	9.9	17.6	25.9	21.6
Azospirillum						3.9	12.6	10.0
Blastochloris								1.1
Magnetospirillum								1.6
Marispirillum								1.6
Porphyrobacter							2.5	1.6
Betaproteobacteria		8.6	16.2	10.0	7.3	14.5	37.2	46.3
Curvibacter			3.0	1.3	1.3			
Dechloromonas						2.0	5.0	1.6
Hydrogenophaga							5.0	6.3
Hydrogenophilus								5.8
Janthinobacterium			1.4					
Methyloversatilis								2.1
Polaromonas			1.0					
Rhodoferax		1.6	2.5	2.1	1.6			

Table 12. Dominant Bacteria phyla observed in the various sampling sites surrounding the bathhouse and bunkhouse (continued).

Phylum	Site # Temp (°C)	9 6.8	7 7.2	8 7.4	41 8.0	39 37.0	38 44.0	43 45.0
Tepidimonas						3.1	12.6	15.3
Deltaproteobacteria			3.2	2.8	2.7			
Geobacter				1.1	1.1			
Gammaproteobacteria			2.5	2.3		1.2		
Spirochaetes						1.2	1.0	1.1
SR1			3.6					
TM7		3.5		2.6	2.2			
Unclassified_Bacteria		34.0	31.2	34.8	32.3	18.8	8.0	9.5

Eukaryotic 18S rDNA gene amplicons were only detected from sites sampled within the intake ditch near the bunkhouse and bathhouse (sites 38, 39 and 43, Table 13), all of which were locations with elevated water temperatures due to the cryptic vents mentioned above (sites 38, 39 and 43, Table 13). Eukaryotic OTU counts (clustered at 97% identity) were negatively correlated with temperature, decreasing from 126 OTU's at 37°C to 30 OTU's at 45°C (Table 10). This result was not unexpected, given that most eukaryotic microbes are sensitive to temperatures exceeding 35°C. Eukaryote phyla representing > 1% of the pyrosequencing reads in any specific sample are listed in Table 13. The super phylum *Alveolata* was common and dominant at all sites where 18S rDNA gene amplicons were detected. The *Alveolata* are comprised of the ciliates (common protozoa), apicomplexa (parasitic protozoa), and the dinoflagellates (many are photosynthetic). Though an assortment of *Alveolata* family members was detected, parasitic protozoa belonging to the *Eimeriidae* family of *Apicomplexa* eukaryotes were clearly abundant at all three locations. The *Eimeriidae* are not known to tolerate elevated temperature and thus sequences detected at Serpentine could potentially represent a new genus of thermophilic protozoa.

The identification and distribution of eukaryotic 18S rDNA sequences from the genus *Naegleria* at intake ditch sites 38, 39 and 43 represents the possible identification of the thermo-tolerant parasitic amoeba *Naegleria fowleri*, which is known to thrive at temperatures of upwards of 45°C and localize to hot spring habitats (Sheehan et al., 2003). The pathogen *N. fowleri* can invade the human nervous system and outbreaks in human populations have often been associated with recreational use in geothermal waters (Szenasi et al., 1998). In this study, taxonomic resolution could only be determined down to the genus-level and so it is not possible to determine if the *Naegleria* detected was the pathogenic species *fowleri*, or one of the other 46 characterized *Naegleria* species.

The family *Philodinidae* and genus *Macropharyngomonas* dominated the pyroreads derived from the highest temperature intake ditch location (i.e. site 43), comprising 34% and 33% of the read total. Interestingly, *Philodinidae* belongs to an order of rotifers that have been found to inhabit hot spring environments, while *Macropharyngomonas* is a genus of halophilic protozoa. The extremophilic nature of these eukaryotes is consistent with the high water temperature (45°C) measured at this

location. Sites sampled directly above (i.e. site 39) and below (i.e. site 38) the structures had a noticeable green biofilm along the bottom of the water channel. This corresponds to the prevalence of chlorophytes at both locations (Table 13).

Table 13. Dominant Eukarya phyla observed in the various sampling sites surrounding the bathhouse and bunkhouse. Family or Genus level taxonomy is highlighted in orange.

	Site #	43	38	39
Superphylum	Temp (°C)	45.0	44.0	37.0
Eukaryote		99.6	99.7	95.0
Environmental samples		1.1	5.6	27.1
Alveolata		23.9	58.8	23.7
Apicomplexa		15.2	37.5	8.7
Colpodellidae		1.5		
Eimeriidae		13.3	37.3	8.7
Ciliophora		6.1	18.5	13.1
Colpodidae		1.5	7.0	
Cyclidiidae			1.4	
Cyrtolophosididae			1.7	
Deltopylidae				2.8
Euplotidae		1.9	3.6	
Metopidae		1.5	2.5	3.7
Prorodontidae				2.5
Animalia		36.7	2.5	15.0
Arthropoda			1.1	
Nematoda				1.9
Monhysteridae				1.9
Rotifera		36.7		2.5
Philodinidae		33.7		
Cercozoa				2.5
Discicristata		34.5	7.6	1.6
Euglenozoa			2.0	
Percolozoa		34.5	7.6	1.9
Macropharyngomonas		33.3	1.7	
Naegleria		1.1	3.9	1.6
Fungi			5.9	8.1
Ascomycota			1.7	2.2
Chytridiomycota				2.2
Stramenopiles			3.9	9.3
Bacillariophyta				1.2
Heterokontophyta			2.5	1.9
Pythiaceae			2.0	
Viridiplantae			3.4	7.2
Chlorophyta			2.8	6.9
Chaetophoraceae			2.2	2.5
Unclassified_Eukaryota		3.0	11.5	

Synthesis

At the DNA sampling and sequencing depth employed, it is reasonable to conclude that the sites assessed around the Serpentine Hot Spring structures contain few potentially pathogenic prokaryotic microorganisms. Bacterial pyrosequencing libraries from sites where TC and FC counts were highest contained low levels of the γ -*Proteobacteria* taxonomic class organisms and a complete lack of genera that are indicators of water contamination, suggesting that water resources around the study site were not impaired at the time of sampling. The possible presence of pathogenic bacteria in addition to the γ -*Proteobacteria* cannot be ruled out, though the vast majority of water-borne bacterial pathogens (including non-coliform bacteria) fall within this taxonomic unit. Coliform bacteria are known to merely be indicators of possible water pollution; most persist naturally in water and soil environments and are not a concern to human health. The low number of FCs detected at all sites during water quality testing, as well as the complete lack of *Escherichia* pyroreads, also provide evidence for the low prevalence of fecal contamination at the Serpentine Hot Spring site. The identification and distribution of eukaryotic 18S rDNA sequences from the genera *Naegleria* at intake ditch sites 38, 39 and 43 does not rule out the possibility of the deadly free-living amoeba *N. fowleri*, which proliferates at elevated water temperatures. However, taxonomic resolution achieved by the molecular-based data could not determine if the *Naegleria* detected was the pathogenic species *fowleri*. Additional molecular work employing other techniques (e.g. near full-length 18S rDNA gene PCR cloning and sequencing, or using *fowleri*-specific PCR primers) is warranted in order to clarify this particular issue.

Microbial Diversity in Thermal Waters

The waters of Serpentine Hot Springs (SHS) (Figure 4E, 4F) and Arctic Hot Springs (AHS) (Figure 4A, 4B, 4C) were each sampled for total microbial diversity. Sampling focused on aqueous environments (i.e. submerged microbial mats) that varied with respect to temperature and/or shifts in the visual appearance of the mat material (which was interpreted as a change in microbial community composition). Water temperatures at the SHS sample sites ranged from 35 to 75°C, similar to those at AHS which ranged from 37 to 62°C. The pH values for all sampling locations were circumneutral. Representative images of microbial mats sampled at SHS and AHS are shown in Figures 23 and 24. Mat colors at each sampling site ranged from green to brown, displaying the chlorophylls and pigments of the dominant microbial populations located in the uppermost layer of the mat structure. For all samples, pyrosequencing of PCR-amplified and barcoded 18S rDNA and 16S rDNA amplicons generated using the bacterial, archaeal, and eukarya primers (described above) were mixed in equal proportion, and used to infer the relative distribution and abundance of each microbial taxonomic domain within each sampling site.

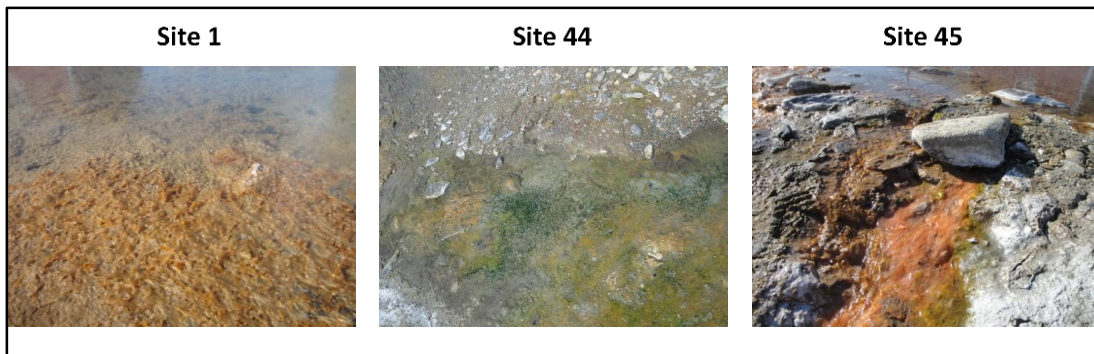


Figure 23. Photographs of microbial growth in and adjacent to the hot pool at Serpentine Hot Springs.



Figure 24. Photographs of microbial growth in Arctic Hot Springs, 2010.

Serpentine Hot Springs

The main Serpentine hot pool (Figure 4e; Figure 23; site 1) and two sites within the adjacent geothermal seep area (Figure 4e; Figure 23; sites 44 and 45) were assessed for total microbial diversity. Of the three sites sampled, archaeal 16S rDNA amplicons were only detectable at site 44, located in the cooler reaches of the geothermal seep. Here, archaeal OTU (phylotype richness) counts were the highest of all SHS sampling locations (Table 14). Bacterial OTU counts were also quite high for this locale, much higher than those observed at sites 1 and 45, which were located near or directly above the spring source vent (Table 14). Similar to the archaeal populations, eukaryotic 18S rDNA sequences were only detected at site 44 (Table 14). At the 97% sequence identity level, 45 *Eukarya* OTUs were observed (Table 14).

Table 14. Archaeal, bacterial, and eukaryotic phylotype richness (97% ID) in the Serpentine Hot Spring study location.

Sample	Temp (°C)	% ID	OTU	ACE (95% CI)	Chao (95% CI)
Archaea					
44	35	97	567	271 (210 - 361)	193 (122 - 359)
Bacteria					
1	75	97	47	166 (122 - 233)	66 (46 - 124)
45	59	97	49	94 (69 - 137)	55 (43 - 91)
44	35	97	202	730 (602 - 896)	483 (356 - 698)
Eukarya					
44	35	97	45	146 (105 - 209)	82 (46 - 205)

The RDP classifier was unable to categorize a majority (62%) of archaeal reads amplified from SHS site 44 (Table 15). RDP classified roughly 29% of the archaeal amplicons as *Bacteria* and only 9% as *Archaea*. Of the latter, most were classified in the phylum *Euryarchaeota*, with *Halobacteria*-like organisms being the most prevalent taxonomic class. Taxonomic resolution of SHS archaeal pyrosequencing reads was poor, in part because the RDP classifier is based on 16S rDNA gene sequences of cultivated and characterized *Archaea* represented in Bergey's Manual (Garrity et al., 2002). Due to the relatively low number of cultured *Archaea*, the RDP bioinformatic training set is relatively small. In other recent work, we have found that computer-based classifiers have trouble correctly classifying archaeal pyrosequencing reads, often incorrectly placing reads in the wrong domain (Kan et al., 2011). Another factor constraining taxonomic resolution was read length for archaeal sequences derived from site 44. The average length of the roughly 2000 reads was only 80 bp (range, 50-354 bp), which placed a severe limitation on taxonomic resolution. At this time, it is not clear why the average read length was so poor. Identical techniques employed by our group in a previous study in Yellowstone Lake, Wyoming (Clingenpeel et al., 2011; Kan et al., 2011), yielded pyroreads that averaged 360 nucleotides. Technical issues at the commercial sequencing facility may have been a contributing factor.

Table 15. Dominant Archaea phyla in Serpentine Hot Spring sampling site 44.

Phylum	Temp (°C)	35
Unclassified_Root		62
Bacteria		29
Archaea		8.6
Unclassified_Archaea		
Crenarchaeota		
Thermoprotei		
Euryarchaeota		8.2
Unclassified_Euryarchaeota		1.4
Methanobacteria		1.1
Methanobacterium		
Methanothermobacter		
Methanococci		
Methanomicrobia		1.3
Halobacteria		4.3

With regards to taxonomic classification of bacterial pyrosequencing reads amplified from SHS sampling locations, the RDP classifier placed all sequences in the domain Bacteria (Table 16). Temperature effects on genus distribution were apparent. There was but a single taxon, *Chloroflexus*, observed at all temperatures. Temperature constraints on phototrophic microbial communities are known to occur (Miller et al., 2009), though it would appear that most of the *Chloroflexus* detected at SHS are adapted to high temperature environments, as their prevalence decreased from ~76% to 2.6% as temperature levels declined from 75 to 35°C. With declining temperatures there was a noticeable shift in the SHS phototrophic bacterial community (Table 16), as the *Chloroflexi*-dominated mat shifted to a predominantly cyanobacterial mat in the cooler reaches of the outflow channel. Phototrophs were not present and would not be expected at SHS site 1, a site sampled directly above the main hot spring vent where temperatures exceeded the known limit of photosynthesis.

Eukarya 18S rDNA amplicons were only obtained from DNA extracted from the SHS sampling site with the lowest temperatures (Table 17, site 44). Here, as seen in the water quality samples (discussed above), rotifer members from the *Philodinidae* family dominated the pyrosequencing library, making up 57% of the reads; another 8% of the sequences represented an unclassified group of rotifers. Many sequences (~16%) were also of an unknown origin, simply classified as Animalia environmental eukaryotic 18S sequences, with no further taxonomic resolution.

Table 16. Dominant Bacteria phyla observed in the Serpentine Hot Spring sampling sites. Genus level taxonomy is highlighted in orange.

Phylum	Site # Temp (°C)	Serpentine Hot Springs		
		1 75	45 59	44 35
Bacteroidetes			3	15.5
Sphingobacteria			1.1	9.3
Haliscomenobacter				1.3
Chloroflexi		75.7	45.5	13.5
Anaerolineae				4.4
Chloroflexi		75.7	45.5	3.3
Chloroflexus		75.7	45.5	2.6
Cyanobacteria			3.5	29.4
Cyanobacteria			3.5	29.4
GpI			1.4	2.2
GpVIII				1.5
GpXII				2.4
Deinococcus-Thermus		9.3	5.8	
Deinococci		9.3	5.8	
Meiothermus		3.2	5.8	
Thermus		6		
Proteobacteria			13.9	11.5
Alphaproteobacteria				6.6
Betaproteobacteria				2
Unclassified_Bacteria		12.1	27.3	26.8

Table 17. Dominant Eukarya phyla observed in Serpentine and Arctic Hot Springs. Family or Genus level taxonomy is highlighted in orange.

Superphylum	Serpentine Hot Springs		Arctic Hot Springs							
	Site #	44	Upper Hot Springs			Main Hot Springs				
		Temp (°C)	48	47	46	50	55	53	52	54
Bacteria					22.3	2.8		1.2	2.0	
Eukaryote	99.5	100.0	100.0	100	77.7	97.2	99.6	98.2	97.9	99.6
Unclassified_Eukaryota					3.6					
Alveolata	4.3		1.5			42.7	9.4	5.2	7.0	1.4
Apicomplexa						34.3	6.8	3.4	6.8	
Eimeriidae						34.3	5.1	3.4	3.0	
Sphaerocystidae							1.7			
Ciliophora			1.5			8.4		1.2		1.4
Cyrtolophosididae						2.8				
Dysteriidae						5.1				
Amoebozoa	1.1					15.7		1.2	2.6	1.1
Tubulinea						14.0			2.6	
Echinamoebidae						12.9			2.4	
Animalia	88.2	100.0	94.3	63	65.5	9.6	52.8	80.9	69.4	95.4
Arthropoda	20.3		3.6	8.3	50.4	1.1	32.3	56.6	67.0	6.4
Canthocamptidae								1.2		
Chironomidae				0.8			1.3	3.1		
Cyprididae								1.2		
Drosophilidae					6.5	1.1	6.4	43.7	65.8	
Oribatida	12.8			5.5	44.6		19.6	7.4		6.0
Tephritidae	2.1			0.5			1.3			
Chordata						4.5		2.5	1.5	
Environmental samples	15.5			0.3			2.1			
Gastrotricha				2.1						
Chaetonotidae				2.1						
Nematoda	1.6					1.7	3.8	1.5		
Cephalobidae						1.7				
Mononchidae								1.5		
Plectidae							3.0			
Porifera						1.1				
Coelospheridae						1.1				
Rotifera	65.8	99.4	90.1	52	1.4	1.1	16.2	20.0		87.9
Adinetida	1.1	1.9		1						1.4
Brachionidae						1.1	3.8			
Philodinidae	57.2	89.7	80.5	48			8.5	16.3		77.9
Pythiaceae							9.0			
Unclassified_Rotifera	7.5	7.7	8.7	3.1	1.4		1.7	2.8		8.5
Bacillariophyta			2.7				3.8	2.5		
Fragilariaceae							1.3			
Naviculaceae			1.2							
Cercozoa						1.7	4.3	1.5		
Environmental samples						10.7	6.8	2.8	15.8	

Table 17. Dominant Eukarya phyla observed in Serpentine and Arctic Hot Springs (continued).

Superphylum	Site #	Serpentine Hot Springs	Arctic Hot Springs								
		44	Upper Hot Springs			Main Hot Springs					
			48	47	46	50	55	53	52	54	56
	Temp (°C)	35	39	38	36	62	59	41	39	39	38
Fungi		2.7					15.2	14.5	1.5	1.4	1.1
Ascomycota							5.6				
Environmental samples									6.8		
Trichocomaceae							3.4				
Blastocladiomycota								6.4			
Catenariaceae								6.4			
Uncultured		2.1					8.4	6.0			1.1
Viridiplantae				36		2.9	1.1	3.4			

Arctic Hot Springs

Fourteen samples were collected in and around Arctic Hot Springs (AHS) (Table 1; Figure 25: sites 2, 3 and 46 thru 57). Samples were often collected within meters of one another due to the steepness of the temperature gradients. Collection locations were grouped into two main areas: “AHS Main Vent”, referring to samples collected between the AHS source vent (Figure 4a, Figure 25) and the “old hot tub” (Figure 4b, Figure 25); and “AHS Upper Thermal Area” referring to samples collected in a separate moist area above the source vent (Figure 4c, Figure 25).

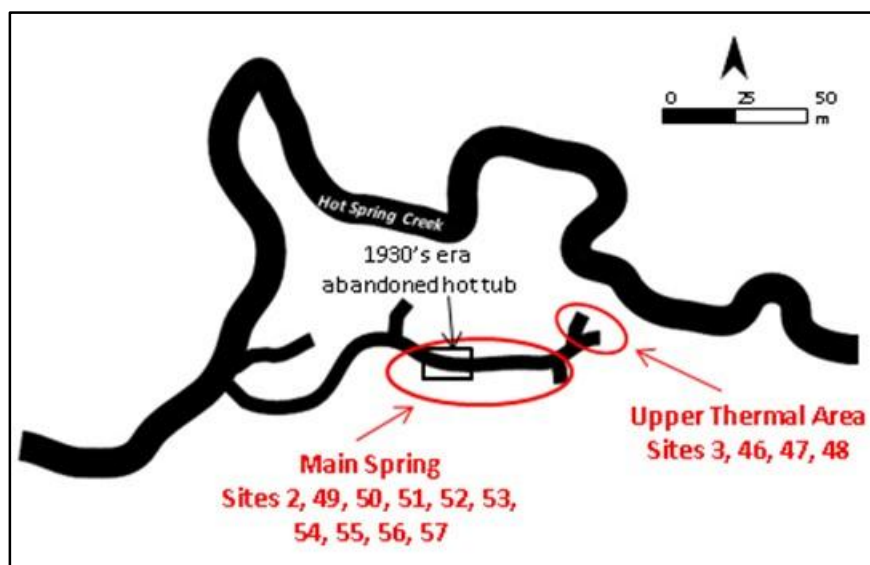


Figure 25. Arctic Hot Springs microbiology collection sites, 2010.

Number of archaeal OTUs identified in the AHS mat samples were inversely correlated with temperature (Table 18). At the 97% identity level, 48 OTUs were identified in the highest temperature sample (62 °C, site 50), whereas 468 OTUs were found at site 52, where the temperature was 39°C. For analysis of archaeal phylotype richness (ACE and Chao estimators), the pyrosequencing data sets were normalized to the same number of reads (150 reads). After this

trimming, the extrapolated total richness estimates no longer showed a negative correlation with site temperature (Table 18).

Table 18. Archaeal, bacterial, and eukaryotic phylotype richness (97% ID) in the Arctic hot springs sampling sites.

Sample	Temp (°C)	OTU	ACE (95% CI)	Chao (95% CI)
Archaea- Main Hot Springs				
50	62	48	126 (81 - 231)	180 (95 - 419)
51	37	161	105 (67 - 199)	91 (62 - 166)
52	39	468	98 (72 - 146)	69 (49 - 127)
53	41	184	342 (253 - 474)	213 (123 - 436)
54	39	172	179 (133 - 251)	103 (71 - 182)
55	59	59	268 (201 - 367)	126 (85 - 226)
Archaea- Upper Hot Springs				
48	39	173	442 (334 - 592)	147 (92 - 2778)
47	38	229	413 (299 - 584)	176 (119 - 299)
46	36	292	188 (120 - 337)	171 (109 - 314)
Bacteria- Main Hot Springs				
50	62	33	83 (60 - 123)	67 (43 - 147)
55	59	110	608 (413 - 910)	257 (137 - 564)
49	50	108	283 (220 - 373)	146 (104 - 242)
57	42	77	224 (171 - 304)	131 (89 - 236)
53	41	73	221 (153 - 333)	188 (91 - 477)
52	39	57	88 (64 - 133)	75 (49 - 155)
54	39	40	164 (102 - 223)	90 (56 - 189)
56	38	137	491 (382 - 642)	280 (192 - 453)
51	37	63	117 (87 - 139)	113 (67 - 253)
Bacteria- Upper Hot Springs				
48	39	159	578 (465 - 726)	266 (191 - 408)
47	38	182	565 (467 - 693)	339 (259 - 479)
46	36	195	928 (774 - 1112)	522 (372 - 784)
3	36	193	558 (466 - 677)	311 (243 - 431)
Eukarya- Main Hot Springs				
50	62	38	83 (55 - 154)	80 (53 - 160)
55	59	42	94 (62 - 155)	66 (37 - 167)
53	41	100	512 (386 - 687)	222 (141 - 396)
52	39	67	173 (111 - 310)	150 (99 - 267)
54	39	70	39 (25 - 92)	34 (23 - 76)
56	38	36	52 (37 - 84)	45 (31 - 91)
Eukarya- Upper Hot Springs				
47	38	25	104 (60 - 202)	59 (34 - 150)
46	36	47	112 (75 - 179)	58 (40 - 113)

Taxonomic identification of the AHS *Archaea* pyrosequencing reads was again problematic, though less so than in the SHS samples. Among the AHS samples, sites 46, 47, 48, and 52 proved difficult for the RDP classifier and were again constrained by read length. The average archaeal 16S rDNA

read length for these sampling locations ranged from 102-176 bp. Among the pyrosequencing reads classified as *Archaea*, *Crenarchaeota* were only detected at sites 50 and 55 (Table 19), with the Thermoprotei being prevalent at site 50. The localization of *Crenarchaeota* populations to high temperature ($\geq 59^{\circ}\text{C}$) and circum-neutral pH has been previously observed in other geothermal sites such as Long Valley Caldera, California, and Yellowstone National Park, Wyoming (Barns et al., 1994; Vick et al., 2010). The *Euryarchaeota* were dominant at most AHS sites, with *Halobacteria*-like organisms dominant at certain lower-temperature locations (e.g., sites 51, 53, and 54). At site 55, the *Methanomicrobia* were the most dominant *Euryarchaeota* (Table 19). It should be noted that while the cultured *Halobacteria* are extreme halophiles (DasSarma et al., 2006), uncultured *Archaea* that phylogenetically fall into the class *Halobacteria* have been found in various environments that, like Arctic Hot Spring, are not saline environments.

Table 19. Dominant Archaea phyla observed in the Arctic Hot Springs sampling sites. Dominant genera are highlighted in orange.

Phylum	Site # Temp ($^{\circ}\text{C}$)	Arctic Hot Springs								
		Upper Hot Springs			Main Hot Springs					
		48 39	47 38	46 36	50 62	55 59	53 41	52 39	54 39	51 37
Unclassified_Root		28.2	32.5	43.5	2.0	7.9	8.5	45.0	1.3	1.0
Bacteria		10.6	20.4	21.5	4.7	12.0	3.9	49.6	3.3	4.5
Archaea		61.2	47.1	35.0	93.3	80.1	87.6	5.4	95.4	94.4
Unclassified_Archaea		2.6	8.3	1.4	28.7	19.6	1.1		1.1	1.6
Crenarchaeota					42.0	6.8				
Thermoprotei					27.3	6.8				
Euryarchaeota		58.2	38.5	33.6	24.7	53.7	86.5	4.8	94.0	92.5
Unclassified_Euryarchaeota		33.9	27.0	21.0		8.2	12.4	2.2	14.4	8.4
Halobacteria		20.3	3.6	11.4	8.0	1.1	73.4	2.5	79.3	82.3
Haladaptatus										1.2
Halalkalicoccus							2.3		3.6	5.2
Haloarcula		2.2		1.6	1.3		15.5		14.4	13.5
Halobacterium										1.1
Haloferax							1.1		2.8	5.8
Halogeometricum									1.1	
Halomicrobium		1.3					10.2		10.3	9.1
Haloquadratum							1.7		1.7	
Halorubrum		1.8					1.1		1.9	2.5
Natrinema							3.5		3.6	1.9
Methanothermobacter					1.3					
Methanobacteria		2.0	6.6	0.7	1.3					1.6
Methanobacterium		1.5	4.5	0.3						
Methanothermobacter						44.4				1.5
Methanococci		1.8		0.1						
Methanomicrobia			1.1	0.4		44.4				

Pyrosequencing of the bacterial PCR amplicons generated 444 - 810 quality reads, depending on the sampling location. A comparison of OTU counts with the ACE and Chao1 total richness data (Table 18) showed a strong correlation; it would appear that the species richness captured in the sampling is fairly representative of that present in these hot springs. As at SHS, *Chloroflexus* was a dominant phylotype at many sampling sites, showing increased prevalence at sites with higher temperatures (Table 20). Group 1 *Cyanobacteria* were also prevalent at all sites except 47, where this phylum was absent.

Table 20. Dominant Bacteria phyla observed in the Arctic Hot Springs sampling sites. Dominant genera are highlighted in orange.

Phylum	Site # Temp (°C)	Upper Hot Springs				Main Hot Springs								
		48	47	46	3	50	55	49	57	53	52	54	56	51
		39	38	36	36	62	59	50	42	41	39	39	38	37
Actinobacteria				2.5	1.4									
Aquificae					1.6									
Bacteroidetes		3.4	8.6	9.3	14.3		1.9	2.5	13.1	5.9	8.5	7.7	6.9	
Flavobacteria									1.6					
Sphingobacteria		2.1	5.0	7.8	13.1				6.1	3.7	5.6	2.8	3.7	
Haliscomenobacter				2.6	7.3									
Chloroflexi		2.7	9.8	3.4	9.3	83.1	62.8	55.0	3.8	8.6	11.1	38.7	7.1	48.2
Anaerolineae		2.6	3.0		1.2		6.5							2.5
Anaerolinea							3.0							
Belliinea							3.1							
Caldilineae								2.1						
Caldilinea								2.1						
Chloroflexi														
Chloroflexus		2.0	8.8	2.2	8.4	83.1	62.8	55.0	3.5	8.6	11.1	38.7	5.9	48.2
Cyanobacteria		46.9	23.1	33.9	19.9		4.6	4.7	16.8	66.1	53.9	33.2	25.9	24.2
Cyanobacteria		46.9	23.1	33.9	19.9		4.6	4.7	16.8	66.1	53.9	33.2	25.9	24.2
GpI		19.5	1.4	5.4	5.0		1.5	2.2	8.3	36.5	27.0	26.9	0.3	17.4
GpIV				1.9										
GpVIII			1.4										1.3	
GpXII				1.2										
Streptophyta					2.8									
Deinococcus-Thermus		1.3		1.7		8.6	7.0	8.9	5.8		1.0		4.4	
Deinococci														
Deinococcus		1.2		1.6										
Meiothermus						2.0	6.9	7.2	5.8					4.2
Thermus						6.3		1.4						
Firmicutes							1.7	3.5						
Clostridia							1.4	3.4						
Planctomycetes			1.3	1.1	1.0									

Table 20. Dominant Bacteria phyla observed in the Arctic Hot Springs sampling sites (continued).

Phylum	Site # Temp (°C)	Upper Hot Springs				Main Hot Springs								
		48	47	46	3	50	55	49	57	53	52	54	56	51
Proteobacteria		16.2	32.7	23.8	21.8		3.2	2.7	10.5	4.7	5.0	2.2	13.3	2.7
Alphaproteobacteria		6.9	15.4	11.0	11.0		1.0		3.5	2.2	2.5		6.5	
Methylocystis														1.0
Porphyrobacter									1.3					
Betaproteobacteria		4.7	3.0	2.3	3.3									2.0
Caenimonas		2.1												
Hydrogenophaga				1.4										
Deltaproteobacteria							1.0							
Gammaproteobacteria			9.8	1.6										3.4
Allochromatium			6.6											2.5
Unclassified_Bacteria		19.2	18.1	21.0	25.1	6.1	10.1	19.5	46.1	13.6	20.2	15.8	22.9	18.7

Similar to SHS, the *Cyanobacteria* were a dominant component of the microbial community at temperatures below ~57°C, highlighting a shift in the microbial population as a function of decreasing water temperature. Previous work examining the dominant microorganisms of a geothermal stream in the neutral-pH Hunter's Hot Springs complex, Oregon, found that *Chloroflexus* organisms dominated the mat structure when temperatures ranged from 70-48°C, whereas from 54-35°C the mat was primarily composed of a cosmopolitan mix of several cyanobacterial genera (Wickstrom and Castenholz, 1985). Similar shifts in microbial populations likely occur in the Serpentine and Arctic Hot Spring systems.

For the eukaryote PCR amplicons, the PCR primers appeared to be highly selective for the eukaryote 18S rDNA gene except at site 50, where roughly 22% of the reads were classified as Bacteria (Table 17). As judged by OTU counts as well as ACE and Chao1 richness estimators, the apparent eukaryote phylotype richness was not related to temperature in a consistent manner, regardless of identity level (Table 18). There were clear and significant differences between geothermal features with respect to the degree of taxon identification. Approximately 35% of the site 55 (59°C) pyroreads were classified to the family *Eimeriidae* (Table 17) and an additional 16% of the reads to the family *Echinamoebidae*. Such large proportional composition likely reflects actual composition and is not without precedent, as the extremely thermophilic protozoa *Echinamoeba thermanum* has been isolated from hot-spring habitats with temperatures measuring as high as 85°C (Baumgartner et al., 2003). For the higher eukaryotes represented in the pyrosequencing libraries, temperature again appeared to be a strong selective force (Table 17). Interestingly, the presence of *Orbitaba* (a family within the mite taxon) and multiple families within the fly taxon (*Drosophilidae*, *Tephritidae*, and *Chironomidae*) (Table 17) were usually detected at the same site locations. Previous work in the outflow channel of an alkaline hot spring in Yellowstone National Park found an ecological intersect between water mites and grazing flies (Wiegert and Mitchell, 1973), where cyanobacterial mats (40-

60°C) are fed on by larvae and adult brine flies. Between temperatures of 25-35°C, the brine fly will also lay eggs in the mat (Wiegert and Mitchell, 1973). A red water mite has also been found to lay its eggs in the cyanobacterial mat at upwards of 36°C; once developed into larvae, the mite will parasitize adult brine flies by attaching to them while they feed (Wiegert and Mitchell, 1973). The high representation of *Orbitaba* and/or various fly taxonomic families at sites 44, 50, 52, and 53 (Table 17), and a corresponding dominance of cyanobacterial phylotypes at sites with temperatures >57°C, suggests similar ecological relations may be occurring at SHS and AHS. High representation of these eukaryotes likely results from pockets of larvae inhabiting the sampled microbial mat. The DNA extracts could be dominated by these two organisms and thus represent a significant pyroread signature. Members of the *Philodinida* family of rotifers were dominant eukaryotic members at sites with measured temperatures of >41°C (Table 17). Though far less investigated, members of the *Bdelloid* order are the only rotifers to be observed in hot spring habitats at temperature ranges of 40-45°C. The *Philodinida* represent a family of rotifers in this taxonomic order (Pejler, 1995). All members of the *Bdelloid* order are able to undergo cryptobiosis, a process by which these eukaryotes enter a stage of dormancy in response to extreme environmental conditions (Pejler, 1995). Dominant *Philodinida* phylotypes detected at SHS and AHS provide evidence for the prevalence of these poorly understood organisms in hot spring ecosystems.

Synthesis

Assessment of the microbial diversity at Arctic and Serpentine Hot Springs considerably expands the current understanding of thermophilic microbial communities in the Bering Land Bridge National Preserve, and is also relevant to other neutral pH hot spring systems. The prevalence of *Chloroflexus* and cyanobacterial bacterial phylotypes at both hot spring locations correlates well with previous microbial community assessments in other globally distributed hot spring environments with circumneutral pH (Pierson and Castenholz, 1974; Ruff-Roberts et al., 1994), demonstrating shifts in the dominant bacterial phototrophic phyla as a function of temperature. Data collected on archaeal microbial populations also shows good correlation with previously characterized hot spring habitats (Barns et al., 1994), with the *Crenarchaeota* phylum only detected at or near the geothermal source waters where temperature levels exceeded 59°C. Below this threshold, a variety of *Euryarchaeota* phylotypes dominated the archaeal populations. Most notable with respect to the diversity analysis, however, was the wide variety of eukaryotic community members detected at both Arctic and Serpentine Hot Springs. Data concerning the diversity of higher-order thermophilic eukaryotes are sparse in the literature. The sequence signature of numerous fly, water mite, protozoa, and rotifer species represents a novel contribution to our understanding of the diversity and prevalence of eukaryotes in geothermal hot spring systems. We are aware that variable eukaryotic 18S rDNA gene copy number per organism may lead to an over-representation of these higher-order eukaryotes in pyrosequencing datasets (Amaral-Zettler et al., 2009). However, the high level of eukaryotic diversity uncovered at both locations suggests that, regardless of abundance, the prevalence and contribution of eukaryotic life to hot spring ecosystems is perhaps more important than previously thought.

The unique and diverse microbial communities uncovered in this study also underline the vulnerability of thermophilic microbial populations to the impacts of tourism-based activities. Of

particular concern in this study is the close proximity of Serpentine Hot Spring to the bunkhouse and bathhouse structures (Figure 4E). Thermal features in other national parks have been subject to acts of vandalism by tourists (Bryan, 2008). Using springs as a repository for coins, clothing, and other items have caused vents to become partially or completely clogged. When geothermal inputs are blocked, environmental factors such as temperature, pressure, and circulation are quickly altered (Bryan, 2008), which in turn changes the structure of thermophilic microbial communities that form based on specific physical and chemical gradients. Microbial mats can subsequently form in regions of the spring formerly too hot to support growth (Steingisser and Marcus, 2009).

Literature Cited

- Aiken, G.R. 1992. Chloride interference in the analysis of dissolved organic carbon by the wet oxidation method. *Environmental Science and Technology*, v. 26, p. 2435-2439.
- Akinin, V.V., Miller, E.L., and Wooden, J.L. 2009. Petrology and geochronology of crustal xenoliths from the Bering Strait region: Linking deep and shallow processes in extending continental crust in Miller, R.B., and Snoke, A.W., eds., *Crustal Cross Sections from the Western North American Cordillera and Elsewhere: Implications for Tectonic and Petrologic Processes*. Geological Society of America Special Paper 456:39-68.
- Amaral-Zettler, L.A., McCliment, E.A., Ducklow, H.W., and Huse, S.M. 2009. A method for studying protistan diversity using massively parallel sequencing of V9 hypervariable regions of small-subunit ribosomal RNA genes. *PLOS One* 4:1-9.
- American Public Health Association. 1980. Method 421B. Pages 390-393 in *Standard Methods for the Examination of Water and Wastewater*, 15th ed., American Public Health Association, Washington, D. C.
- Ball, J.W. and Nordstrom, D.K. 1991. User's manual for WATEQ4F, with revised database and test cases for calculating speciation of major, trace, and redox elements in natural waters. U.S. Geological Survey Open-File Report 91-183.
- Baker, G.C., Smith, J.J., Cowan, D.A. 2003. Review and re-analysis of domain-specific 16S primers. *Journal of Microbiological Methods* 55:541-555.
- Barns, S.M, Fundyga, R.E., Jefferies, M.W., and Pace, N.R. 1994. Remarkable archaeal diversity detected in a Yellowstone National Park hot spring environment. *PNAS* 91:1609-1613.
- Barringer, J.L., and Johnsson, P.A. 1996. Theoretical considerations and a simple method for measuring alkalinity and acidity in low-pH waters by Gran titration. U.S. Geological Survey Water-Resources Investigations Report 89-4029, p. 36.
- Baumgartner, M., A. Yapi, R. G.-F., and Stetter, K.O.. 2003. Cultivation and properties of *Echinamoeba thermarum* n. sp., an extremely thermophilic amoeba thriving in hot springs. *Extremophiles* 7:267-274.

- Beget, J.E., Hopkins, D.M., and Charron, S.D. 1996. The largest known maars on Earth, Seward Peninsula, northwest Alaska. *Arctic* 49:62-69.
- Brinton, T.I., Antweiler, R.C., and Taylor, H.E. 1995. Method for the determination of dissolved chloride, nitrate, and sulfate in natural water using ion chromatography. U.S. Geological Survey Open-File Report 95-426A, 16 p
- Book, P.A., Dixon, M., and Kirchner, S. 1983. Native healing in Alaska – Report from Serpentine Hot Springs. *Western Journal of Medicine* 139:923-927.
- Brooks, A.H. 1901. A new occurrence of cassiterite in Alaska. *Science* 13:593.
- Brooks, A.H., Richardson, G.B., Collier, A.J., and Mendenhall, W.C. 1901. Reconnaissance in the Cape Nome and Norton Bay regions, Alaska, in 1900. U.S. Geological Survey Special Publication.
- Bryan, T.C. 2008. Upper Geyser Basin. Pages 24-172 in T.C. Bryan, editor. *The Geysers of Yellowstone*. Geological Society of America, The University Press of Colorado, Boulder, Colorado.
- Buchanan, T.J., and Somers, W.P. 1969. Discharge measurements at gaging stations, U.S. Geological Survey Techniques of Water-Resources Investigations Book 3, Chapter A8.
- Carter, R.W., and Davidian, J. 1968. General procedures for gaging streams. U.S. Geological Survey Techniques of Water-Resources Investigations, Book 3, Chapter A6.
- Climate Zone, 2011. Average monthly climate and weather indicators in Kotzebue Alaska. <http://www.climate-zone.com/climate/united-states/alaska/kotzebue/> (accessed 22 February 2011).
- Clingenpeel, S., R.E. Macur, J. Kan, W.P. Inskeep, D. Lovalvo, J. Varley, E. Mathur, K. Nealson, Y. Gorby, H. Jiang, T. LaFracois, and T.R. McDermott. 2011. Yellowstone Lake: high-energy geochemistry and rich bacterial diversity. *Environmental Microbiology* 13:2172-2185.
- Collier, A.J. 1902. A reconnaissance of the northwestern portion of Seward Peninsula, Alaska. U.S. Geological Survey Professional Paper 2.
- Cox, A., and Engebretson, D. 1985. Change in motion of Pacific plate at 5 m.y. B.P. *Nature* 313: 472-474.
- Craig, H. 1961a. Isotopic variations in meteoric waters. *Science* 133:1702–1703.
- Craig, H. 1961b. Standard for reporting concentrations of deuterium and oxygen-18 in natural waters. *Science* 133:1833–1834.
- Craig, H. 1963. The isotopic geochemistry of water and carbon in geothermal areas. Pages 17-53 in E. Tongiorgi, editor, *Nuclear Geology on Geothermal Areas*, Pisa, Consiglio Nazionale delle Ricerche.

- DasSarma, S., B.R. Berquist, J.A. Coker, P. DasSarma, and J.A. Müller. 2006. Post-genomics of the model haloarchaeon *Halobacterium* sp. NRC-1. *Saline Systems* 2:3, doi:10.1186/1746-1148-2-3.
- Deming, D., Sass, J.H., Lachenbruch, A.H., and De Rito, R.F. 1992. Heat flow and subsurface temperature as evidence for basin-scale ground-water flow, North Slope of Alaska. *Geological Society of America Bulletin* 104:528-542.
- Dumitru, T.A., Miller, E.L., O'Sullivan, P.B., Amato, J.M., Hannula, K.A., Calvert, A.T., and Gans, P.B. 1995. Cretaceous to Recent extension in the Bering Strait region, Alaska. *Tectonics* 14:549-563.
- Eastabrook, C.H., Stone, D.B., and Davies, J.N. 1988. Seismotectonics of northern Alaska. *Journal of Geophysical Research* 93:12026-1040.
- Ellis, A.J., and Wilson, S.H. 1955. The heat from the Wairakei-Taupo thermal region calculated from the chloride output. *New Zealand Journal of Science and Technology B, General Research Section* 36:622-631.
- Faure, G. 1986. *Principles of Isotope Geology*, 2nd edition. John Wiley and Sons, New York, New York.
- Fournier, R.O. 1977. Chemical geothermometers and mixing models for geothermal systems. *Geothermics* 5:41-50.
- Fournier, R.O. 1991. Water geothermometers applied to geothermal energy. Pages 37-69 in F. D'Amore, editor. *Applications of geochemistry in geothermal reservoir development*, UNITAR/UNDP Center on Small Energy Resources, Rome, Italy.
- Friedman, I., and Smith, G.I. 1970. Deuterium content of snow cores from Sierra Nevada area. *Science* 169:467-470.
- Gamble, B.M. and Till, A.B. 1993. Maps showing metallic mineral resources of the Bendeleben and Soloman Quadrangles, western Alaska. U.S. Geological Survey Miscellaneous Field Studies Map MF-1838-D, scale 1:250,000.
- Garbarino, J.R. and Taylor, H.E. 1995. Inductively-coupled plasma-mass spectrometric method for the determination of dissolved trace elements in natural water. U.S. Geological Survey Open-File Report 94-358, 88 p
- Garrity, G.M., Winters, M., Kuo, A.W., and Searles, D.B. 2002. Taxonomic outline of the Prokaryotes. *Bergey's Manual of Systematic Bacteriology*, 2nd edition, Springer-Verlag, NY.
- Giggenbach, W.F. 1981. Geothermal mineral equilibria. *Geochimica et Cosmochimica Acta* 45:393-410.
- Hayba, D.O., and Ingebritsen, S.E. 1997. Multiphase groundwater flow near cooling plutons. *Journal of Geophysical Research* 102:12235-12252.

- Hinzman, L.D., Kane, D.L., Yoshikawa, K., Carr, A., Bolton, W.R., and Fraver, M. 2003. Hydrological variations among watersheds with varying degrees of permafrost. Pages 407-411 in M. Phillips, S.M. Springman, and L.U. Arenson, editors. Permafrost – Proceedings of the 8th International Conference on Permafrost. A.A. Balkema, Leiden, The Netherlands.
- Hopkins, J.P, and Hopkins, D.M. 1958. Seward Peninsula. Pages 104-110 in H. Williams, editor. Landscapes of Alaska, their geological evolution. University of California Press, Berkeley, California.
- Hudson, T. 1979. Igneous and metamorphic rocks of the Serpentine Hot Springs area, Seward Peninsula, Alaska. U.S. Geological Survey Professional Paper 1079.
- Huse, S.M., Welch, D.M., Morrison, H.G., and Sogin, M.L. 2010. Ironing out the wrinkles in the rare biosphere through improved OTU clustering. *Environmental Microbiology* 12:1889–1898.
- Ingebritsen, S.E., Galloway, D.L., Colvard, E.M., Sorey, M.L., and Mariner, R.H. 2001. Time-variation of hydrothermal discharge at selected sites in the western United States: Implications for monitoring. *Journal of Volcanology and Geothermal Research* 111:1-23.
- Ingebritsen, S.E., Mariner, R.H., and Sherrod, D.R. 1994. Hydrothermal systems of the Cascade Range, north-central Oregon. U.S. Geological Survey Professional Paper 1044-L.
- Ingebritsen, S.E., and Mariner, R.H. 2010. Hydrothermal heat discharge in the Cascade Range, northwestern United States. *Journal of Volcanology and Geothermal Research* 196: 208-218.
- Ingebritsen, S.E., Sherrod, D.R., and Mariner, R.H. 1989. Heat flow and hydrothermal circulation in the Cascade Range, north-central Oregon. *Science* 243:1458-1462.
- Kan, J., S. Clingenpeel, R.E. Macur, W.P. Inskeep, D. Lovalvo, J. Varley, Y. Gorby, T.R. McDermott and K. Nealson. 2011. *Archaea* in Yellowstone Lake. *International Society for Microbial Ecology Journal* 5:1784-1795.
- Kendall, C., and McDonnell, J. J., editors. 1998. *Isotope Tracers in Catchment Hydrology*. Elsevier, Amsterdam, Netherlands.
- Knopf, A. 1908. Geology of the Seward Peninsula tin deposits Alaska. U.S. Geological Survey Bulletin 358.
- Kunin, V., Engelbrekton, A., Ochman, H., and Hugenholtz, P. 2010. Wrinkles in the rare biosphere: Pyrosequencing errors can lead to artificial inflation of diversity estimates. *Environmental Microbiology* 12:118-123.
- Mackey, K.G., Fujita, K., Gunbina, L.V., Kovalev, V.N., Imaev, V.S., Koz'min, B.M., and Imaeva, L.P. 1997. Seismicity of the Bering Strait region: Evidence for a Bering block. *Geology* 25:979-982.

- McCleskey, R. B., Nordstrom, D. K., and Naus, C. A. 2004. Questa baseline and pre-mining ground-water-quality investigation. 16. Quality assurance and quality control for water analyses. U.S. Geological Survey Open-File Report 2004-1341.
- Miller, S.R., Strong, A.L., Jones, K.L., and Ungerer, M.C. 2009. Bar-coded pyrosequencing reveals shared bacterial community properties along the temperature gradients of two alkaline hot springs in Yellowstone National Park. *Applied and Environmental Microbiology* 75:4565-4572.
- Miller, T.P., Barnes, Ivan, and Patton, W.W., Jr. 1973. Geologic setting and chemical characteristics of hot springs in west-central Alaska. U.S. Geological Survey Open-File Report 73-188.
- Miller, T.P., Barnes, Ivan, and Patton, W.W., Jr. 1975. Geologic setting and chemical characteristics of hot springs in west-central Alaska. *Journal of Research of the U.S. Geological Survey* 3:149-162.
- Moll-Stalcup, E.J. 1994. Latest Cretaceous and Cenozoic magmatism in mainland Alaska. Pages 589-619 in G. Plafker and H.C. Berg, editors. *The Geology of Alaska, G-1*, Geological Society of America, *The Geology of North America*, Boulder, Colorado.
- Moll-Stalcup, E.J., Brew, D.A., and Vallier, T.L. 1994. Latest Cretaceous and Cenozoic rocks of Alaska. Plate 5 in G. Plafker and H.C. Berg, editors. *The Geology of Alaska, G-1*, Geological Society of America, *The Geology of North America*, Boulder, Colorado.
- Moxham, R.M. and West, W.S. 1953. Radioactivity investigations in the Serpentine–Kougarok area, Seward Peninsula, Alaska, 1946. U.S. Geological Survey Circular 265.
- National Park Service (NPS). 1987. Bering Land Bridge National Preserve, Alaska: General management plan, land protection plan, wilderness suitability review. U.S. Department of the Interior, National Park Service, Washington, D.C.
- National Park Service. 2003. Cultural landscape inventory: Iyat (Serpentine Hot Springs). U.S. Department of Interior, National Park Service, Washington, D.C.
- National Park Service. 2009. Bering Land Bridge National Preserve foundation statement. U.S. Department of Interior, National Park Service, Washington, D.C.
- National Park Service. 2011. Shared Beringian Heritage Program web site. <http://www.nps.gov/akso/beringia/beringia/index.cfm/> (accessed 23 January 2011).
- Page, R.A., Biswas, N.N., Lahr, J.C., and Pulpan, H. 1991. Seismicity of continental Alaska. Pages 47-68 in D.B. Slemmons, E.R. Engdahl, M.D. Zoback, and D.D. Blackwell, editors. *Neotectonics of North America*. Geological Society of America, *The Geology of North America*, Boulder, Colorado.
- Pandey, R.V., Nolte, V., and Schlotterer, C. 2010. CANGS: A user friendly utility of processing and analyzing 454 GS-FLX data in biodiversity studies. *BMC Research Notes* 3:3.

- Panichi, C. and Gonfiantini, R. 1977. Environmental isotopes in geothermal fluids. *Geothermics* 6:143-161.
- Pejler, B. 1995. Relation to habitat in rotifers. *Hydrobiologia* 313/314:267-278.
- Pewe, T.L. 1975. Quaternary geology of Alaska. U.S. Geological Survey Professional Paper 835.
- Pierson, B.K., and Castenholz, R.W. 1974. A phototrophic gliding filamentous bacterium of hot springs, *Chloroflexus aurantiacus*, gen. and sp. nov. *Archives of Microbiology* 100:5-24.
- Plafker, G., Gilpin, L.M., and Lahr, J.C. 1994. Neotectonic map of Alaska. Plate 12 in G. Plafker, and H.C. Berg, editors. *The Geology of Alaska*. Geological Society of America, *The Geology of North America*, Boulder, Colorado.
- Poage, M.A., and Chamberlain, C.P. 2001. Empirical relationships between elevation and the stable isotopic composition of precipitation and paleowaters: Considerations for studies of paleoelevation change. *American Journal of Science* 301:1-15.
- Rantz, S.E. 1982. Measurement and computation of streamflow: Volume 1. Measurement of stage and discharge. U.S. Geological Survey Water-Supply Paper 2175.
- Richards, M., and Blackwell, D. D., 2002, The Nevada story – Turning loss into gain: Geothermal Resources Council Bulletin, v. 31, no. 3, p. 107-110.
- Reed, M.H. and Spycher, N.F. 1984. Calculation of pH and mineral equilibria in hydrothermal waters with application to geothermometry and studies of boiling and dilution. *Geochimica et Cosmochimica Acta* 48:1479-1492.
- Robinson, M.S., and Stevens, D.L. 1984. Geologic map of the Seward Peninsula. Alaska Division of Geological & Geophysical Surveys Special Report 34, 1 sheet, scale 1:500,000.
- Roth, D.A., Taylor, H.E., Domagalski, J.L., Dileanis, P.D., Peart, D.B., Antweiler, R.C., and Alpers, C.N. 2001. Distribution of inorganic mercury in Sacramento River water and suspended colloidal sediment material: *Archives of Environmental Contamination and Toxicology*, v. 40, p. 161-172.
- Ruff-Roberts, A. L., Kuenen, G. J., and Ward, D. M. 1994. Distribution of cultivated and uncultivated cyanobacteria and *Chloroflexus*-like bacteria in hot spring microbial mats. *Applied and Environmental Microbiology*. 60:697–704.
- Sainsbury, C. L. 1975. Geology, ore deposits, and mineral potential of the Seward Peninsula, Alaska. U.S. Bureau of Mines Open-File Report.
- Sainsbury, C. L., Kachadoorian, R., Smith, T.E., and Todd, W.C. 1968. Cassiterite in gold placers at Humboldt Creek Serpentine–Kougarok area, Seward Peninsula, Alaska, U.S. Geological Survey Circular 565.

- Scholl, M.A., Ingebritsen, S.E., Janik, C.J., and Kauahikaua, J.P. 1996. Use of precipitation and groundwater isotopes to interpret regional hydrology on a tropical volcanic island: Kilauea volcano area, Hawaii. *Water Resources Research* 32:3525-3537.
- Schloss, P.D., Westcott, S.L., Ryabin, T., Hall, J.R., Hartmann, M., Hollister, E.B., Lesniewski, R.A., Oakley, B.B., Parks, D.H., Robinson, C.J., Sahl, J.W., Stres, B., Thallinger, G.G., Van Horn, D.J., and Weber, C.F. 2009. Introducing mothur: Open-source, platform-independent, community-supported software for describing and comparing microbial communities. *Applied and Environmental Microbiology* 75:7537-7541.
- Sheehan, K.B, Fagg, J.A., Ferris, M.J., and Henson, J.M. 2003. PCR detection and analysis of the free-living amoeba *Naegleria* in hot springs in Yellowstone and Grand Teton national parks. *Applied and Environmental Microbiology* 69:5914–5918.
- Smith, R.L., and Shaw, H.R. 1975. Igneous-related geothermal systems. Pages 58-63 in D.E. White, and D.L. Williams, editors. *Assessment of geothermal resources of the United States – 1975*. U.S. Geological Survey Circular 726.
- Smith, R.L., and Shaw, H.R. 1979. Igneous-related geothermal systems. Pages 12-17 in L.J.P. Muffler, editor. *Assessment of geothermal resources of the United States – 1978*. U.S. Geological Circular 790.
- Steingisser, A., and Marcus, A.W. 2009. Human impacts on geyser basins. *Yellowstone Science* 17:7-18.
- Stookey, L.L. 1970. Ferrozine - a new spectrophotometric reagent for iron. *Analytical Chemistry*, v. 42, p. 779-781.
- Szenasi, Z, Endo, T, Yagita, K., and Nagy, E. 1998. Isolation, identification and increasing importance of ‘free-living’ amoebae causing human disease. *Journal of Medical Microbiology* 47:5-16.
- Taylor, H. P., Jr. 1968. The oxygen isotope geochemistry of igneous rocks. *Contributions to Mineralogy and Petrology* 19:1-71.
- Taylor, H.E. and Garbarino, J.R. 1991. The measurement of trace metals in water resources—Monitoring samples by inductively coupled plasma-mass spectrometry. *Spectrochimica Acta Reviews*, v.14, no. 1-2, p. 33-43.
- Till, A.B., and Dumoulin, J.A. 1994. Geology of the Seward Peninsula and Saint Lawrence Island. Pages 141-152 in G. Plafker, and H.C. Berg, editors. *The Geology of Alaska*. Geological Society of America, *The Geology of North America, G-1*, Boulder, Colorado.
- Till, A.B., Dumoulin, J.A., Werdon, M.B., and Bleick, H.A. 2010. Preliminary bedrock geologic map of the Seward Peninsula, Alaska, and accompanying conodont data: U.S. Geological Survey Open-File Report 2009-1254, 2 plates, scale 1:500,000.

- To, T.B., Nordstrom, D.K., Cunningham, K.M., Ball, J.W., and McCleskey, R.B. 1999. New method for the direct determination of dissolved Fe(III) concentration in acid mine waters. *Environmental Science & Technology*, v. 33, p. 807-813.
- Turner, D.L., and Swanson, S.E. 1981. Continental rifting: A new tectonic model for the central Seward Peninsula. Pages 7-36 in E.M. Westcott and D.L. Turner, editors. *Geothermal reconnaissance study of the central Seward Peninsula, Alaska*. University of Alaska Geophysical Institute Report UAGR-284, Fairbanks, Alaska.
- Verplanck, P.L., Antweiler, R.C., Nordstrom, D.K., and Taylor, H.E. 2001. Standard reference water samples for rare earth element determination. *Applied Geochemistry*, v 16, p.231-244.
- Vick, T.J., Dodsworth, J.A., Costa, K.C., Shock, E.L., and Hedlund, B.P. 2010. Microbiology and geochemistry of Little Hot Creek, a hot spring environment in the Long Valley Caldera. *Geobiology* 8:140-154.
- Von Damm, K.L., Buttermore, L.G., Oosting, S.E., Bray, A.M., Fornari, D.J., Lilley, M.D., and Shanks, W.C., III. 1997. Direct observation of the evolution of a seafloor “black smoker” from vapor to brine. *Earth and Planetary Science Letters* 149:101-111.
- Waring, G.A. 1917. Mineral springs of Alaska. U.S. Geological Survey Water-Supply Paper 418.
- Wickstrom, C.E., and Castenholz, R.W. 1985. Dynamics of cyanobacterial and ostracod interactions in an Oregon hot spring. *Ecology* 66:1024-1041.
- Wiegert, R.G., and Mitchell, R. 1973. Ecology of Yellowstone thermal effluent systems: intersects of blue-green algae, grazing flies (*Paracoenia*, *Ephydriidae*) and water mites (*Partnuniella*, *Hydrachnellae*). *Hydrobiologia* 41:251-271.
- Wimmler, N.L. 1926, Notes on lode deposits in Seward Peninsula. Alaska Territorial Department of Mines Miscellaneous Report 192-1.
- Woo, M.-K. 1986. Permafrost hydrology in North America. *Atmosphere-Ocean* 24:210-234.
- Wood, C.A., and Kienle, J. 1990. *Volcanoes of North America*. Cambridge University Press, Cambridge, UK.
- Yoshikawa, K., and Hinzman, L.D. 2003. Shrinking permafrost ponds and groundwater dynamics in discontinuous permafrost near Council, Alaska. *Permafrost and Periglacial Processes* 14:151-160. Fung Associates Inc. and SWCA Environmental Consultants. 2010. Assessment of natural resources and watershed conditions for Kalaupapa National Historical Park. Natural Resource Report. NPS/NPRC/WRD/NRR—2010/261. National Park Service, Fort Collins, Colorado.
- Greater Yellowstone Whitebark Pine Monitoring Working Group. 2014. Whitebark Pine Monitoring Working Group. 2014. Monitoring whitebark pine in the Greater Yellowstone Ecosystem: 2013

annual report. Natural Resource Data Series. NPS/GRYN/NRDS—2014/631. National Park Service. Fort Collins, Colorado.

National Park Service. 2010. Instructions to authors — Natural Resource Technical Report, Natural Resource Technical Report, and Natural Resource Data Series: version 3.1. Natural Resource Technical Report. NPS/NPRC/IMD/NRTR—2010/256. National Park Service, Fort Collins, Colorado.

U.S. Forest Service (USFS). 1993. ECOMAP. National hierarchical framework of ecological units. U. S. Forest Service, Washington, D.C.

Appendix A : Details of analytical methods for water chemistry

The tables in Appendix A are summaries of analytical techniques, detection limits, typical precision, and references used to determine the chemical composition of sampled waters. Estimates of detection limits are assumed equal to 3 times the standard deviation of several dozen measurements of the constituent in a blank solution treated as a sample. Typical analytical precision, expressed as percent relative standard deviation, is based on several analytical runs and calculated using analytical data for standard reference water samples. Precision for any single analytical run is better than that for multiple analytical runs, but using multiple analytical runs to calculate precision provides a more realistic estimate of error when comparing results for samples analyzed at different times. The typical relative standard deviations, or precision estimates, are for analyte concentrations greater than 10 times the detection limit and less than the high standard. When an analyte concentration was greater than that of the high standard, the sample was diluted, introducing an additional source of error. Techniques, general conditions, and variants of standard procedures are discussed in the following sections.

All reagents were of purity at least equal to the reagent-grade standards of the American Chemical Society. Double-distilled or deionized water and re-distilled or trace-metal-grade acids were used in all preparations. Samples were diluted as necessary to bring analyte concentrations within the optimal range of the method. Each sample was analyzed in at least duplicate for each dilution for all constituents. Reagent blanks were analyzed to evaluate contamination from reagents used to prepare standards and dilutions.

Table A-1. Analytical techniques, detection limits, typical precision, equipment used, and analytical method references.

[CVAFS, cold-vapor atomic fluorescence spectrometry; IC, ion chromatography; ICP-MS, inductively-coupled plasma-mass spectrometry; ICP-AES, inductively coupled plasma-optical emission spectrometry; GFAAS, graphite furnace atomic absorption spectroscopy; ISE, ion-selective electrode; mg/L, milligrams per liter; mM, millimolar; MS, mass spectrometry; µg/L, micrograms per liter; ng/L, nanograms per liter; nm, nanometer; °C, degrees centigrade; RSD, relative standard deviation; TOC, total organic carbon; ---, not measured or calculated %, percent]

Constituent	Analytical Technique	Detection limit ¹ / Typical precision ²	Equipment Used	Reference(s) and comments
Calcium (Ca)	ICP-AES	0.4 mg/L / 5%	Leeman Labs Direct Reading Echelle	Analytical wavelength: 315.887 nm, view: radial
Magnesium (Mg)	ICP-AES	0.04 mg/L / 5%	Leeman Labs Direct Reading Echelle	Analytical wavelength: 280.270 nm, view: axial
Sodium (Na)	ICP-AES	0.05 mg/L / 5%	Leeman Labs Direct Reading Echelle	Analytical wavelength: 589.592 nm, view: radial
Potassium (K)	ICP-AES	0.02 mg/L / 5%	Leeman Labs Direct Reading Echelle	Analytical wavelength: 766.490 nm, view: axial
Sulfate (SO ₄)	IC	0.3 mg/L / 3%	Dionex model 600 ion chromatograph with AG4A guard and AS4A separator columns and Anion Self-Regenerating Suppressor	1.8 mM NaHCO ₃ + 1.7 mM Na ₂ CO ₃ eluent (Brinton and others, 1995)
Alkalinity (as HCO ₃)	Titration	1.0 mg/L / 2%	Orion Research model 960/940 autotitrator, potentiometric detection, end-point determined by the first derivative technique	(Barringer and Johnsson, 1989)
Fluoride (F)	IC	0.1 mg/L / 4%	Dionex model 600 ion chromatograph with AG4A guard and AS4A separator columns and Anion Self-Regenerating Suppressor	.8 mM NaHCO ₃ + 1.7 mM Na ₂ CO ₃ eluent (Brinton and others, 1995)
Chloride (Cl)	IC	0.09 mg/L / 4%	Dionex model 600 ion chromatograph with AG4A guard and AS4A separator columns and Anion Self-Regenerating Suppressor	1.8 mM NaHCO ₃ + 1.7 mM Na ₂ CO ₃ eluent (Brinton and others, 1995)
Silica (SiO ₂)	ICP-AES	0.06 mg/L / 5%	Leeman Labs Direct Reading Echelle	Analytical wavelength: 251.611 nm, view: axial

Table A-1. Analytical techniques, detection limits, typical precision, equipment used, and analytical method references (continued).

Constituent	Analytical Technique	Detection limit ¹ / Typical precision ²	Equipment Used	Reference(s) and comments
Aluminum (Al)	ICP-AES	0.07 mg/L / 5%	Leeman Labs Direct Reading Echelle	Analytical wavelength: 308.215 nm, view: axial
	GFAAS ³	0.001 mg/L / 7%	Perkin-Elmer model 4110ZL	Analytical wavelength: 309.3 nm, modifier: 15 µg Mg(NO ₃) ₂ , atomization temperature: 2300°C
Total iron (Fe(T))	ICP-AES	0.007 mg/L / 5%	Leeman Labs Direct Reading Echelle	Analytical wavelength: 238.204. nm, view: axial
	Colorimetry	0.001 mg/L / 3%	Hewlett-Packard model 8452A diode array spectrometer with 1 and 5 cm cells	FerroZine method (Stookey, 1970; To and others, 1999)
Ferrous iron (Fe(II))	Colorimetry	0.002 mg/L / 3%	Hewlett-Packard model 8452A diode array spectrometer with 1 and 5 cm cells	(Stookey, 1970; To and others, 1999)
Boron (B)	ICP-AES	0.010 mg/L / 7%	Leeman Labs Direct Reading Echelle	Analytical wavelength: 249.678 nm, view: axial
	ICP-MS ⁴	0.002 mg/L / 5%	Perkin-Elmer SCIEX ELAN DRC II	Isotope: 11 (Garbarino and Taylor, 1995; Taylor and Garbarino, 1991)
Lithium (Li)	ICP-AES	0.001 mg/L / 5%	Leeman Labs Direct Reading Echelle	Analytical wavelength: 670.784 nm, view: axial
Strontium (Sr)	ICP-AES	0.0003 mg/L / 4%	Leeman Labs Direct Reading Echelle	Analytical wavelength: 421.552 nm, view: axial
Barium (Ba)	ICP-AES	0.0008 mg/L / 4%	Leeman Labs Direct Reading Echelle	Analytical wavelength: 455.403 nm, view: axial
Manganese (Mn)	ICP-AES	0.002 mg/L / 5%	Leeman Labs Direct Reading Echelle	Analytical wavelength: 257.610 nm, view: axial
Zinc (Zn)	ICP-AES	0.005 mg/L / 5%	Leeman Labs Direct Reading Echelle	Analytical wavelength: 206.200 nm, view: radial

Table A-1. Analytical techniques, detection limits, typical precision, equipment used, and analytical method references – Continued.

Constituent	Analytical Technique	Detection limit¹ / Typical precision²	Equipment Used	Reference(s) and comments
Lead (Pb)	ICP-AES	0.008 mg/L / 6%	Leeman Labs Direct Reading Echelle	Analytical wavelength: 220.353 nm, view: axial
	ICP-MS ⁴	0.00001 mg/L / 2%	Perkin-Elmer SCIEX ELAN DRC II	A weighted average of the 206, 207 and 208 isotopes was used (Garbarino and Taylor, 1995; Taylor and Garbarino, 1991)
Nickel (Ni)	ICP-AES	0.002 mg/L / 3%	Leeman Labs Direct Reading Echelle	Analytical wavelength: 231.604. nm, view: axial
	GFAAS ³	0.0005 mg/L / 5%	Perkin-Elmer model 4110ZL	Analytical wavelength: 231.604 nm, view: axial, atomization temperature: 2300°C
Copper (Cu)	ICP-AES	0.002 mg/L / 7%	Leeman Labs Direct Reading Echelle	Analytical wavelength: 324.754. nm, view: axial
Cadmium (Cd)	ICP-AES	0.002 mg/L / 5%	Leeman Labs Direct Reading Echelle	Analytical wavelength: 214.428. nm, view: axial
Chromium (Cr)	ICP-AES	0.002 mg/L / 5%	Leeman Labs Direct Reading Echelle	Analytical wavelength: 206.149. nm, view: axial

Table A-1. Analytical techniques, detection limits, typical precision, equipment used, and analytical method references – Continued.

Constituent	Analytical Technique	Detection limit¹ / Typical precision²	Equipment Used	Reference(s) and comments
Cobalt (Co)	ICP-AES	0.007 mg/L / 5%	Leeman Labs Direct Reading Echelle or	Analytical wavelength: 228.616. nm, view: axial
Beryllium (Be)	ICP-AES	0.001 mg/L / 4%	Leeman Labs Direct Reading Echelle	Analytical wavelength: 313.042 nm, view: axial
Molybdenum (Mo)	ICP-AES	0.007 mg/L / 7%	Leeman Labs Direct Reading Echelle	Analytical wavelength: 277.540 nm, view: axial
	ICP-MS	0.0005 mg/L / 3%	Perkin-Elmer SCIEX ELAN DRC II	Isotope: 95 (Garbarino and Taylor, 1995)
Vanadium (V)	ICP-AES	0.002 mg/L / 5%	Leeman Labs Direct Reading Echelle	Analytical wavelength: 292.401 nm, view: axial
	ICP-MS ⁴	0.0003 mg/L / 2%	Perkin-Elmer SCIEX ELAN DRC II	Isotope: 51 (Garbarino and Taylor, 1995)
Arsenic (As)	ICP-AES	0.04 mg/L / 7%	Leeman Labs Direct Reading Echelle	Analytical wavelength: 188.977. nm, view: axial
Selenium (Se)	ICP-AES	0.04 mg/L / ---	Leeman Labs Direct Reading Echelle	Analytical wavelength: 196.026. nm, view: axial
	ICP-MS	0.0002 mg/L / 3%	Perkin-Elmer SCIEX ELAN DRC II	Isotope: 77 (Garbarino and Taylor, 1995)

Table A-1. Analytical techniques, detection limits, typical precision, equipment used, and analytical method references – Continued.

Constituent	Analytical Technique	Detection limit¹ / Typical precision²	Equipment Used	Reference(s) and comments
Mercury (Hg)	CVAFS	0.4 ng/L / 4%	PS Analytical, model Galahad, direct cold-vapor atomic fluorescence spectrometry	Taylor and others (1997), Roth and others (2001)
Bismuth (Bi)	ICP-MS	0.001 µg/L / ---	Perkin-Elmer SCIEX ELAN DRC II	Isotope: 209
Cerium (Ce)	ICP-MS	0.0004 µg/L / 3%	Perkin-Elmer SCIEX ELAN DRC II	Isotope: 140 (Verplanck and others, 2001)
Cesium (Cs)	ICP-MS	0.002 µg/L / ---	Perkin-Elmer SCIEX ELAN DRC II	Isotope: 133
Dysprosium (Dy)	ICP-MS	0.0004 µg/L / 7%	Perkin-Elmer SCIEX ELAN DRC II	Isotope: 163 (Verplanck and others, 2001)
Erbium (Er)	ICP-MS	0.0004 µg/L / 6%	Perkin-Elmer SCIEX ELAN DRC II	Isotope: 167 (Verplanck and others, 2001)
Europium (Eu)	ICP-MS	0.001 µg/L / 5%	Perkin-Elmer SCIEX ELAN DRC II	Isotope: 151, problems with Ba interference (Verplanck and others, 2001)
Gadolinium (Gd)	ICP-MS	0.0006 µg/L / 3%	Perkin-Elmer SCIEX ELAN DRC II	Isotope: 158 (Verplanck and others, 2001)
Hafnium (Hf)	ICP-MS	0.0005 µg/L / ---	Perkin-Elmer SCIEX ELAN DRC II	Isotope: 178
Holmium (Ho)	ICP-MS	0.0002 µg/L / 3%	Perkin-Elmer SCIEX ELAN DRC II	Isotope: 165 (Verplanck and others, 2001)
Lanthanum (La)	ICP-MS	0.0004 µg/L / 3%	Perkin-Elmer SCIEX ELAN DRC II	Isotope: 139 (Verplanck and others, 2001)
Lutetium (Lu)	ICP-MS	0.0002 µg/L / 5%	Perkin-Elmer SCIEX ELAN DRC II	Isotope: 175 (Verplanck and others, 2001)
Neodymium (Nd)	ICP-MS	0.0008 µg/L / 3%	Perkin-Elmer SCIEX ELAN DRC II	Isotope: 146 (Verplanck and others, 2001)
Praseodymium (Pr)	ICP-MS	0.0002 µg/L / 3%	Perkin-Elmer SCIEX ELAN DRC II	Isotope: 141 (Verplanck and others, 2001)
Rubidium (Rb)	ICP-MS	0.001 µg/L / ---	Perkin-Elmer SCIEX ELAN DRC II	Isotope: 85

Table A-1. Analytical techniques, detection limits, typical precision, equipment used, and analytical method references – Continued.

Constituent	Analytical Technique	Detection limit ¹ / Typical precision ²	Equipment Used	Reference(s) and comments
Rhenium (Re)	ICP-MS	0.0007 µg/L / ---	Perkin-Elmer SCIEX ELAN DRC II	Isotope: 187
Antimony (Sb)	ICP-MS	0.004 µg/L / 2%	Perkin-Elmer SCIEX ELAN DRC II	Isotope: 121 (Garbarino and Taylor, 1995; Taylor and Garbarino, 1991)
Samarium (Sm)	ICP-MS	0.0008 µg/L / 3%	Perkin-Elmer SCIEX ELAN DRC II	Isotope: 147 (Verplanck and others, 2001)
Tantalum (Ta)	ICP-MS	0.002 µg/L / ---	Perkin-Elmer SCIEX ELAN DRC II	Isotope: 181
Terbium (Tb)	ICP-MS	0.0002 µg/L / 3%	Perkin-Elmer SCIEX ELAN DRC II	Isotope: 159 (Verplanck and others, 2001)
Tellurium (Te)	ICP-MS	0.008 µg/L / ---	Perkin-Elmer SCIEX ELAN DRC II	Isotope: 126
Thorium (Th)	ICP-MS	0.001 µg/L / ---	Perkin-Elmer SCIEX ELAN DRC II	Isotope: 232
Thallium (Tl)	ICP-MS	0.004 µg/L / 3%	Perkin-Elmer SCIEX ELAN DRC II	Isotope: 205 (Garbarino and Taylor, 1995; Taylor and Garbarino, 1991)
Thulium (Tm)	ICP-MS	0.0002 µg/L / 4%	Perkin-Elmer SCIEX ELAN DRC II	Isotope: 169 (Verplanck and others, 2001)
Uranium (U)	ICP-MS	0.0005 µg/L / 3%	Perkin-Elmer SCIEX ELAN DRC II	Isotope: 238 (Garbarino and Taylor, 1995; Taylor and Garbarino, 1991)
Tungsten (W)	ICP-MS	0.006 µg/L / 6%	Perkin-Elmer SCIEX ELAN DRC II	Isotope: 182
Yttrium (Y)	ICP-MS	0.0003 µg/L / 3%	Perkin-Elmer SCIEX ELAN DRC II	Isotope: 89
Ytterbium (Yb)	ICP-MS	0.0005 µg/L / 4%	Perkin-Elmer SCIEX ELAN DRC II	Isotope: 174 (Verplanck and others, 2001)
Zirconium (Zr)	ICP-MS	0.001 µg/L / ---	Perkin-Elmer SCIEX ELAN DRC II	Isotope: 90
Dissolved organic carbon (DOC)	TOC	0.1 mg/L	Oceanography International Model 700 TOC Analyzer	Wet oxidation method (Aiken, 1992)

Table A-1. Analytical techniques, detection limits, typical precision, equipment used, and analytical method references – Continued.

Constituent	Analytical Technique	Detection limit ¹ / Typical precision ²	Equipment Used	Reference(s) and comments
Hydrogen sulfide (H ₂ S)	ISE	0.002 mg/L	Accumet model 13-620-551 Silver/Sulfide combination electrode	Sample mixed 1:1 on-site with Orion Research 941609 Sulfide Anti-Oxidant Buffer and analyzed within 24 hours of collection (APHA, 1998)
¹⁸ O/ ¹⁶ O (δ ¹⁸ O)	MS	0.1 per mil ²	DuPont model 21-491 mass spectrometer	Standardization against Vienna Standard Mean Ocean Water (VSMOW) (δ ¹⁸ O = 0 per mil) and Standard Light Antarctic Precipitation (SLAP) (δ ¹⁸ O = -55.5 per mil) (Epstein and Mayeda, 1953)
² H/ ¹ H (δ ² H)	MS	0.1 per mil ²	V.G. Micromass model 602 mass spectrometer	Standardization against VSMOW (δ ² H = 0 per mil) and SLAP (δ ² H = -428 per mil) (Coplen and others, 1991)

¹Some samples were diluted for ICP-MS analysis; reported detection limits must be multiplied by the dilution factor for these samples (for example, the detection limit for a sample diluted to 1:10 is ten times the undiluted detection limit reported in this table).

²Percent relative standard deviations, or precision, are for analyte concentrations greater than 10 times the detection limit and less than the high standard. Percent relative standard deviations are based on several analytical runs. The precision likely would be better for any single analytical run.

Appendix B: Quality Assurance Quality Control

Table B-1. Results for standard reference water samples.

Constituent		Technique	SRWS	n	mean	MPV
Al	mg/L	ICP-AES	T197	2	0.098	0.110
Al	mg/L	ICP-AES	T199	2	0.094	0.092
Al	µg/L	ICP-MS	T135	6	12.9	10.5
Al	µg/L	ICP-MS	T173	6	69.9	71
Al	µg/L	ICP-MS	T175	6	52.9	52
Alkalinity (as CaCO ₃)	mg/L	Titration	M186	2	50.5	50.4
Alkalinity (as CaCO ₃)	mg/L	Titration	M182	2	23.3	24.0
As	mg/L	ICP-AES	T173	2	<0.03	0.003
As	mg/L	ICP-AES	T197	2	<0.03	0.001
As	mg/L	ICP-AES	T199	2	<0.03	0.000
As	µg/L	ICP-MS	T135	6	10.2	10
As	µg/L	ICP-MS	T173	6	2.65	2.67
As	µg/L	ICP-MS	T175	6	7.46	7.38
B	µg/L	ICP-MS	T135	6	12.1	13.1
B	µg/L	ICP-MS	T173	6	157	158
B	µg/L	ICP-MS	T175	6	51.3	48.3
Ba	mg/L	ICP-AES	T173	2	0.042	0.042
Ba	mg/L	ICP-AES	T197	2	0.036	0.036
Ba	mg/L	ICP-AES	T199	2	0.007	0.007
Ba	µg/L	ICP-MS	T135	6	68.2	67.8
Ba	µg/L	ICP-MS	T173	6	41.4	42.2
Ba	µg/L	ICP-MS	T175	6	17.8	18
Be	mg/L	ICP-AES	T173	2	0.002	0.002
Be	µg/L	ICP-MS	T135	6	59.0	59
Be	µg/L	ICP-MS	T173	6	1.91	2
Be	µg/L	ICP-MS	T175	6	2.99	2.92
Br	mg/L	IC	M186	2	1.42	1.42
Br	mg/L	IC	M192	2	0.200	0.191
Ca	mg/L	ICP-AES	T173	2	34.9	34.8
Ca	mg/L	ICP-AES	T197	2	54.3	55.0
Ca	mg/L	ICP-AES	T199	2	3.72	3.8
Cd	mg/L	ICP-AES	T173	2	0.001	0.001
Cd	mg/L	ICP-AES	T197	2	0.003	0.003
Cd	mg/L	ICP-AES	T199	2	0.001	0.002
Cd	µg/L	ICP-MS	T135	6	50.5	50.5

Table B-1. Results for standard reference water samples – Continued.

Constituent		Technique	SRWS	n	mean	MPV
Cd	µg/L	ICP-MS	T173	6	1.26	1.26
Cd	µg/L	ICP-MS	T175	6	8.35	8.2
Ce	µg/L	ICP-MS	PPREE (1:100)	4	1.63	1.63
Ce	µg/L	ICP-MS	SCREE (1:100)	4	0.252	0.246
Cl	mg/L	IC	M186	2	24.6	23.6
Cl	mg/L	IC	M192	2	12.9	12.9
Co	mg/L	ICP-AES	T173	2	<0.003	0.001
Co	mg/L	ICP-AES	T197	2	0.005	0.006
Co	µg/L	ICP-MS	T135	6	40.0	40
Co	µg/L	ICP-MS	T173	6	1.21	1.26
Co	µg/L	ICP-MS	T175	6	7.46	7.44
Cr	mg/L	ICP-AES	T173	2	0.004	0.005
Cr	mg/L	ICP-AES	T197	2	<0.002	0.001
Cr	mg/L	ICP-AES	T199	2	<0.002	0.001
Cr	µg/L	ICP-MS	T135	6	79.0	79
Cr	µg/L	ICP-MS	T173	6	4.77	4.88
Cr	µg/L	ICP-MS	T175	6	1.99	1.93
Cu	mg/L	ICP-AES	T173	2	0.007	0.008
Cu	mg/L	ICP-AES	T197	2	0.028	0.028
Cu	mg/L	ICP-AES	T199	2	<0.003	0.002
Cu	µg/L	ICP-MS	T135	6	62.0	62
Cu	µg/L	ICP-MS	T173	6	7.33	7.5
Cu	µg/L	ICP-MS	T175	6	1.98	1.85
Dy	µg/L	ICP-MS	PPREE (1:100)	4	0.215	0.22
Dy	µg/L	ICP-MS	SCREE (1:100)	4	0.084	0.0814
Er	µg/L	ICP-MS	PPREE (1:100)	4	0.117	0.12
Er	µg/L	ICP-MS	SCREE (1:100)	4	0.045	0.0437
Eu	µg/L	ICP-MS	PPREE (1:100)	4	0.060	0.06
Eu	µg/L	ICP-MS	SCREE (1:100)	4	0.015	0.0148
F	mg/L	IC	M186	2	0.854	0.960
F	mg/L	IC	M192	2	0.125	0.128
Fe	mg/L	ICP-AES	T173	2	0.022	0.021
Fe	mg/L	ICP-AES	T197	2	1.91	1.900
Fe	mg/L	ICP-AES	T199	2	0.161	0.171

Table B-1. Results for standard reference water samples – Continued.

Constituent		Technique	SRWS	n	mean	MPV
Fe	mg/L	FerroZine	T173	1	0.0214	0.0214
Gd	µg/L	ICP-MS	PPREE (1:100)	4	0.236	0.24
Gd	µg/L	ICP-MS	SCREE (1:100)	4	0.092	0.0829
Hg	ng/L	CVAAS	Hg7	3	3.1	2.2
Hg	ng/L	CVAAS	Hg8	3	13.8	14.3
Hg	ng/L	CVAAS	Hg21	3	27.7	30.3
Hg	ng/L	CVAAS	Hg27	3	7.1	8.2
Ho	µg/L	ICP-MS	PPREE (1:100)	4	0.044	0.0443
Ho	µg/L	ICP-MS	SCREE (1:100)	4	0.017	0.0162
K	mg/L	ICP-AES	T173	2	3.80	3.85
K	mg/L	ICP-AES	T197	2	5.07	5.37
K	mg/L	ICP-AES	T199	2	1.61	1.87
La	µg/L	ICP-MS	PPREE (1:100)	4	0.804	0.804
La	µg/L	ICP-MS	SCREE (1:100)	4	0.102	0.099
Li	mg/L	ICP-AES	T173	2	0.019	0.017
Li	mg/L	ICP-AES	T197	2	0.010	0.009
Li	mg/L	ICP-AES	T199	2	<0.001	0.001
Li	µg/L	ICP-MS	T135	6	62.3	73.7
Li	µg/L	ICP-MS	T173	6	17.1	17.1
Li	µg/L	ICP-MS	T175	6	3.09	3.2
Lu	µg/L	ICP-MS	PPREE (1:100)	4	0.011	0.0111
Lu	µg/L	ICP-MS	SCREE (1:100)	4	0.005	0.00453
Mg	mg/L	ICP-AES	T173	2	9.10	9.38
Mg	mg/L	ICP-AES	T199	2	6.18	6.20
Mn	mg/L	ICP-AES	T173	2	0.509	0.495
Mn	mg/L	ICP-AES	T197	2	1.64	1.59
Mn	mg/L	ICP-AES	T199	2	0.012	0.014
Mn	µg/L	ICP-MS	T135	6	422	423
Mn	µg/L	ICP-MS	T173	6	497	495
Mn	µg/L	ICP-MS	T175	6	47.0	49.4
Mo	µg/L	ICP-MS	T135	6	62.9	63
Mo	µg/L	ICP-MS	T173	6	7.25	7.22
Mo	µg/L	ICP-MS	T175	6	1.87	1.79
Na	mg/L	ICP-AES	T173	2	37.1	36.5

Table B-1. Results for standard reference water samples – Continued.

Constituent		Technique	SRWS	n	mean	MPV
Na	mg/L	ICP-AES	T197	2	38.9	37.8
Na	mg/L	ICP-AES	T199	2	7.59	7.72
Nd	µg/L	ICP-MS	PPREE (1:100)	4	0.932	0.934
Nd	µg/L	ICP-MS	SCREE (1:100)	4	0.233	0.222
Ni	mg/L	ICP-AES	T173	2	0.004	0.005
Ni	mg/L	ICP-AES	T197	2	0.018	0.019
Ni	mg/L	ICP-AES	T199	2	0.0004	0.0004
Ni	µg/L	ICP-MS	T135	6	65.7	65.6
Ni	µg/L	ICP-MS	T173	6	4.25	5.38
Ni	µg/L	ICP-MS	T175	6	3.12	3.18
Pb	mg/L	ICP-AES	T173	2	<0.007	0.005
Pb	mg/L	ICP-AES	T197	2	<0.007	0.002
Pb	mg/L	ICP-AES	T199	2	<0.007	0.001
Pb	µg/L	ICP-MS	T135	6	103	103
Pb	µg/L	ICP-MS	T173	6	4.73	4.59
Pb	µg/L	ICP-MS	T175	6	3.10	3
Pr	µg/L	ICP-MS	PPREE (1:100)	4	0.211	0.212
Pr	µg/L	ICP-MS	SCREE (1:100)	4	0.045	0.0431
Sb	mg/L	ICP-AES	T173	2	<0.02	0.005
Sb	mg/L	ICP-AES	T197	2	<0.02	0.000
Sb	mg/L	ICP-AES	T199	2	<0.02	0.000
Sb	µg/L	ICP-MS	T135	6	80.7	76.3
Sb	µg/L	ICP-MS	T173	6	5.25	5.2
Sb	µg/L	ICP-MS	T175	6	1.95	1.9
Se	mg/L	ICP-AES	T173	2	<0.03	0.002
Se	mg/L	ICP-AES	T197	2	<0.03	0.001
Se	mg/L	ICP-AES	T199	2	<0.03	0.000
Se	µg/L	ICP-MS	T135	6	12	10
Se	µg/L	ICP-MS	T173	6	2.25	2.47
Se	µg/L	ICP-MS	T175	6	2.30	2.1
SiO ₂	mg/L	ICP-AES	T173	2	11.3	11.1
SiO ₂	mg/L	ICP-AES	T197	2	14.4	14.2
SiO ₂	mg/L	ICP-AES	T199	2	5.59	5.46
Sm	µg/L	ICP-MS	PPREE (1:100)	4	0.202	0.204

Table B-1. Results for standard reference water samples – Continued.

Constituent		Technique	SRWS	n	mean	MPV
Sm	µg/L	ICP-MS	SCREE (1:100)	4	0.071	0.0674
SO ₄	mg/L	IC	M186	2	14.9	14.6
SO ₄	mg/L	IC	M192	2	4.76	4.54
Sr	mg/L	ICP-AES	T173	2	0.296	0.279
Sr	mg/L	ICP-AES	T197	2	0.440	0.407
Sr	mg/L	ICP-AES	T199	2	0.017	0.021
Sr	µg/L	ICP-MS	T135	6	45.6	46
Sr	µg/L	ICP-MS	T173	6	279	279
Sr	µg/L	ICP-MS	T175	6	62.5	63.6
Tb	µg/L	ICP-MS	PPREE (1:100)	4	0.035	0.0367
Tb	µg/L	ICP-MS	SCREE (1:100)	4	0.013	0.0134
Tl	µg/L	ICP-MS	T173	6	5.93	5.94
Tl	µg/L	ICP-MS	T175	6	1.98	1.97
Tm	µg/L	ICP-MS	PPREE (1:100)	4	0.015	0.0148
Tm	µg/L	ICP-MS	SCREE (1:100)	4	0.006	0.00585
U	µg/L	ICP-MS	T173	6	1.94	1.92
U	µg/L	ICP-MS	T175	6	1.46	1.48
V	mg/L	ICP-AES	T173	2	0.004	0.004
V	mg/L	ICP-AES	T197	2	<0.001	0.001
V	mg/L	ICP-AES	T199	2	<0.001	0.001
V	µg/L	ICP-MS	T135	6	52.8	52.8
V	µg/L	ICP-MS	T173	6	4.11	4.31
V	µg/L	ICP-MS	T175	6	2.87	2.94
Y	µg/L	ICP-MS	PPREE (1:100)	4	1.35	1.348
Y	µg/L	ICP-MS	SCREE (1:100)	4	0.478	0.472
Yb	µg/L	ICP-MS	PPREE (1:100)	4	0.081	0.0818
Yb	µg/L	ICP-MS	SCREE (1:100)	4	0.036	0.034
Zn	mg/L	ICP-AES	T173	2	0.360	0.348
Zn	mg/L	ICP-AES	T197	2	1.11	1.100
Zn	mg/L	ICP-AES	T199	2	0.004	0.006
Zn	µg/L	ICP-MS	T135	6	46.9	48.2
Zn	µg/L	ICP-MS	T173	6	332	348
Zn	µg/L	ICP-MS	T175	6	72.8	71.6

Appendix C: Water Chemistry Analyses

Site data and water analyses are presented in Tables C-1 to C-3. Results of field parameters, water analyses for constituent concentrations greater than 0.002 mg/L, and sampling coordinates are shown in Table C-1. Trace element concentrations (less than 0.002 mg/L) are reported in Table C-2, water isotope determinations ($\delta^{18}\text{O}$ and δD) are reported in Table C-3. Photographs of most of the samples sites are in Appendix D.

Table C-1. Results of water analyses, field parameters, and sampling coordinates.

Site ID		1	2	3	4	5	6
Location		Serpentine Hot Spring	Arctic Hot Springs - above old bath house	Arctic Hot Springs - upper site	Cold water intake for bath house	Hot Springs Creek - North Fork	Hot Springs Creek - South Fork
Collection Date		6/23/2010	6/24/2010	6/24/2010	6/23/2010	6/25/2010	6/25/2010
Collection Time		16:30	12:30	14:00	15:30	11:30	12:30
Field Determinations							
pH		7.52	7.47	7.23	7.64	7.47	6.32
Specific Conductance	μS/cm	4535	4570	4750	4660	126	28
Temperature	°C	74.8	72.8	36.3	61	6.5	5.2
Flow Cell Temperature	°C	60.6	66	34.1	52.8	9.7	11.1
DO	mg/L	0.6	<0.05	5.2	2.45	11.5	11.8
DOC	mg/L	1	1.9	2.7	0.9	3.2	7.3
Eh	V	-0.064	-0.086	0.154	-0.019	0.394	0.394
H ₂ S	mg/L	1.04	0.944	0.054	0.627	---	---
Constituent							
Ca	mg/L	84.5	84.6	79.3	84.1	15.6	1.3
Mg	mg/L	0.312	0.317	0.259	0.306	2.56	0.59
Na	mg/L	789	789	807	797	2.2	2.24
K	mg/L	37.3	36.7	41.7	37.4	0.737	0.313
Li	mg/L	4.91	4.95	5.26	5.01	<0.001	<0.001
Cs	mg/L	0.606	0.607	0.760	0.618	<0.000003	<0.000003
Rb	mg/L	0.527	0.522	0.619	0.530	0.0013	0.0010
Sr	mg/L	2.52	2.64	2.51	2.61	0.060	0.009
Ba	mg/L	0.049	0.049	0.053	0.049	0.01	0.009
SO ₄	mg/L	4.89	4.17	2.8	4.22	31.8	1.72
S ₂ O ₃	mg/L	0.7	<0.1	<0.1	---	---	---
Alkalinity as HCO ₃ ⁻	mg/L	56.8	56.1	59.5	58	24.9	10.5
F	mg/L	7.26	7.17	7.96	7.12	0.07	0.07
Cl	mg/L	1460	1430	1460	1480	6.28	2.53
Br	mg/L	5.41	5.43	5.84	5.75	<0.05	<0.05
NO ₃	mg/L	<0.05	0.43	1.17	<0.05	<0.05	0.23
NH ₄	mg/L	1.2	1.4	1.9	1.2	<0.1	<0.1
SiO ₂	mg/L	80.2	80.8	78	81.2	5.71	6.82
B	mg/L	3.53	3.64	3.72	3.74	0.0019	0.0024
Al	mg/L	0.0090	0.0054	0.0078	0.033	0.023	0.102
Fe(T)	mg/L	0.004	0.003	0.434	0.008	0.010	1.19
Fe(II)	mg/L	0.004	0.003	0.22	0.008	0.01	0.406
Mn	mg/L	0.031	0.034	0.044	0.030	0.0015	0.076
W	mg/L	0.055	0.054	0.070	0.054	0.00003	<0.00002
EPMA _n	meq	40.4	40.4	41.1	40.7	1.07	0.25
EPMA _c	meq	42.6	41.9	42.6	43.2	1.22	0.28
Speciated CI	%	-5.4	-3.8	-3.6	-5.9	-12.7	-11.3
SCI	%	-3.8	-5.1	-3.4	-3.6	6.2	2.0

EPMA_n, equivalents per million for anions; EPMA_c, equivalents per million for cations; CI, charge imbalance; SCI, specific conductance imbalance

Table C-1. Results of water analyses, field parameters, and sampling coordinates — Continued.

Site ID		7	8	9	10	11	12
Location		Hot Springs Creek - upstream from bath house	Pooled up water south east of bathhouse	outflow from bath house / stream south of bath house	Hot Springs Creek - about 200 m downstream from bath house	Hot Springs Creek - above Arctic Hot Springs	Hot Springs Creek - downstream from Arctic Hot Springs
Collection Date		6/23/2010	6/23/2010	6/23/2010	6/23/2010	6/24/2010	6/24/2010
Collection Time		12:45	13:30	11:00	9:40	14:35	11:30
Field Determinations							
pH		6.87	6.80	6.96	7.15	7.25	7.30
Specific Conductance	µS/cm	99	101	121	198	232	235
Temperature	°C	7.2	7.4	6.8	6.6	9.5	7.8
Flow Cell Temperature	°C	10.8	10.7	10.7	7.5	13.3	10.4
DO	mg/L	12.2	11.7	12.4	12.2	12.3	12.3
DOC	mg/L	3.8	4.5	3.5	10.9	4.9	4.9
Eh	V	0.378	---	0.268	0.279	0.274	0.349
H2S	mg/L	---	---	0.004	0.004	0.003	0.003
Constituent							
Ca	mg/L	11	10.8	11.1	12.1	10.5	10.8
Mg	mg/L	1.93	1.9	1.91	1.95	1.56	1.51
Na	mg/L	2.98	3.29	6.78	18.7	21.45	26.85
K	mg/L	0.648	0.674	0.763	1.38	1.34	1.69
Li	mg/L	0.006	0.009	0.028	0.099	0.109	0.143
Cs	mg/L	0.00041	0.0005	0.0031	0.012	0.014	0.019
Rb	mg/L	0.0017	0.0020	0.0044	0.013	0.014	0.018
Sr	mg/L	0.047	0.048	0.060	0.099	0.098	0.116
Ba	mg/L	0.012	0.012	0.013	0.017	0.014	0.014
SO4	mg/L	22.7	21	21.3	20.9	18.1	17
S2O3	mg/L	---	---	---	---	---	---
Alkalinity as HCO3-	mg/L	19.6	19.7	19.8	20.3	18.4	18.8
F	mg/L	0.06	0.12	0.08	0.14	0.24	0.28
Cl	mg/L	3.55	3.98	10	31.4	37.2	46.1
Br	mg/L	<0.05	<0.05	<0.05	0.13	0.14	0.18
NO3	mg/L	0.43	0.23	0.17	1.04	0.28	0.24
NH4	mg/L	<0.1	<0.1	<0.1	<0.1	<0.1	<0.1
SiO2	mg/L	5.89	5.93	6.47	7.63	7.4	8.05
B	mg/L	0.0052	0.0067	0.020	0.065	0.076	0.109
Al	mg/L	0.037	0.034	0.112	0.597	0.047	0.054
Fe(T)	mg/L	0.301	0.297	0.337	0.646	0.326	0.382
Fe(II)	mg/L	0.160	0.187	0.125	0.281	0.191	0.205
Mn	mg/L	0.021	0.029	0.033	0.028	0.024	0.023
W	mg/L	0.00008	0.00002	0.00025	0.00065	0.0013	0.0017
EPMA _n	meq	0.85	0.85	1.02	1.63	1.63	1.89
EPMCat	meq	0.88	0.86	1.04	1.66	1.73	1.97
Speciated Cl	%	-4.6	-1.7	-1.5	-1.8	-5.9	-3.9
SCI	%	1.5	-1.8	-0.5	-1.2	-12.8	-1.0

Table C-1. Water analyses, field parameters, and sampling coordinates — Continued.

Site ID	13	20	27	34	35	37
Location	Unnamed Spring	moderate size, high-gradient stream below continental divide	hillside seep NE of Serpentine HS	spring orifice that debouches into a well-defined, narrow perennial channel	flow-through pool on continental divide	headwaters of north fork Hot Spring Creek below continental divide
Collection Date	6/23/2010	6/23/2010	6/24/2010	6/24/2010	6/24/2010	6/24/2010
Collection Time						
Field Determinations						
pH	6.85	7.71	6.85	6.81	7.94	7.94
Specific Conductance	μS/cm 34.9	240	19.8	99.9	182	---
Temperature	°C 2.8	6.2	4.3	1	15.4	---
Flow Cell Temperature	°C ---	---	---	---	---	---
DO	mg/L ---	---	---	---	---	---
DOC	mg/L ---	---	---	---	---	---
Eh	V ---	---	---	---	---	---
H2S	mg/L ---	---	---	---	---	---
Constituent						
Ca	mg/L 0.84	32.7	0.779	9.86	21.3	49.8
Mg	mg/L 0.445	5.791	0.351	1.623	0.644	8.885
Na	mg/L 2.47	1.99	2.13	2.93	1.63	1.50
K	mg/L 0.058	0.786	0.073	0.491	0.655	0.155
Li	mg/L 0.001	<0.001	0.001	<0.001	<0.001	<0.001
Cs	mg/L ---	---	---	---	---	---
Rb	mg/L ---	---	---	---	---	---
Sr	mg/L 0.011	0.119	0.004	0.040	0.037	0.207
Ba	mg/L 0.009	0.015	0.009	0.029	0.005	0.001
SO4	mg/L 1.1	72	0.9	30.7	4.3	121
S2O3	mg/L ---	---	---	---	---	---
Alkalinity as HCO3-	mg/L 15.2	42.5	8.0	21.9	64.3	48.5
F	mg/L 0.16	0.10	0.43	0.08	0.09	0.10
Cl	mg/L 2.9	1.7	2.0	1.7	1.2	1.2
Br	mg/L <0.05	<0.06	<0.07	<0.08	<0.09	<0.10
NO3	mg/L <0.1	<0.1	<0.1	0.2	<0.1	0.3
NH4	mg/L ---	---	---	---	---	---
SiO2	mg/L 5.99	4.14	5.10	6.92	7.22	1.86
B	mg/L <0.01	<0.01	<0.01	<0.01	<0.01	<0.01
Al	mg/L 0.533	<0.08	<0.08	<0.08	<0.08	<0.08
Fe(T)	mg/L 0.235	0.006	0.092	0.027	0.011	<0.003
Fe(II)	mg/L ---	---	---	---	---	---
Mn	mg/L 0.002	<0.001	0.004	0.002	0.010	<0.001
W	mg/L ---	---	---	---	---	---
EPMA _n	meq 0.36	2.11	0.23	1.03	1.17	3.03
EPMA _{cat}	meq 0.22	2.08	0.17	0.75	1.19	2.96
Speciated Cl	% -48.2	-1.4	-31.7	-31.8	2.1	-2.3
SCI	% -17.2	-1.1	7.3	4.6	-35.0	---

Table C-2. Water analyses for trace elements (<0.002 mg/L).

Site ID		1	2	3	4	5	6
Cu	µg/L	0.2	0.2	0.6	0.4	0.58	1.1
Zn	µg/L	0.9	0.3	0.5	2.4	1.3	0.99
Cd	µg/L	< 0.007	< 0.007	< 0.007	0.007	0.029	0.0100
Cr	µg/L	<0.7	<0.5	<0.6	<0.9	0.05	0.22
Co	µg/L	0.1	3	0.1	0.4	0.64	1.4
Ni	µg/L	< 2	< 2	< 2	2	0.22	0.90
Pb	µg/L	0.05	0.06	0.07	0.07	0.009	0.060
Be	µg/L	0.76	0.84	0.31	0.63	0.024	0.044
V	µg/L	< 1	< 1	< 1	< 1	< 0.1	0.8
Mo	µg/L	< 0.7	< 0.7	< 0.7	< 0.7	0.14	< 0.07
Sb	µg/L	< 0.03	0.13	0.04	0.07	0.10	0.054
Se	µg/L	< 0.6	< 0.6	< 0.6	< 0.6	0.17	< 0.06
As	µg/L	<1	<1	<2	<1	0.16	0.64
Bi	µg/L	< 0.08	< 0.08	< 0.08	< 0.08	< 0.008	< 0.008
Ce	µg/L	0.014	0.011	0.082	0.032	0.51	7.5
Dy	µg/L	< 0.001	< 0.001	0.005	0.002	0.039	0.25
Er	µg/L	0.002	< 0.001	0.004	< 0.001	0.025	0.15
Eu	µg/L	< 0.0008	< 0.0008	0.0013	< 0.0008	0.0055	0.039
Ga	µg/L	1.2	1.1	0.32	1.1	0.0047	0.047
Gd	µg/L	0.0034	0.0016	0.0086	0.0027	0.045	0.28
Hg	ng/L	2.3	3.9	1.8	3.5	1.5	1.9
Ho	µg/L	< 0.0003	< 0.0003	0.0010	< 0.0003	0.0081	0.048
La	µg/L	0.011	0.009	0.045	0.020	0.36	3.0
Lu	µg/L	< 0.0009	< 0.0009	0.0010	< 0.0009	0.0052	0.024
Nd	µg/L	0.005	0.004	0.036	0.014	0.380	3.1
P	µg/L	< 40	< 40	43	50	< 4	7
Pr	µg/L	0.0014	0.0019	0.010	0.0036	0.099	0.85
Re	µg/L	< 0.001	< 0.001	< 0.001	< 0.001	0.0080	0.0002
Sm	µg/L	< 0.002	0.003	0.008	0.003	0.071	0.49
Sn	µg/L	< 0.2	< 0.2	< 0.2	< 0.2	< 0.02	< 0.02
Tb	µg/L	< 0.001	< 0.001	0.002	< 0.001	0.0063	0.044
Te	µg/L	< 0.02	0.02	< 0.02	< 0.02	0.003	< 0.002
Th	µg/L	< 0.07	< 0.07	< 0.07	< 0.07	0.084	0.94
Tl	µg/L	0.90	0.87	0.069	0.87	0.0034	0.0053
Tm	µg/L	< 0.0003	< 0.0003	0.0004	< 0.0003	0.0040	0.022
U	µg/L	0.026	< 0.01	0.078	0.16	0.90	1.0
Y	µg/L	0.023	0.020	0.047	0.028	0.24	1.3
Yb	µg/L	0.001	< 0.001	0.003	0.002	0.032	0.15
Zr	µg/L	0.28	0.29	0.30	1.1	0.084	0.50

Table C-2. Water analyses for trace elements (<0.002 mg/L) — Continued.

Site ID		7	8	9	10	11	12
Cu	µg/L	0.69	0.72	0.79	1.4	0.80	0.83
Zn	µg/L	0.82	0.91	1.4	3.6	0.55	0.70
Cd	µg/L	0.017	0.018	0.021	0.025	0.015	0.015
Cr	µg/L	0.15	0.09	0.18	0.74	0.11	0.11
Co	µg/L	1.7	0.73	0.25	0.40	0.33	1.2
Ni	µg/L	0.46	0.42	0.45	0.91	0.38	0.46
Pb	µg/L	0.031	0.026	0.10	0.46	0.030	0.039
Be	µg/L	0.028	0.022	0.032	0.069	0.042	0.044
V	µg/L	0.3	0.3	0.5	1.3	0.4	0.4
Mo	µg/L	0.14	0.08	0.10	0.34	0.08	0.10
Sb	µg/L	0.17	0.082	0.074	0.077	0.065	0.12
Se	µg/L	0.07	0.08	< 0.06	< 0.06	< 0.06	< 0.06
As	µg/L	0.27	0.27	0.32	0.50	0.33	0.32
Bi	µg/L	< 0.008	< 0.008	< 0.008	< 0.008	< 0.008	< 0.008
Ce	µg/L	2.2	2.1	2.4	5.3	3.3	3.7
Dy	µg/L	0.084	0.077	0.091	0.18	0.11	0.12
Er	µg/L	0.050	0.046	0.051	0.091	0.061	0.066
Eu	µg/L	0.012	0.011	0.014	0.029	0.016	0.019
Ga	µg/L	0.016	0.016	0.037	0.17	0.036	0.042
Gd	µg/L	0.093	0.085	0.10	0.19	0.12	0.14
Hg	ng/L	2.9	1.5	2.0	4.2	1.8	1.7
Ho	µg/L	0.016	0.015	0.018	0.033	0.021	0.023
La	µg/L	1.1	1.1	1.2	2.6	1.6	1.9
Lu	µg/L	0.0088	0.0080	0.0092	0.015	0.011	0.012
Nd	µg/L	0.92	0.90	1.0	2.1	1.3	1.5
P	µg/L	< 4	< 4	< 4	13	< 4	< 4
Pr	µg/L	0.26	0.25	0.29	0.61	0.37	0.42
Re	µg/L	0.0057	0.0051	0.0054	0.0054	0.0039	0.0042
Sm	µg/L	0.15	0.15	0.17	0.34	0.20	0.23
Sn	µg/L	< 0.02	< 0.02	< 0.02	0.05	< 0.02	< 0.02
Tb	µg/L	0.014	0.013	0.016	0.031	0.018	0.022
Te	µg/L	0.002	< 0.002	0.002	0.002	0.003	0.002
Th	µg/L	0.20	0.20	0.25	0.66	0.34	0.31
Tl	µg/L	0.0044	0.0054	0.0095	0.029	0.019	0.028
Tm	µg/L	0.0070	0.0068	0.0077	0.014	0.0093	0.010
U	µg/L	0.64	0.60	0.65	1.1	0.69	0.70
Y	µg/L	0.47	0.45	0.49	0.90	0.59	0.66
Yb	µg/L	0.053	0.052	0.055	0.096	0.065	0.071
Zr	µg/L	0.17	0.16	0.18	0.25	0.24	0.24

Table C-2. Water analyses for trace elements (<0.002 mg/L) — Continued.

Site ID		13	20	27	34	35	37
Cu	µg/L	<3	<3	<3	<3	<3	<3
Zn	µg/L	<2	<2	4	2	<2	<2
Cd	µg/L	<1	<1	<1	1	<1	<1
Cr	µg/L	<2	<2	<2	<2	<2	<2
Co	µg/L	<3	<3	<3	<3	<3	<3
Ni	µg/L	<2	<2	<2	6	<2	<2
Pb	µg/L	<7	<7	<7	<7	<7	<7
Be	µg/L	<0.5	<0.5	<0.5	<0.5	<0.5	<0.5
V	µg/L	<1	1	2	2	<1	<1
Mo	µg/L	<5	6	<5	<5	<5	10
Sb	µg/L	<20	<20	<20	<20	<20	<20
Se	µg/L	<30	<30	<30	<30	<30	<30
As	µg/L	<30	<30	<30	<30	<30	<30
Bi	µg/L	---	---	---	---	---	---
Ce	µg/L	---	---	---	---	---	---
Dy	µg/L	---	---	---	---	---	---
Er	µg/L	---	---	---	---	---	---
Eu	µg/L	---	---	---	---	---	---
Ga	µg/L	---	---	---	---	---	---
Gd	µg/L	---	---	---	---	---	---
Hg	ng/L	---	---	---	---	---	---
Ho	µg/L	---	---	---	---	---	---
La	µg/L	---	---	---	---	---	---
Lu	µg/L	---	---	---	---	---	---
Nd	µg/L	---	---	---	---	---	---
P	µg/L	---	---	---	---	---	---
Pr	µg/L	---	---	---	---	---	---
Re	µg/L	---	---	---	---	---	---
Sm	µg/L	---	---	---	---	---	---
Sn	µg/L	---	---	---	---	---	---
Tb	µg/L	---	---	---	---	---	---
Te	µg/L	---	---	---	---	---	---
Th	µg/L	---	---	---	---	---	---
Tl	µg/L	---	---	---	---	---	---
Tm	µg/L	---	---	---	---	---	---
U	µg/L	---	---	---	---	---	---
Y	µg/L	---	---	---	---	---	---
Yb	µg/L	---	---	---	---	---	---
Zr	µg/L	---	---	---	---	---	---

Table C-3. Water isotope data.

Site ID	Location	Collection Date	$\delta^{18}\text{O}$ (‰)	δD (‰)
1	Serpentine Hot Spring	6/23/2010	-15.50	-122.15
2	Arctic Hot Springs - above old bath house	6/24/2010	-15.50	-122.99
3	Arctic Hot Springs - upper site	6/24/2010	-14.84	-118.70
4	Cold water intake for bath house	6/23/2010	-15.43	-123.13
5	Hot Springs Creek - North Fork	6/25/2010	-17.36	-127.91
6	Hot Springs Creek - South Fork	6/25/2010	-17.15	-128.33
7	Hot Springs Creek - upstream from bath house	6/23/2010	-17.50	-130.93
8	Pooled up water south east of bathhouse	6/23/2010	-17.46	-129.80
9	outflow from bath house / stream south of bath house	6/23/2010	-17.53	-130.10
10	Hot Springs Creek - about 200 m downstream from bath house	6/23/2010	-17.57	-130.08
11	Hot Springs Creek - above Arctic Hot Springs	6/24/2010	-17.25	-128.92
12	Hot Springs Creek - downstream from Arctic Hot Springs	6/24/2010	-17.21	-128.21
13	Spring/pool	6/23/2010	-16.37	-122.17
14	Thermokarst outflow	6/23/2010	-16.27	-122.35
15	Stream headwaters	6/23/2010	-17.24	-130.58
16	Stream headwaters	6/23/2010	-18.31	-135.90
17	Pool/seep	6/23/2010	-17.13	-126.93
18	Snowbank	6/23/2010	-21.44	-160.84
19	Headwaters spring	6/23/2010	-16.32	-120.52
20	High-gradient stream	6/23/2010	-17.03	-126.24
21	Headwaters spring	6/23/2010	-17.13	-126.67
22	Snowbank	6/23/2010	-21.22	-157.78
23	Snowbank	6/23/2010	-17.95	-132.25
24	Seep	6/23/2010	-17.89	-132.87
25	Steam below tors	6/23/2010	-17.76	-132.22
26	Mid-valley stream	6/23/2010	-17.67	-132.22
27	Hillside seep	6/24/2010	-18.63	-138.83
28	Hillside spring	6/24/2010	-17.51	-130.28
29	Ridgetop spring	6/24/2010	-16.64	-125.34
30	Snowbank	6/24/2010	-20.49	-151.59
31	Spring near divide	6/24/2010	-18.63	-138.50
32	Headwaters spring	6/24/2010	-16.75	-130.78
33	Headwaters spring	6/24/2010	-17.62	-130.77
34	Spring (C. palustra)	6/24/2010	-16.28	-122.03
35	Pool on divide	6/24/2010	-15.70	-119.04
36	Ephemeral(?) spring	6/24/2010	-16.42	-122.76
37	Headwaters N fork	6/24/2010	-16.45	-128.01

The Department of the Interior protects and manages the nation's natural resources and cultural heritage; provides scientific and other information about those resources; and honors its special responsibilities to American Indians, Alaska Natives, and affiliated Island Communities.

NPS 182/129651, September 2015

National Park Service
U.S. Department of the Interior



Natural Resource Stewardship and Science
1201 Oakridge Drive, Suite 150
Fort Collins, CO 80525

www.nature.nps.gov